72-12,558

JANSMA, Wilmar Bruce, 1944-
ULTRASTRUCTURE AND HISTOCHEMISTRY OF
FIBRICOLA CRATERA (TREMATODA: DIPLOSTOMATIDAE).

Iowa State University, Ph.D., 1971
Zoology

University Microfilms, A XEROX Company, Ann Arbor, Michigan

THIS DISSERTATION HAS BEEN MICROFILMED EXACTLY AS RECEIVED

Ultrastructure and histochemistry of *Fibricola cratera* (Trematoda: Diplostomatidae)

by

Wilmar Bruce Jansma

A Dissertation Submitted to the
Graduate Faculty in Partial Fulfillment of
The Requirements for the Degree of
DOCTOR OF PHILOSOPHY

Major Subject: Zoology (Parasitology)

Approved:

Signature was redacted for privacy.

In Charge of Major Work

Signature was redacted for privacy.

For the Major Department

Signature was redacted for privacy.

For the Graduate College

Iowa State University
Ames, Iowa

1971

PLEASE NOTE:

Some pages have indistinct print. Filmed as received.

UNIVERSITY MICROFILMS.

TABLE OF CONTENTS

INTRODUCTION

Host-parasite interfaces are of considerable interest to parasitologists for they represent unique sites for interaction of two genetically distinct types of tissue. The existence of these interfaces and the physiological, pathological, and immunological conditions and factors allowing two vastly phylogenetically different organisms to live in close contact with one another is a biological phenomenon which recently has attracted the attention of many workers. In the present study, various host-parasite interfaces of a strigeoid trematode were studied using light microscopy, histochemistry, and transmission and scanning electron microscopy.

During a course in helminthology at Iowa Lakeside Laboratory, Milford, Iowa in the summer of 1967, many amphibian hosts from the surrounding area (Dickinson and Clay Counties, Iowa) were examined and leopard frogs (Rana pipiens) were found to be heavily parasitized by strigeoid metacercariae (diplostomula) within hindleg and pelvic musculature. It had previously been shown by Ulmer (1955) and Turner (1958) that these metacercariae, when fed to mammalian hosts, mature rapidly to the adult stage of Fibricola cratera (Barker and Noll, 1915) Dubois, 1932. Preliminary feeding experiments and developmental studies utilizing laboratory-reared mice (Mus musculus)

and both adult raccoons (Procyon lotor) and opossums (Didelphis virginiana) from nature, demonstrated that all life cycle stages of this duodenal parasite could be maintained in the laboratory, thus providing abundant material for subsequent cytological and histochemical studies.

This thesis concerns itself with detailed studies on several organ systems of F. cratera. Because of the recently revised interpretation of trematode tegument indicating that the processes of respiration, pinocytosis, absorption and secretion may be associated with this cytoplasmic host-parasite interface, a complete study of regional specializations of the tegument was included to assess their role in some of these functions. One objective of this investigation was to examine the histochemistry, ultrastructure, and possible function of the unusual holdfast (tribocytic) organ of this species. Study of the alimentary tract of the adult worm was included to determine its absorptive and/or secretory capabilities. Because of the paucity of information on trematode sensory structures and the limited knowledge of the nervous system at the ultrastructural level, a complete study of this system of F. cratera was also undertaken. Additionally, various aspects of male and female reproductive systems as well as primary and reserve excretory systems were

investigated.

This investigation of several organ systems of F. cratera should prove useful in understanding general trematode structure and physiology, and in elucidating the complex host-parasite relationships common to digenetic trematodes.

HISTORICAL REVIEW

The genus Fibricola was established by Dubois (1932) with cratera as type species for a diplostomatid trematode described by Barker (1915) as Hemistomum craterum (Barker and Noll, 1915) from the intestine of the muskrat, Fiber zibethicus. This species was subsequently reported from the muskrat, Ondatra (Fiber) zibethicus, in Minnesota by Cuckler (1940) and in Illinois by Guilford (1954). It has also been reported as an intestinal parasite from mink (Mustela vison) in Ontario by Law and Kennedy (1932), in Texas by Read (1948), and in Louisiana by Lumsden and Zischke (1961); from the raccoon (Procyon lotor) in Iowa by Morgan and Waller (1940), Hoffman (1955), Turner (1958), in Michigan by Chandler and Rausch (1946), and in Lousiana by Lumsden and Zischke (1961). Other hosts reported are the opossum (Didelphis virginiana) in Georgia and Tennessee by Byrd, Reiber, and Parker (1942) and in Michigan by Chandler and Rausch (1946); the Norway rat (Rattus norvegicus) in Wisconsin by Schiller and Morgan (1949), in Michigan by DeGiusti (1957); and the skunk (Mephitis nigra) in Michigan by Chandler and Rausch (1946). In life cycle studies on F. cratera, Cuckler (1940) also reported this species from domestic cats, a spotted skunk, a short-tailed shrew, rats, and a meadow mouse. Experimentally this trematode has been recovered from laboratory rats (Ulmer, 1954;

Hoffman, 1955; Turner, 1958), laboratory white mice (Ulmer, 1954, 1955; Turner, 1957, 1958), and domestic chickens (Ulmer, 1955). A single natural avian infection was reported by Lumsden (1961) in Louisiana from the white ibis (Eudocimis albus).

Dubois (1953) concluded that three valid species of the genus Fibricola occur in the United States, namely: 1) Fibricola cratera (Barker and Noll, 1915) Dubois, 1932 [Synonyms: Hemistomum craterum Barker and Noll, 1915; F. laruei Miller, 1940, F. nana Chandler and Rausch, 1946]; 2) Fibricola lucida (LaRue and Bosma, 1927) Dubois and Rausch, 1950 [Synonyms: Neodiplostomum lucidum LaRue and Bosma, 1927, Theriodiplostomum lucidum LaRue and Bosma, 1944]; and 3) Fibricola texensis Chandler, 1942 [Theriodiplostomum texensis (Chandler) Dubois, 1944]. F. cratera (described as F. laruei) was reported from the small intestine of the raccoon (Procyon lotor) in Quebec, Canada by Miller (1940); this species was also reported as F. nana from the red squirrel (Tamiasciuris hudsonicus) in Michigan by Chandler and Rausch (1946), and from the gray squirrel (Sciuris hudsonicus) in several North Central States by Rausch and Tiner (1948).

Fibricola texensis has been reported from the raccoon (Procyon lotor) in Texas by Chandler (1942), who also described the life cycle of this species, and in Georgia

by Babero and Shepperson (1958) and Sawyer (1958). In studies on the life cycle of F. texensis, Leigh (1954) successfully used rats, hamsters, and chicks as experimental hosts.

Other species reported by Dubois (1953) are: Fibricola caballeroi Cerecero, 1943, from gray rats in Mexico and Fibricola minor Dubois, 1936 from the Australian water rat, Hydromys chrysogaster.

All members of the genus Fibricola belong to the family Diplostomatidae Poirier, 1886, whose members parasitize birds and mammals. The family is part of a large group of digenetic trematodes known as strigeoids which differ from many other trematodes in possessing two distinct body divisions, namely: 1) a flattened mobile forebody (anterior segment) and 2) a hindbody filled with reproductive organs. The conspicuous holdfast (tribocytic) organ characteristic of all strigeoids is the focal point of a portion of this study. Characteristics of members of the family Diplostomatidae according to Dubois (1953, 1963) include: massive and well defined tribocytic organ with or without a central cleft; distinct proteolytic glands; absence of a paraprostate gland; testes either club-shaped, pear-shaped, heart-shaped, bilobed in the form of dumbells, recurved as a horseshoe, entire or lobed, or sometimes ovoid.

The family is divided into subfamilies Diplostomatinae and Alariinae on the basis of host-specificity and distribution of vitelline follicles. Members of the subfamily Diplostomatinae (14 genera) are parasites of birds and possess vitellaria limited to the hindbody. Members of Alariinae Hall and Wigdor, 1918 are parasites of mammals, and have vitelline follicles generally limited to the forebody (anterior segment) of the adult. Dubois (1953) listed Fibricola and seven other genera in this subfamily and separated Fibricola from them by the following characters: 1) transverse constriction between the fore- and hindbody; 2) testes in tandem arrangement; 3) absence of pseudosuckers or auriculae; and 4) absence of a genital cone.

Pearson (1959, 1961) questioned the validity of the genus Fibricola and proposed that Fibricola, Conodiplostomum, and Neodiplostomum be placed as subgenera of Neodiplostomum, F. cratera thus becoming N. (Fibricola) craterum. Dubois (1963), however, retained the genus Fibricola and also placed F. texensis Chandler, 1942 in synonymy with F. cratera. Existent species of the genus Fibricola thus are: 1) F. cratera (Barker and Noll, 1915) Dubois, 1932 [Synonyms: Hemistomum craterum Barker and Noll, 1915, F. laruei Miller, 1940, F. nana Chandler and Rausch, 1946, F. texensis Chandler, 1942]; 2) F. lucida (LaRue and Bosma, 1927) Dubois and Rausch, 1950;

3) F. minor Dubois, 1936; 4) F. caballeroi Cerecero, 1943; F. sarcophila Sandars, 1957 from the Tasmanian devil (Sarcophilus harrisii); 6) F. sudarikovi Sadovaskaia, 1951 from the muskrat (Ondatra zibethicus), the wood mouse (Apodemus agrarius), and the hamster (Cricetululus triton nestor) in Russia; and 7) F. intermedia Pearson, 1959 from the Australian water rat (Hydromys chrysogaster).

Cuckler (1940, 1949) first reported on the life cycle of F. cratera which involves physid snails and several species of tadpoles and frogs as intermediate hosts. Ulmer (1954, 1955) and Hoffman (1955) presented additional life cycle observations. Turner (1957, 1958) provided descriptions of developmental stages of this species. References relating to ultrastructural and histochemical studies of adult organ systems will be presented within subsequent sections of this thesis.

SUMMARY OF LIFE CYCLE

Briefly, the life cycle of Fibricola cratera (as determined by Hoffman, 1955; Turner, 1958) is as follows: Adults are located in the duodenum of the mammalian host and oval, operculate eggs are voided with host feces. After incubation in water (usually 24-30 days), hatched miracidia penetrate physid snails (Physa gyrina) in which mother and daughter sporocyst generations develop. Furcocercous cercariae emerge 24 to 31 days later and penetrate amphibian tadpoles of several kinds, especially Rana pipiens. Metacercariae (diplostomula) first develop within the tadpole peritoneal cavity and later in the tail stem. At metamorphosis, diplostomula migrate to developing hindleg muscles. After metamorphosis, encapsulated metacercariae are localized principally in the hindleg musculature (primarily the gastrocnemius muscle in light infections) of adult frogs (Rana pipiens), or in heavy infections they may occur throughout pelvic and pectoral musculature. Encapsulated metacercariae when fed to experimental hosts (laboratory white mice) mature rapidly, hindbody and adult reproductive organs being fully formed within 5-6 days.

METHODS AND MATERIALS

Adult F. cratera were recovered from the duodenum of laboratory-reared white mice and from raccoons collected near Little Miller's Bay, West Lake Okoboji, Dickinson Co., Iowa. These hosts had been fed lower leg muscles of frogs (Rana pipiens) containing metacercariae (diplostomula) of F. cratera. Naturally infected frogs were collected near Center Lake, Dickinson Co., Iowa, and Trumbull Lake, Clay Co., Iowa, or were obtained from commercial sources (E. B. Steinhilber, Oshkosh, Wisconsin).

Light Microscopy

Specimens for whole mount preparations were fixed in A.F.A., dehydrated, stained with Mayer's paracarmine, counterstained with fast green, cleared in methyl salicylate and mounted in a synthetic medium (Permount). Specimens for histological sectioning were fixed in 10% neutral buffered formalin, A.F.A., or Ristroph's fixative, dehydrated through ethanol and embedded in 56-57° C Paraplast (Sherwood Medical Industries, St. Louis, Missouri). Sections (8-10 μ thick) were stained with Harris' acid haematoxylin counterstained with eosin, Ehrlich's acid haematoxylin, Mallory's triple stain, Weigert's collagen stain, neutral red or paraldehyde-fuchsin with Halmi's counterstain. Plastic (epon)

sections (approximately 1.0 u thick) were stained with 1% toluidine blue, 2% safranin O, or Paragon-1301 (C and C. Paragon Co., Bronx, New York). Histochemical techniques on neutral buffered formalin-fixed specimens included methods reported by Pearse (1968), Lillie (1965), Bancroft (1967), and Luna (1968), as well as the gold chloride technique for trematodes developed by Gorirossi and DeGiusti (1950), and the methods of Bueding, Schiller, and Bourgeois(1967) for localization of cholinesterase.

Photomicrographs were made using a 35 mm Pentax Spotmatic camera in conjunction with an AO Spencer Microstar research microscope and a Leitz Labolux microscope, equipped with bright field and phase objectives. Line drawings were made with the aid of a Leitz microprojector.

Transmission Electron Microscopy

Specimens for transmission electron microscopy were initially fixed for 2-3 hours at 4° C in 6% glutaraldehyde, buffered with 2.26% monobasic phosphate-2.52% NaOH (Millonig, 1961) to a pH of 7.2-7.3. To aid in cytological preservation, 10 drops of 1% $CaCl_2$ per 100 cc of buffer and sucrose to a concentration of 5% were added to the fixative (Lumsden, 1970). After initial fixation, specimens were washed in the above buffer for three consecutive 20-minute periods. Postfixation of specimens in 1%

osmium tetroxide for one hour at 4° C was completed using the above buffer minus $CaCl_2$ or sucrose, and this buffer was also used in two subsequent buffer washes of five minutes each. Specimens were dehydrated through a graded ethanol series including three changes of absolute ethanol before being placed in cold propylene oxide. After passage through a propylene oxide-epon series, specimens were embedded in the following epon mixture: Araldite 502 (10 ml); Epon 812 (13 ml); DDSA (30 ml); DMC (1.5 ml) (Anderson and Ellis, 1965; Mollenhauer, 1964). After curing at 37° C (12 hours), 45° C (24 hours), and 60° C (3 days), hardened blocks were trimmed, and ultrathin sections displaying silver to gold interference colors (600-900 A) were made with glass or diamond knives on LKB III or Reichart OmU2 ultramicrotomes. Sections were placed on bare copper grids and doubly stained with uranyl acetate (20% UrAc in absolute methanol) (Stempak and Ward, 1964) and lead citrate (Reynolds, 1963). Specimens were examined using RCA-3F, Hitachi 11C and 11E-1 electron microscopes, all operating at an accelerating voltage of 50 kilovolts. Negatives were taken on either Dupont Cronar film or Kodak medium contrast projection plates at magnifications of 3,200 X to 51,000 X. Images were subsequently enlarged photographically using Schneider-Companon lenses.

Scanning Electron Microscopy

After initial repeated washing in double distilled water, specimens for scanning electron microscopy were fixed using a solution consisting of 6 parts 2% osmium tetroxide and 1 part saturated mercuric chloride (after Parducz, 1967) for one minute at 0° C. Following fixation, specimens were again washed in distilled water, placed on aluminum weighing pans, blotted dry, and then immediately frozen using liquid nitrogen (Marszalek and Small, 1969). Frozen specimens were then quickly transferred to a freeze dryer (Edwards) and kept at -30° C for 24-28 hours. Dried specimens were coated with gold-palladium and viewed in a JEOLCO SCM-S1 scanning electron microscope operating at either 4 or 10 kilovolts. Negatives were taken at magnifications of 100 X to 10,000 X using Kodak Ektapan projection sheet film.

ULTRASTRUCTURAL STUDIES

Tegument

The structure, physiology and embryonic development of the body covering of digenetic trematodes has been the subject of numerous investigations. Until relatively recent times, most studies (reviewed by Ødlaug, 1948) concluded that the body is covered by a cuticle--in some instances homogenous, in others, two layered. The relationship of the "subcuticular" parenchymal cells to the body covering was also variously interpreted and as recently as 1951, Hyman outlined five theories of cuticular origin and structure among the Digenea. A review of these theories was presented by Threadgold (1963b) and by Lee (1966).

Electron microscopy, however, has shown the body covering of digenetic flukes to be of a protoplasmic syncytial nature and the term cuticle hence is inappropriate. Threadgold (1963b) proposed instead the term tegument, and his studies demonstrated the cellular nature and presence of mitochondria, endoplasmic membranes and vacuoles within the tegument. He further showed the existence of a direct association of the tegument with underlying subtegumental parenchymal cell bodies by means of protoplasmic tubules.

Subsequent studies (reviewed by Lee, 1966; Morris and Threadgold, 1968) confirm the syncytial nature of the tegument and numerous publications based on ultrastructural

observations include those by Bils and Martin (1966) on Acanthoparyphium spinulosum, by Inatomi et al. (1968) on Clonorchis sinensis, by Erasmus and Öhman (1965) and Erasmus (1967b) on Cyathocotyle bushiensis, by Reznik (1966) on Dicrocoelium lanceatum, and by Threadgold (1963a, 1963b, 1967) and Björkman and Thorsell (1964) on Fasciola hepatica. Other studies are those by Burton (1966) on Gorgodera sp., by Threadgold (1968a) on Haplometra cylindracea, by Burton (1964) on Haematoloechus medioplexus and by Bogitsh (1968) on Megalodiscus temperatus. Bogitsh and Aldridge (1967) reported on the tegumental ultrastructure of Posthodiplostomum minimum and the tegument of Schistosoma mansoni has been studied by Senft et al. (1961), Lee (1966), Morris and Threadgold (1968), Silk, Spence, and Gear (1969) and Smith, Reynolds, and Lichtenburg (1969).

Ultrastructural studies on the tegument of Fibricola cratera reported below confirm the syncytial nature of the tegument and the presence of underlying subtegumental cell bodies. Considerable variation in structure of the tegument is apparent, however, in various body regions.

Dorsal surface tegument (Figs. 1-4, 6) Dorsally, the tegument of the forebody is roughened and averages 1.5 μ (1.3-1.67 μ) in thickness. Intrategumental spines (Figs. 1-3) in general do not protrude from the dorsal surface as they do ventrally (Figs. 7, 8, 10, 13, 14), at

the forebody edge (Fig. 12), and from the tegument of the holdfast (Fig. 11). The dorsal tegument is bounded by a typical trilaminate unit membrane approximately 110 A wide (PM, Fig. 3). Within the surface syncytium (distal tegument) are numerous mitochondria, vesicles and spines. Vesicles in the surface syncytium appear to be of two types: 1) elongate, narrow ones measuring 0.2 μ in length, usually situated near the surface plasma membrane, and 2) larger oval or circular vesicles (av. diam. 0.36 μ) located throughout the surface syncytium (Figs. 3, 4). The latter often appear filled with particulate matter of varying density (Figs. 2, 4) and resemble those within the cytoplasm of the underlying tegumental cell bodies. Below the surface syncytium is a basal membrane (230 A wide) often elevated into the syncytial surface matrix for a short distance (arrows, Figs. 1, 2). Underlying this membrane is a conspicuous fibrous layer 0.43 u (0.32-0.52 μ) thick composed of numerous intertwined fibers (diam. 110 A). Within circular tegumental muscle bands (CM, Fig. 1) beneath the fibrous layer, individual muscle fibers are discernible. Longitudinal muscle bands (LM) lying below the circular muscle include two types of muscle fibers: larger dense ones having an average diameter of 360 A (330-400 A), and more numerous smaller fibers (90-110 A diam.) surrounding them. No distinct numerical ratio

between the two types could be determined, but the smaller ones outnumber the larger by a ratio of more than 6:1, a ratio also known to occur in vertebrate striated muscle (Huxley, 1965). Large mitochondria and beta glycogen particles fill the intermuscular and lower parenchymal areas (Figs. 1, 2). Also present are oblique (dorsoventral) muscle bands (shown in tangential section, Fig. 1) located below longitudinal muscle.

Below the oblique muscle in Fig. 1 a portion of a tegumental cell body is shown. Its cytoplasm is filled with numerous vesicles and individual ribosomes. Heterochromatin appears along the periphery of the nucleus (NU) and is also scattered within the less dense euchromatin. Centrally located within the nucleus is a granular nucleolonemar nucleolus (NUC, Fig. 1). Several tight junctions between the tegumental cell body and an adjacent parenchymal cell are shown in Fig. 1.

Hindbody tegument (Figs. 5, 9) Scattered mitochondria, few vesicles, and absence of spines characterize the irregular hindbody surface syncytium, 1.65 µ (1.4-1.9 µ) thick. Covering the external surface is a typical unit membrane. Several elevations of the basal plasma membrane can be seen in Fig. 5 (arrows). Fibrous elements in the underlying fibrous layer as well as circular and longitudinal muscle bands occur below the

surface syncytium. In addition, dorso-ventral muscle bands also traverse the parenchymal region. Adjacent to the fibrous layer is a small tegumental nerve (N) with synaptic vesicles, the latter measuring 400-540 A. Several nerves with similar synaptic vesicles and large oval vesicles (diam. 0.27-0.36 μ) permeate the underlying tissue.

Ventral surface tegument (forebody) (Figs. 7, 8, 10, 13, 14) Two vesicle types also occur in the ventral surface syncytium: 1) elongate vesicles (0.3 μ X 0.036 μ) near the surface plasma membrane (Fig. 13), and 2) large rounded vesicles measuring 0.3-0.45 μ in diameter (Figs. 10, 13, 14). Associated with the roughened ventral surface are conspicuous protruding spines with deep surrounding crypts (Figs. 7, 10, 13). Spine structure varies greatly in different planes of section as is evidenced in Figs. 13 and 14, where bases of several spines are shown in the same section as outer edges of adjacent spines. Ventral forebody spines are oriented at right angles to the longitudinal axis of the body and cover the entire surface (Fig. 7). Triangular spines in the holdfast region (Figs. 15, 17) and those on the lateral edge of the forebody (Fig. 12) measure 1.2-2.0 μ in height and taper to a point.

Spine structure (Figs. 15, 16, 17) Surfaces of tegumental spines are bounded by a typical unit membrane (PM, Figs. 15, 17). Spines possess a definite lattice

infrastructure (Figs. 15, 16, 17), said to resemble a protein lattice crystal (Burton, 1964; Smith, Reynolds, and Lichtenburg, 1969). Horizontal rods (HR) situated 280-290 A apart traverse the spine and are connected by smaller vertical bars spaced at 80 A intervals (Fig. 17). Spines rest on a basal membrane (BM) contiguous with the membrane underlying the adjacent surface syncytium.

Tegumental spines are most extensive on the ventral surface, where they are especially well developed around the holdfast organ. Although they are prominent at the lateral edges of the forebody and protrude from the lateral and ventral surfaces of the forebody, they do not do so dorsally and appear to be entirely absent from the tegument of the hindbody.

Holdfast (Tribocytic) Organ

Characteristic of strigeoid trematodes is the presence of a large, densely staining, glandular holdfast organ (tribocytic organ, adhesive organ) situated posterior to the acetabulum on the ventral body surface. In a review on the structure and function of the holdfast, Erasmus and Öhman (1963) considered two main structural types: 1) acetabular--superficially resembling the acetabulum with a close aggregation of gland cells surrounding the external opening and central chamber of the holdfast, and exemplified by Diplostomum, Alaria, Cyathocotyle and Fibricola;

2) lobular--with walls extending as finger-like processes usually enclosed in a forebody cup, with a compact glandular mass at the base of the lobes and characteristic of Apatemon, Cotylurus, and related species of Strigeidae. Fibricola with its acetabular holdfast represents the family Diplostomatidae which Dubois (1953) considers to be a morphological and evolutionary step between the primitive Cyathocotylidae and the more advanced Strigeidae. Previous studies on the ultrastructure of strigeoid holdfasts include those by Erasmus and Öhman (1965), Erasmus (1967b, 1968) on Cyathocotyle bushiensis; by Erasmus (1969) on Apatemon gracilis minor; and by Erasmus (1970) on Diplostomum phoxini.

The holdfast of F. cratera when inverted appears as a longitudinal slit-like opening on the ventral surface of the forebody (Figs. 18, 19). In cross section (Figs. 20, 21, 22) the holdfast consists of a central chamber (CCH, Fig. 21) connected externally by means of a holdfast cleft (HC, Figs. 22, 24) separating the two holdfast lobes. Surrounding the central chamber and holdfast cleft are numerous tightly packed gland cells (GC, Figs. 21, 23) with dense staining nuclei.

The tegument of the holdfast cleft (T, Fig. 24) contains numerous elongate spines (SP) (av. length 2.5 μ) and is continuous with the ventral surface tegument and

with the tegumental folds (TF) characterizing the more dorsal central chamber of the holdfast. Several large muscle bands (MU, Fig. 24) (av. 1.65 μ X 0.8 μ) underlie the tegument of this region. At the opening of the central holdfast chamber (HO, Fig. 24), the tegument becomes devoid of spines and large irregularly shaped folds characterize its surface (TF, Figs. 22, 24-30). Such folds average 675 A (600-800 A) in width, are bounded by a distinct plasma membrane (PM, Fig. 26), and constitute the walls of elaborate small chambers, thus greatly increasing the surface area of the holdfast (Figs. 29, 30).

Associated with these tegumental folds are slender finger-like microvillar processes (MV, Figs. 24, 25, 28, 30) with an average width of 420 A (390-550 A); these fill the central chamber of the holdfast and are also evident in the region of the holdfast cleft (Fig. 24). Such elongate microvillar processes appear membrane bound (small arrows, Fig. 26) and are circular in cross section; these may represent sites of holdfast secretion. Located near the base of the holdfast tegumental folds are large numbers of elongate dense vesicles (DV, Figs. 27, 30), identical to cytoplasmic vesicles within adjacent gland cells and associated ducts (GD, Fig. 28). Underlying the tegument of this area is a basal lamina (membrane) (BM, Figs. 27, 31) approximately 180 A wide, and often forming an extensively

folded interface between tegument and the underlying tissue (Fig. 27). Between tegument and glandular cells is a region containing large numbers of mitochondria (M, Fig. 24) and excretory tubules (EL, Figs. 24, 29, 32). Densely packed mitochondria of this region appear typically elongate (av. 180 μ X 1340 μ) with numerous internal cristae (CR, Fig. 34). Walls of excretory tubules are lined with membrane bound laminar structures (EL, Fig. 32) measuring 235 A in width. Densely staining protein bodies (PB, Figs. 24, 33) composed of innumerable 100 A subunits may occur within the wall of the excretory tubule or near its nucleus (NU, Fig. 33).

Glandular cells of the holdfast (GC, Figs. 21, 23, 35, 38) form a dense aggregation in which individual cell plasma membranes are only infrequently discerned (PM, Fig. 37). Individual gland cells possess large nuclei (NU, Figs. 35, 36, 37, 40) containing areas of dense staining heterochromatin and less dense euchromatin. Nuclear pores (NP, Fig. 36) connecting the nucleoplasm with the surrounding cytoplasm were frequently observed. Within the cytoplasm, the presence of extensive cisternae of endoplasmic reticulum are indicative of a secretory function. Scattered mitochondria and densely staining vesicles (DV, Figs. 39, 40) similar to those observed near the holdfast tegumental folds are also seen in the

cytoplasm of holdfast gland cells.

The holdfast (tribocytic) organ of Fibricola closely resembles the "adhesive" organ of Diplostomum phoxini, as described by Erasmus (1970).

Nervous System and Sensory Receptors

Nervous system

Detailed studies on the nervous system of digenetic trematodes, other than early morphological studies by European workers near the turn of the century have largely been neglected. Among the more comprehensive works are those by Bettendorf (1897) and by Zailer (1914), whose investigations on gross neuroanatomy of adult trematodes involved the use of certain techniques including methylene blue and heavy metal stains. Bullock and Horridge (1965) in their monograph of invertebrate nervous systems noted the paucity of and infrequent additions to the literature regarding trematode nervous anatomy and physiology. They characterized trematode nervous systems as being primitive and less well developed than those of free-living triclad and polyclad turbellarians. Several authors of general parasitology texts currently in use seem to concur with the idea of a primitive nervous system, e.g., "The (trematode) nervous system is relatively simple, sensory elements being feebly developed", (Smyth, 1962); "Organs and structures that are important or even essential for

free living organisms often become lost or greatly modified in parasitic forms. Structures for locomotion and special sensory organs have become modified or even disappear completely", (Baer, 1951); "The nervous system and sense organs require no long discussion. All parasites, especially the endoparasites, have a more or less simplified nervous system. The simplification is best reflected in the loss of sense organs, which can be present in the free-living developmental stages and disappear with the transition to the parasitic way of life", (Dogiel, 1964); and, "The development of the nervous system is of low grade and sense organs are almost lacking", (Chandler and Read, 1965). Stunkard (1967) in a symposium of parasites of invertebrates noted that regression of sensory and nervous structures appears to coincide with the adoption of the parasitic habit.

More recent studies, however, involving biochemical assays, enzyme histochemistry, as well as transmission and scanning electron microscopy of trematodes indicate that a highly specialized nerve network and many types of specialized sensory receptors occur in both larval and adult trematodes. Bueding (1952) first reported acetylcholinesterase in adult Schistosoma mansoni and noted that enzymatic levels of this substance were similar in magnitude to those of mammalian brain tissue. Chance

and Mansour (1953) also localized this enzyme from the nervous system of Fasciola hepatica. Numerous biochemical studies since then have indicated that neural impulse transmission and neuromuscular activation in trematodes bears marked similarity to nervous systems of higher animals. Accurate descriptions of gross nerve structure and nerve fiber ramifications have been made possible with the development of precise histochemical techniques for localization of acetylcholine within nerve tissues. This technique was first developed by Koelle and Friedenwald (1949) and was later modified by Gomori (1952). Still later it was adapted for helminths by Bueding, Schiller, and Bourgeois (1967) who clearly depicted the nervous system of adult Schistosoma mansoni. Halton and Morris (1969) also used a similar technique to describe the nervous system of the monogenetic trematode, Diclidophora merlangi, and found high cholinesterase activity in the cerebral ganglia, main ventral nerve cords and nerve plexi in the oral suckers, pharynx and cirrus. Localization of acetylcholinesterase has also been used in this study to describe the nervous system of Fibricola cratera at the light microscope level.

In general, the structure of the nervous system of digenetic trematodes follows a basic morphological pattern. Two large cerebral ganglia located near the

pharynx are connected by a large dorsal commissure. From these ganglia several nerve trunks or cords (usually three pairs) proceed anteriorly and three pairs (dorsal, lateral, and ventral) extend posteriorly. Nerve commissures connect major longitudinal nerves at right angles, thus forming the rungs of the "ladder-like" network characteristic of trematode nervous systems. In F. cratera, ventral and lateral nerve trunks are very prominent (Figs. 41, 42) but the dorsal cord was not observed. Cerebral ganglia (CG, Figs. 41, 42, 43, 45) consisting of nerve cell bodies and axons appear as triangular dark-staining masses located at the posterolateral edges of the pharynx (P, Fig. 41). Joining the cerebral ganglia dorsally is the cerebral commissure (CC, Figs. 43, 44, 45) measuring approximately 6.0 μ in width. Proceeding anteriorly from the cerebral ganglia are the anterior ventral nerve cords (AN, Fig. 43) which give rise to small nerve branches to the pharynx, esophagus, and well innervated oral sucker. Within the oral sucker, as well as within the acetabulum (Figs. 41, 42), nerve fibers ramify between alternating muscle bands resulting in the dense staining of acetylcholine in these areas. Arching outwardly from the anterior ventral nerve is the lateral nerve cord (LN, Figs. 41, 42) which then proceeds posteriorly near the edge of the forebody and continues into the hindbody to the region of the genital

pore (GP, Fig. 41). The lateral nerve cord (LN) and the transverse nerve commissures (NC) are of similar diameter (3.2-4.0 μ) but generally are smaller than the conspicuous posterior ventral nerves (7.8-9.0 μ) (Fig. 42). The latter (VN, Figs. 41, 42, 44) originate from the cerebral ganglia and extend to the posterior of the hindbody and lie lateral to the intestinal crura, acetabulum, and the entire holdfast (HF, Fig. 41). Nerve commissures (NC, Figs. 42, 44, 46) connecting lateral and ventral nerve cords traverse the entire fore- and hindbody at right angles to the longitudinal axis. Commissures are more numerous (16-18) in the forebody than in the hindbody, and although much variation occurs, are spaced 24.0-33.0 μ apart in the forebody.

Two well defined structures, here tentatively considered as unipolar cells (UC, Figs. 43, 45), similar in position to those described by Halton and Morris (1969), were observed anteromedial to the cerebral ganglia at the level of the pharynx. These bodies (4.5 μ diam.) appear stalked with a small internal nerve fiber arising from the underlying ganglionic tissue and extending distally. These structures in Fibricola cratera differ from described trematode eyespots (Kümmel, 1960; Isseroff, 1964; Pond and Cable, 1966) in lacking pigmented cells or particles visible at the light level; they may represent specialized sensory

receptors of similar function for they are located precisely in the same position as are photoreceptors in the miracidium of this species and in larval stages of other trematodes. Eyespots in adult trematodes are very rare, however, and have been reported only infrequently. Faust (1918) in his study of trematode eyespots noted that among distomes only members of the family Allocreadiidae or closely related groups do adults possess pigmented eyespots. He also stated that in many cases pigmentation is faint and the "lens" appears degenerate in adults. Although pigmented eyespots occur in some adult aspidogastrid trematodes, e.g., Cotylapsis insignis as reported by Osborn (1903), they have not been reported from strigeoid trematodes. Further studies involving ultrastructural investigations on these bodies should prove fruitful.

The ultrastructure of trematode nerve fibers, cell bodies, nerve synapses and neuromuscular junctions remains largely unexplored. Previous reports are those by Dixon and Mercer (1965) on the cercariae of Fasciola hepatica, Reissig (1970) on nerve cell bodies in adult Schistosoma mansoni, and Wilson (1970) on the nervous system of Fasciola hepatica miracidia. Fine structure of cerebral ganglia, major nerve cords, and nerve fibers, of Fibricola cratera are depicted in Figs. 47 through 54.

Nerve axons within the cerebral ganglia (Fig. 47) possess at least two distinct types of vesicles: 1) numerous membrane bound synaptic vesicles (SV, Fig. 47), approximately 400-450 A in diameter, with clear or slightly electron dense contents, and 2) large dense vesicles, less abundant, approximately 580-600 A diameter, and filled with electron dense material. These types of vesicles correspond in size, density, and appearance with vesicles reported by Dixon and Mercer (1965) from the cerebral ganglion of Fasciola hepatica cercariae. A probable synaptic cleft is seen in Fig. 47 (arrow) where dense vesicles have accumulated at the junction of two neurons.

Cross sections of major nerves of F. cratera (Figs. 48, 49) illustrate that numerous synaptic vesicles (SV) of nearly uniform size (400-450 A) are tightly packed and form the bulk of the nerve cord. Dense amorphous masses also occur within nerves but are dissimilar to typical mitochondria (M, Fig. 48) which are located in parenchymal tissue surrounding the nerve proper. Several smaller nerves (N) possessing typical synaptic vesicles and dense bodies were observed within gastrodermal cells adjacent to the gut lumen (LU, Fig. 50) and within holdfast gland cell cytoplasm (Fig. 52). Tegumental nerves (N, Figs. 51, 53, 54, 60) possess synaptic vesicles and are situated between the fibrous layer (FL) of the tegument

(T, Fig. 51) and the underlying circular muscle tissue (MU, Figs. 53, 54). Nerves underlying the dorsal forebody tegument (Fig. 51), the ventral forebody tegument (Fig. 53), and hindbody tegument (Fig. 54) appear similar in their position (subtending the fibrous layer) and internal composition (possessing synaptic vesicles). Occasionally, unidentified dense bodies within nerves (N, Fig. 53) were interspersed among the numerous synaptic vesicles (400-500 A diam.).

Sensory receptors

Until very recently, trematode sensory receptors received little or no attention and numerous authors (Dogiel, 1964; Smyth, 1962; Rogers, 1962) have implied that the loss of sense organs is common among parasitic organisms. Zailer (1914), who studied the innervation of the oral sucker of Gorgoderina vitelliloba, noted several types of presumed sensory bulbs in this region. Other workers reported similar nerve terminals but their structure, location, and function have remained enigmatic until only recently. Development of transmission and scanning electron microscopes with ancillary biological preparative techniques has resulted in the recent appearance of several detailed studies depicting sensory structures in helminths. It has already been shown that simple and complex sensory receptors occur in large numbers in adult and larval stages

of trematodes, cestodes, and nematodes. In a light microscope study of sensory receptors of monogenetic, aspidogastrid and digenetic trematodes, Rohde (1968) described ten different types of tegumental receptors, but indicated that further ultrastructural confirmation should be made.

At the ultrastructural level, studies on specialized photoreceptors (eyespots) of miracidia of Fasciola hepatica and Philophthalmus were made by Kümmel (1960) and Isseroff (1964), respectively. Pond and Cable (1966) later reported on the fine structure of cercarial eyespots.

Regarding additional receptors, Dixon and Mercer (1965) in an ultrastructural study of the cercarial nervous system of Fasciola hepatica, first reported a presumed ciliated sensory bulb embedded in the tegument near the oral sucker. Similar receptors in Schistosoma mansoni cercariae have been reported by Morris (1971) and by Robson and Erasmus (1970), and in cercariae of Himasthla secunda studied by Chapman and Wilson (1970). Wilson (1970) also reported the presence of four types of sensory structures in the miracidium of Fasciola hepatica. Several reports of sensory receptors of adult digenetic trematodes have recently appeared and include those by Morris and Threadgold (1967), Silk, Spence, and Gear (1969), Smith, Reynolds, and Lichtenburg (1969) on Schistosoma mansoni,

and by Erasmus (1967b, 1969) on Cyathocotyle bushiensis and Apatemon gracilis. Lyons (1969a, b) reported the existence of both single and compound sensory receptors in her studies on monogenetic skin parasites. Morseth (1967) reported a similar type of ciliated receptor from the adult cestode, Echinococcus granulosus. In the present study, transmission and scanning electron microscopy have shown that in addition to single ciliated receptors, other types of sensory structures are strategically located in and on the tegument of Fibricola cratera.

Tegumental sensory receptors in adult F. cratera appear to be of four major types, depicted in four scanning electron micrographs (Figs. 63-66). Each of the four types will be discussed as to its morphology, number, position on the body surface, and comparison with other reported receptors.

Type I (Figs. 55-58, 60, 61, 65) This consists of a sensory bulb embedded within the tegument and is characterized by the presence of a single terminal cilium projecting beyond the surrounding tegumental tissue. The cilium (0.23 μ wide) possesses the typical 9+2 internal microtubule pattern and measures 1.1-1.2 μ in overall length, of which 0.78-0.8 μ is exposed as a central projection within a cylindrical cavity, the latter extending from the external tegument to the bulbous portion of the

sensory receptor (Figs. 55-58, 60, 61, 65). The basal body (BB, Figs. 55, 56) of the cilium lacks the two central microtubules which terminate basally near the junction of the exposed portion of the cilium with the bulb proper. The basal body is expanded laterally near its base and appears to be connected with dense bodies located near septate desmosomes (SD, Fig. 55) and joining the sensory bulb to the surrounding tegument (T). Septate desmosomes (SD, Figs. 55, 56, 58, 61) appear as thickenings of the plasma membrane of both the sensory bulb and surrounding tegument and possess stout cross striations between the two membranes, thus effectively "locking" the terminal portion of the underlying sensory bulb within the tegument. Typical trilaminate plasma membranes (PM, Fig. 56) bound the surrounding tegument externally, as well as the sensory bulb and its exposed cilium (Fig. 57). Internally, these sensory bulbs (1.60 μ av. width) contain synaptic vesicles (SV, Figs. 55-58, 61) varying somewhat in appearance and in size (730-950 A), as well as cristate mitochondria (M, Figs. 55, 56, 58, 60, 61) also varying in size (0.31-0.64 μ max. diam.), number, and profile (circular to oval, Fig. 58). Basally the sensory bulb is continuous with a nerve fiber (N, Figs. 57, 58) connecting with other nerve processes via a synaptic junction (SJ) schematically depicted in Fig. 57. Microtubules (MT,

Figs. 57, 58) (300 A av. width), synaptic vesicles, and mitochondria also are present in such nerve fibers. Sensory bulbs of this type were frequently observed on both the ventral and dorsal forebody surfaces, being especially numerous at the edges of the forebody where direct contact with host tissue would result when the entire forebody is flexed around an intestinal villus. Sensory structures of this type structurally resemble those described by Dixon and Mercer (1965) in Fasciola hepatica cercariae, as well as those noted by Erasmus (1967b, 1969) from the strigeoid trematodes Cyathocotyle bushiensis and Apatemon gracilis, and by Chapman and Wilson (1970) in transmission electron micrographs of tegumental receptors of Himasthla secunda cercariae. Type I receptors appear similar to one of the receptors termed a "lateral sheathed ciliated ending" by Wilson (1970) and located between miracidial tegumental plates in Fasciola hepatica; they also resemble the sensory receptor reported by Morseth (1967) from Echinococcus granulosus, although distinct ciliary rootlet fibers described by him were only infrequently observed in F. cratera receptors. Type I receptors differ from those reported by Morris and Threadgold (1967) and by Silk, Spence, and Gear (1969) from Schistosoma mansoni adults in that the terminal cilium of F. cratera is exposed externally and is not

enclosed within the tegument. Although the bulbous portion of Type I receptors resembles those described for single sense organs by Lyons (1969a) in Gyrodactylus and Entobdella, the exposed ciliary portion of the F. cratera receptors (0.78-0.8 μ long) is drastically shorter than the exposed portion of cilia in monogenetic skin parasites (9.0-11.0 μ in length).

Type II (Fig. 66) Although structurally similar to those of Type I in possessing a single projecting cilium, it differs in lacking a ringed depression around the cilium. In this type, the cilium (C, Fig. 66) projects from the underlying sensory bulb lying flush with the tegumental surface from which nearby tegumental folds (TF, Fig. 66) also arise. Receptors of this type are the most numerous of all receptors, and are located primarily on the dorsal and ventral surfaces of the forebody tegument and also among tegumental folds around the oral sucker (Fig. 70). This receptor type superficially resembles integumentary papillae described by Chapman and Wilson (1970) in scanning electron micrographs of the surface of Himasthla secunda cercariae.

Type III (Figs. 59, 62, 64) This type of sensory bulb (1.5-2.0 μ diam.) projects from the tegumental surface as a large domed structure, lacking a terminal cilium. The entire bulb is covered with tegumental tissue

(T, Figs. 59, 62) with its attendant plasma membrane (PM, Fig. 62). Internally, typical synaptic vesicles (SV, Figs. 58, 62) (850-950 A diam.) and cristate mitochondria (M Fig. 62) were observed. Sensory structures of this type occur on the ventral surface of the forebody (Figs. 59, 62), but are more numerous in the genital region near the posterior of the body (SB, Figs. 68, 69). Although exact numbers of receptors surrounding the genital aperture (GA, Figs. 68, 69, genital cone shown inverted (Fig. 68) and everted (Fig. 69)) could not be determined, an estimate of several hundred receptors in this area seems plausible. Receptors of this type were also observed at the rim of the oral sucker (SB. Fig. 70). Reports of nonciliated sensory structures are very infrequent. Structurally, this receptor (Type III) resembles the "lateral bulbous ending" described by Wilson (1970) from the miracidium of Fasciola hepatica and also several types of receptors described by Rohde (1968) in a light level study of the adult trematode, Diaschistorchis multitesticularis. He noted large numbers of receptors around the oral sucker and genital regions of that species.

Type IV (Figs. 63, 67) Structurally, this sensory structure resembles Type I and II receptors in possession of a terminal cilium (C) projecting from an underlying sensory bulb (SB, Figs. 63, 67) but differs in that the

entire bulbous portion is elevated above the surrounding tegument. Type IV receptors, although less numerous, were observed at the edge of the acetabulum (A, Fig. 67) where six receptors of this type were circumferentially arranged. Occasionally receptors of this type were found in the genital region interspersed among the more numerous domed Type III receptors. Although a receptor similar to Type IV has not previously been reported, sensory bulbs located near the oral sucker of Schistosoma mansoni cercariae (Robson and Erasmus, 1970) are similarly elevated from the surrounding tissue.

Although several functions for the reported sensory structures of various helminths have been mentioned, namely: tangoreception (Dixon and Mercer, 1965; Erasmus, 1967b; Rees, 1968; Robson and Erasmus, 1970; Wilson, 1970), chemoreception (Dönges, 1964; Rees, 1968; Lyons, 1969b; Wilson, 1970), direction of flow of medium (Morris and Threadgold, 1967), gravity reception (Wilson, 1970), the specific function of any or all of these structures remains unknown. In a review of helminth site-finding behavior, Ulmer (1971) emphasized the lack of detailed knowledge of the complex sensory mechanisms involved in the behavior patterns of life cycle stages of all helminths. Based on internal structure, location on the body surface, and comparison with other known invertebrate sensory receptors,

it might seem plausible to assign a tangoreceptive function to some of the receptors described in this study. Their actual function, however, remains unknown.

Future detailed electrophysiological, ultrastructural, and behavioral studies hopefully will elucidate the role of these specialized structures, which most probably are essential to the organism in maintenance of its parasitic way of life. It can be said with certainty that sensory structures are very numerous, being especially well developed around the organs of attachment and genital openings, and that they form an integral part of a highly complex nervous system in this species. Thus, contrary to earlier reports, it has been shown that even in entirely parasitic stages of this helminth, the nervous system with its numerous specialized receptors and nerve fibers remains complex and cannot in any sense be considered degenerate.

Alimentary Tract

The alimentary tract of digenetic trematodes, because of its importance in nutritional metabolism, has been the subject of many histological, histochemical, and ultrastructural studies. Most digenetic trematodes possess a relatively simple digestive tract consisting of a terminal mouth enclosed by a muscular oral sucker, a short esophagus, a muscular pharynx, and intestinal crura

(ceca), the latter extending to the posterior of the body and usually ending blindly. In general, the lining of the oral sucker, esophagus and pharynx consists of a modified tegument structurally similar to the external surface of the worm. Intestinal crura are lined with a single layer of epithelial cells possessing cytoplasmic projections extending into the lumen. In structure, the latter resemble microvilli characteristic of intestinal epithelial cells of higher animals.

Recent ultrastructural and cytochemical studies on a wide variety of digenetic trematodes indicate that the gut lining is chemically complex and that individual gastrodermal cells are structurally highly variable. The epithelium may be of a syncytial nature or may be composed of individual cells (see review by Davis and Bogitsh, 1971b). Although it is generally believed that gut epithelium (gastrodermis) is involved in both secretion and absorption, much controversy as to correlation of these functions to various cellular functions (volume, height, maturation, internal organelles, etc.) exists in the literature (Sommer, 1880; Muller, 1923; Stephenson, 1947a; Gresson and Threadgold, 1959; Dawes, 1962; Thorsell and Björkman, 1965). Recent ultrastructural studies on trematode digestive tracts include those by Gresson and Threadgold (1959), Thorsell and Björkman (1965) and Threadgold (1968b) on Fasciola

hepatica; by Dike (1967, 1969) and Davis, Bogitsh, and Nunnally (1968, 1969) on Haematoloechus medioplexus; by Dike (1967) on Gorgoderina amplicava, (1969) on Paragonimus kellicotti. Additional recent descriptions of gut epithelium include those by Shannon and Bogitsh (1969) on Schistosomatium douthitti and by Davis and Bogitsh (1971b) on Gorgoderina attenuata.

The digestive tract of Fibricola cratera consists of the mouth (MO, Fig. 71) within the terminal oral sucker (OS, Figs. 41, 71), a short esophagus leading to a muscular pharynx (P), and intestinal crura (IC, Figs. 41, 71), the latter extending to the posterior of the hindbody where they end blindly. In a scanning electron micrograph of the mouth (Fig. 70), numerous tegumental sensory bulbs (SB) surround the opening (24-26 μ diam.) and the continuation of the external tegument into the lining of the oral sucker can be seen. The oral sucker (Figs. 72, 74) is lined with a modified tegument (0.5 μ max. thickness) possessing numerous tegumental folds bounded by a trilaminate plasma membrane (PM, Fig. 74). This lining somewhat resembles the esophageal tegumental lining of Schistosoma mansoni recently described by Morris and Threadgold (1968) and Dike (1971). A high magnification micrograph of the tegument (T, Fig. 74) illustrates the presence of vesicles (V) similar to those described from

the external tegumental surface and demonstrates also the basal plasma membrane (BM) and the 130 A fibers comprising the underlying fibrous layer (FL), the latter also clearly shown in Fig. 72. The bulk of the oral sucker consists of alternating bands of circular and longitudinal muscles (MU, Fig. 72). The lining of the muscular pharynx depicted in Fig. 73 is also a modified tegument (T) containing numerous vesicles and small mitochondria (0.35-0.5 μ diam.). An electron translucent fibrous layer (0.25 μ thick) lies between the tegumental lining (T) and the massive muscle bands (MU) of the pharynx (Fig. 73). Within the lumen of the pharynx, ingested material (IM, Fig. 73) can be seen.

In cross sections of intestinal crura (Fig. 75), the gut outline usually appears circular or oval, but is occasionally flattened (Fig. 76) so that the lumen is reduced to a longitudinal slit. The thickness of the gut wall, the height of individual gastrodermal cells, and their structural state are highly variable depending on the plane of sections of cells; thus, sections through bulbous nucleated portions (NU, Fig. 75) appear thicker than adjacent cytoplasmic regions of the same cell. The appearance of the gut also varies in accordance with its nutritional state, and the location (forebody vs. hindbody) from which sections were taken. Although definite correla-

tions between structural and nutritional features are difficult to ascertain, it is of interest that the number of microvilli occurring on gastrodermal cells in the forebody appear similar in sections of the gut whether it is unfilled (Figs. 75, 76) or filled (Fig. 85). In contrast, the gut epithelium of the hindbody (Figs. 86, 87) possesses fewer and shorter microvilli and the gut walls appears reduced in thickness.

The cecal lining of F. cratera is characterized by the presence of septate desmosomes between individual gastrodermal cells, (the cytoplasm of such cells containing extensive granular endoplasmic reticulum, several types of vesicles, and scattered cristate mitochondria), and the universal presence of protoplasmic extensions (microvilli) extending centrally into the gut lumen. Various circular and longitudinal muscle bands (MU, Figs. 75, 76) surround the basal portion of the gut. Several large nuclei (NU, Fig. 75) approximately 2.6 to 4.0 μ in diameter lie within the cytoplasm of their respective gastrodermal cells which are basally bounded by a highly convoluted basal plasma membrane. The cytoplasm (CY, Figs. 75, 77, 81) of gastrodermal cells is filled with endoplasmic reticulum (ER, Figs. 83, 86) studded with ribosomes (140-150 A diam.) (R, Figs. 77, 84) and cristate mitochondria (M. Figs. 83, 84). Densely staining septate

desmosomes (SD, Figs. 75, 76, 79, 83, 87) occur between adjacent gastrodermal cells near the lumenal surface and their dense cross striations are readily seen (Figs. 79, 83). Projecting from the lumenal surface of the gastrodermal cells (GDC) are elongate digitiform processes here referred to as microvilli (MV, Figs. 76-80, 82, 83, 85, 86). Sommer (1880) first reported "pseudopodia" on the gut cells of Fasciola (Distomum) hepatica and later Muller (1923) mentioned "cytoplasmic fibrils" extending from the gut cells of the same species. Although other workers have mentioned the presence of this brush border (Stephenson, 1947a; Wotton and Sogandares-Bernal, 1963), the detailed structure of these processes was first shown in ultrastructural studies of F. hepatica by Gresson and Threadgold (1959) and later by Thorsell and Björkman (1965). Senft et al. (1961) and Ercoli et al. (1963) described these processes in adult Schistosoma mansoni gut cells. Halton (1966), reporting on the occurrence of microvilli in seven species of digenetic trematodes, estimated that these processes increase the available absorptive surface area approximately 115 to 120 times. In all digenetic trematode species studied to date (see review, Davis and Bogitsh, 1971b) similar cytoplasmic extensions, characterized as being either digitiform or lamelloid, have been observed. In Fibricola, these cytoplasmic projections branch freely

from the surface, sometimes appearing lamelloid (Figs. 77, 80) in forming closed loops, but more frequently appearing as finger-like processes having circular or oval outlines in cross section (Fig. 78). Each microvillus (450-550 A diam.) is bounded by a trilaminate plasma membrane and internally is filled with a dense filamentous core. Superficially, microvilli possess a particulate coating similar to the glycocalyx reported from the intestinal microvilli of Haematoloechus medioplexus by Dike (1967) and from Gorgoderina attenuata by Davis and Bogitsh (1971b). In addition to undigested food material (IM, Fig. 85) located centrally within the lumen, dense nondescript particulate matter (Figs. 77, 79) often is seen between individual microvilli (MV). This substance usually appears separated from the microvillar plasma membrane by an electron translucent region, thus suggesting a region of active digestion and/or resorption. Within both the cytoplasm of the gastrodermal cells (Fig. 83) and within the gut lumen (Figs. 80, 82), whorled membrane bodies (WM) consisting of numerous concentric folds were frequently observed. Similar bodies have been reported by Davis, Bogitsh, and Nunnally (1969) who isolated cathepsin in them while studying the nonspecific esterases in Haematoloechus medioplexus. They hypothesized that vesicles containing cathepsin fuse with mitochondria and

other membrane-bound organelles to form cytolysosomes. After autolytic enzymatic digestion of degenerating organelles, the cytolysosomes together with resulting residual bodies (whorled membrane bodies) presumably migrate to the edge of the gastrodermis where they are expelled into the lumen. Davis and Bogitsh (1971a) reported apparently similar arylsulfatase-rich cytolysosomes and membranous remnants from the gastrodermal cytoplasm and lumen of Haematoloechus medioplexus and Gorgoderina attenuata. Additionally, Davis and Bogitsh (1971b) reported myelinated membrane remnants staining positively for acid phosphatase (a marker for lysosomal activity) in gut cells of Gorgoderina attenuata. Although these whorled membrane bodies found in Fibricola structurally resemble the myelinated residual bodies described elsewhere, their functional role must await further cytochemical localization. Another type of cytoplasmic inclusion (heretofore undescribed) is a large dense body (termed "protein body") (PB, Figs. 80, 81) comprised of small rounded subunits, 50-75 A in diameter. These bodies are usually surrounded by cytoplasm (CY, Fig. 81) filled with granular endoplasmic reticulum (ER, Fig. 80) and free ribosomes. It is hypothesized that the substance constituting the "protein body" is formed by the extensive endoplasmic reticulum of the surrounding cytoplasm and

may be expelled into the gut lumen (note the proximity of the "protein body" to the lumen in Fig. 81).

In sections of the intestinal wall in the hindbody (Figs. 86, 87), the lumen (LU) is filled with a wide variety of clear vesicles, lipoid droplets, and particulate matter suggestive of degraded ingested material (IM). The cells comprising the gut lining of this region are flat and possess few shortened microvilli on their apical surfaces. Within the intestinal cytoplasm of the hindbody (Fig. 86) and the forebody (Fig. 85), membrane bound vesicles (V) (0.3-0.5 μ diam.) were frequently seen, usually located superficially near the lumenal border. Dike (1969) and Bogitsh, Davis, and Nunnally (1968) reported ultrastructural localization of acid phosphatase in similarly structured and positioned vesicles in the gastrodermis of Haematoloechus medioplexus. The presence of acid phosphatase in such vesicles suggests that they are involved in secretion of digestive enzymes. Several other authors (Halton, 1967; Threadgold, 1968b; Morris, 1968; Bogitsh, 1970; Bogitsh and Shannon, 1971; Davis and Bogitsh, 1971b) have also localized acid phosphatase in the ceca of a number of digenetic trematodes. Sites of localization were principally the superficial digestive vesicles (mentioned above), the microvillar surfaces within the lumen, and the infoldings of the basal and

lateral plasma membranes of the gastrodermal cells. Although there is a strong structural correlation of acid phosphatase with sites of presumed active transport mechanisms (microvillar and basal plasma membranes), the existence of dephosphorylative transfer mechanisms (using acid phosphatase) for transport of low molecular weight compounds across these membranes remains unproven (review by Read, 1966). Nevertheless, an active transport system of similar mechanism probably exists to permit movement of materials across the physiologically dynamic surface characteristic of trematode gastrodermis.

Although the secretory role of the gut has not been clearly elucidated, the presence of extensive endoplasmic reticulum, Golgi complexes (and their associated vesicles) strongly supports this view. With regard to absorption of nutrients, it has been hypothesized by several authors (see review by Davis and Bogitsh, 1971b) that secreted digestive enzymes (acid phosphatase, esterases, others) initiate the first stages of extracellular digestion of food material within the lumen. Higher molecular weight substances are further degraded at the membrane level and the resulting low molecular weight substances (e.g., monosaccharides) may be absorbed by the gastrodermal cells. In a review of digestion in flatworms, Jennings (1968) noted that digestion is initially extracellular

(possibly entirely extracellular in some species such as Fasciola hepatica), but that in most cases there is absorption of partially digested soluble substances into the gastrodermis, digestion thus being completed intracellularly. Observations reported in this structural study lend support to the interpretation of the gastrodermis functioning concomitantly in both secretion and absorption.

Male Reproductive System

Although spermatogenesis in digenetic trematodes has attracted the attention of many helminthologists in the last century, observations have generally been limited to the more general features of the process. According to Nez and Short (1957), gametogenetic studies on more than 60 species of trematodes have been published, but many of these involve only studies of chromosome numbers and various structural changes of such chromosomes during gametogenesis. More recent light level studies such as those by Burton (1960) on Haematoloechus medioplexus and by Guilford (1961) on Halipegus eccentricus provide a rather complete overall review of trematode gametogenesis, but relatively few ultrastructural studies on germinal cells have been completed and much of the cellular composition of these cells remains obscure. Gresson (1965), in a review of spermatogenesis of digenetic trematodes, noted that although previous studies have shown a common pattern of

spermatogenesis, much controversy as to the structure of spermatozoa, the process of spermiogenesis, and the presence of cellular structures (centrioles, flagella, mitochondria, Golgi complexes) within germinal cells still exists.

Although much of the present study is limited to spermiogenesis and the structure of mature spermatozoa of Fibricola cratera, a review of the male reproductive system of this trematode and a generalized pattern of spermatogenesis common to all digenetic trematodes thus far studied will be presented for purposes of orientation.

The male reproductive system of F. cratera consists of paired testes and vasa efferentia, a vas deferens, a seminal vesicle, and an ejaculatory duct (Ulmer, 1955). The anterior testis (AT, Figs. 41, 88-90) appears oval or triangular, and is situated between the more anterior ovary (OV, Figs. 41, 88, 89) and the posterior testis (PT), the latter constricted medially and hence appearing dumbbell-shaped. The vitelline reservoir (VR, Figs. 41, 88-90) is located medially between the two testes. Paired vasa efferentia from the testes join to form a single vas deferens, the latter expanding posteriorly to form the seminal vesicle. The thin-walled seminal vesicle (SMV, Figs. 89, 91) is filled with large numbers of mature spermatozoa. The terminal portion of the vas deferens

(also known as the ejaculatory duct) joins the uterus, and the common duct so formed opens externally via the genital aperture (GA, Figs. 68, 69, 89, 91).

Histologically, the testis consists of three primary regions, namely: 1) an outer testis wall (TW, Figs. 103, 117) consisting of a sheath of connective tissue with fibrous elements and elongated mitochondria; 2) a germinal layer of primary germinal cells and spermatogonia lying just beneath the testis wall; and 3) the testicular cavity containing primary and secondary spermatocytes, developing spermatids, mature spermatozoa, and cytoplasmic residual bodies, all of which are randomly interspersed. Primary spermatogonia (Figs. 103, 104) possess large nuclei (NU), numerous mitochondria (M) located at the circumference of the nuclear membrane, and a cytoplasm (CY) filled with numerous ribosomes. Within these cells, which display a high nuclear to cytoplasmic volume ratio, centrioles (CE, Fig. 103) and ciliary rootlet fibers are seen. Evidence of the presence of centrioles is of interest for Gresson (1965) stated that they are seldom seen in male germ-cells of digenetic trematodes. Except for the peripherally situated spermatogonia, there appears to be no orderly arrangement of other developmental stages within the testis, thus making sequential study of individual germ cells rather difficult. Using squash preparations and

specific nuclear stains (e.g., Feulgen's), many workers (see reviews by Burton (1960) and Gresson (1965)), have shown a common pattern of spermatogenesis (Fig. 92). Incipient germ cells give rise mitotically to primary spermatogonia located near the testis wall. Each primary spermatogonium produces two secondary spermatogonia which in turn divide mitotically to form four tertiary spermatogonia. The latter do not separate completely but remain attached by a short strand of cytoplasm, thus forming a "rosette" pattern of cells. This characteristic rosette pattern is maintained throughout all subsequent divisions including spermiogenesis so that eventually a cluster of 32 spermatids (termed a spermatomorula by Hendelberg, 1962) remain attached centrally. Yosufzai (1952) in studying Fasciola hepatica called this central cytoplasmic connection a blastophore, but more recently Sato et al. (1967) more correctly termed this region a cytophore and demonstrated it with electron micrographs. Tertiary spermatogonia again divide mitotically to form 8 primary spermatocytes with a diploid (2N) number of chromosomes. After two subsequent maturation divisions typical of animal meiosis, 16 secondary spermatocytes and ultimately 32 spermatids result. A detailed study of chromosomes undergoing meiotic divisions was not undertaken, but the general appearance of chromosomes (CH,

Fig. 105) in spermatocytes resembles that reported in similar cells of Fasciola hepatica by Gresson and Perry (1961). These chromosomes (0.75-0.8 μ wide) are seen coiled throughout the ribosome-filled spermatocyte cytoplasm (CY) and are filled internally with dense filaments or lamellae traversing the chromosome longitudinally, thus giving it a "scroll-like" appearance. It has been shown that this chromatin material in developing spermatids loses its fibrous appearance and becomes very dense and compact (Burton, 1960).

Since the subsequent stages of spermiogenesis (formation of mature spermatozoa from spermatids) are virtually unknown, it was an objective of this study to illustrate the various cellular components and processes involved in sperm formation. To understand this process and to obtain points of reference for this developmental sequence, it seems advisable first to describe mature spermatozoa of Fibricola. Studies on living and fixed trematode spermatozoa have shown that they are typically threadlike structures characterized by their extreme length and small uniform diameter. The sperm of Haematoloechus, for example, has a diameter of 0.5 μ and a length of approximately 400 μ (Burton, 1960). In sectioned testis, spermatozoa of Fibricola measure 0.5-0.6 μ in diameter and approximately 35 to 50 μ in length. Accurate measurement of spermatozoan

length is difficult, due to the extensive coiling of sperm within the testis and seminal vesicle (Figs. 117, 118). Mature sperm (Fig. 102) observed either in the testis (SPE, Fig. 109) or stored in the seminal vesicle (SPE, Figs. 117, 118) consist of two major components, the head and tail, the latter subdivided into neck, middle, and terminal pieces. Sections through the head region reveal the large circular nucleus (NU, Figs. 98, 111) and numerous microtubules (MT, Fig. 111) at the periphery of the sperm head. A single axial filament (AF, Fig. 111) lies parallel to the nucleus and extends to the anterior end of the sperm. The structure of these axial units, although resembling cilia in possessing nine outer doublet microtubule units (DB, Fig. 114) differs markedly from typical 9+2 cilia in possessing an internal axial column instead of two central microtubules characteristic of cilia (Afzelius, 1959). The internal structure and significance of these axial filaments are discussed below. Also present in the head region of the sperm are cristate mitochondria (M, Figs. 98, 111) also found in the neck region of the sperm tail (Fig. 102, B). Within the neck region (Figs. 99, 112, 114, 116) axial filaments (AF), mitochondria (M) and microtubules (MT, Figs. 112, 114, 116), the latter 250 A diameter, are enclosed within the outer plasma membrane. In the middle portion of the

tail (Fig. 100), only two parallel axial filaments and several cytoplasmic microtubules are seen. The cytoplasm also contains glycogen deposits (G, Fig. 118) similar to those reported from tapeworm spermatozoa (Lumsden, 1965). Axial filaments move closer together in the terminal portion of the sperm tail, which tapers distally as two naked axial filaments (ST, Fig. 118), only one of which is seen terminally. Axial filaments consist of nine doublet microtubule units and the central axial column. Doublet microtubule units (DB, Fig. 114) measure 420 A x 260 A in cross section, and possess both A and B subunits similar to those reported from mammalian sperm tails (Afzelius, 1959). Internally, the central axial column (760 A diam.) consists of a dense core termed an axial rod or core (AR, Fig. 114) of approximate 330 A diameter. Surrounding this core is a thin (120 A) translucent zone which in turn is enclosed by a dense outer cortical sheath (CS, Fig. 114). In negative staining studies on axial filaments of Haematoloechus medioplexus sperm, Burton (1967b) interpreted the cortical sheath as a double helical pattern of rounded subunits spiralling around the central axial rod. Silveira (1969) more correctly interpreted the cortical sheath as being composed of 400 A wide tissue bands wrapped around the intermediate translucent zone in a double helix, each gyre having a length of 700 A

and a pitch of 45 degrees. In a longitudinal section of an axial filament (AF) of Fibricola (Fig. 110), a similar helical pattern of the cortical sheath (CS) around the axial core can be seen. Radiating outward from the cortical sheath are spokes (S, Figs. 110, 112, 114, 116) connecting the A subunit of the outer doublet units (DB, Fig. 114) with the central axial column. Such spokes (460 A long) appear to be arranged in a helical pattern along the central axial column, for in individual cross sections of axial filaments (AF, Figs. 112, 116) all nine radiating spokes are rarely seen, thus suggesting that they are arranged spirally along the central axis. Shapiro et al. (1961) who first reported axial filaments from Haematoloechus medioplexus sperm tails also proposed a helical spoke arrangement. The A microtubules to which spokes are attached bear two radiating arms, the latter extending in one direction. Axial filaments similar to those noted above have been described from 14 species of turbellarians, 7 species of trematodes and 3 species of cestodes (see review by Silveira, 1969). Although earlier reports (Shapiro et al., 1961; Gresson and Perry, 1961; Rosario, 1964) mentioned the presence of unique axial filaments, two recent reports (by von Bonsdorff and Telkka (1965) on Diphyllobothrium latum and by Sato et al. (1967) on Paragonimus miyazakii) include selected

sections of entire spermatozoa.

Cytoplasmic microtubules (MT, Figs. 111, 112, 114, 116) within spermatozoa are more numerous in the head region (Figs. 98, 111) where they form a parallel row along one side of the sperm head. These microtubules (260-280 A diam.) diminish in number in the neck and middle tail regions of the sperm (Figs. 112, 114, 116) and are absent from its terminal portion. Sections of Fibricola spermatozoa (Figs. 98-101) confirm the observations of other investigators as to the presence and position of microtubules, mitochondria and axial filaments within sperm tails. Fibricola sperm, however, differ in possession of only one axial filament in the region of the sperm nucleus (Fig. 111) instead of two as reported by other workers.

The formation of these unique spermatozoa from spermatids (spermiogenesis) has not been extensively studied. Early workers noted the extensive coiling of the nucleus within spermatids and the presence of an apical cytoplasmic projection. Each mature sperm was depicted as an elongated nucleus complete with a "flagellum". Several authors considered sperm to be entirely of nuclear origin, but more recently it has been recognized that both cytoplasmic and nuclear components are involved in sperm formation (see review by

Gresson, 1965). Spermatozoa originally were considered to be uniflagellate, but recently Dhingra (1954a) reported two "flagella-like" processes projecting from sperm of Isoparorchis eurytremum. Nez and Short (1957), as well as Burton (1960) also reported biflagellate sperm in Schistosomatium douthitti and Haematoloechus medioplexus, respectively. Guilford (1961) reported "cytoplasmic filaments" extending from spermatids of Halipegus eccentricus. Since much confusion over sperm formation exists, clarification of the process of spermiogenesis at ultrastructural level and correlation of these findings with light level observations seem promising. Hendelberg (1962), using a Feulgen-osmium staining technique to study spermiogenesis in Fasciola hepatica and Dicrocoelium dentriticum, correctly described the entire process. He demonstrated three distinct processes arising from spermatids, two "flagella" (axial filaments) and a central "middle snook" (mid-piece). Hendelberg showed that the elongated nucleus leaves the spermatid body and migrates to the distal end of the mid-piece. Axial filaments (flagella) lying on either side of the mid-piece then fuse with the latter to form the composite sperm tail described above. Upon maturation, the terminal piece of the sperm tail detaches from the former spermatid body and a residual cytoplasmic body remains within the testis.

This entire process in Fibricola cratera is depicted in sequential diagrams (Figs. 93-97), with special reference to the structure of the mid-piece and the formation of the mature sperm tail. Although all 32 spermatids undergo concomitant development, the maturation process of only one is depicted. A newly formed spermatid (Fig. 93) contains a large nucleus (NU), several mitochondria and membrane-bound vesicles within its cytoplasm. Apically the cytoplasm bulges outward and a centriole (CE) is located in this region. Centrioles (or centrosomes) have been reported in similar locations in spermatids of Haematoloechus medioplexus by Burton (1960) and also by Dhingra (1954a, b, 1955a, b) in Isoparorchis eurytremum, Cyclocoelum bivesiculatum, Cotylophoran elongatum, and Gastrothylax crumenifer. Burton (1960) noted that after division of primary spermatocytes of Haematoloechus, each secondary spermatocyte receives a pair of centrioles. After subsequent division of secondary spermatocytes, each resulting spermatid receives a single centriole. In the next developmental stage (Fig. 94), the nucleus (NU) undergoes elongation and moves apically toward the centriole (CE). Two axial filaments (AF) arise from the centriole and grow laterally. Ciliary rootlet fibers (RT, Fig. 94) attached to the basal portion of the developing axial filaments may serve to position these filaments during

their formation and possibly may later be involved in movement of these filaments from the horizontal position (Fig. 94) to a more vertical plane (Figs. 96, 97). Hendelberg (1962) observed that these axial filaments in Fasciola hepatica extend laterally for 240 μ before they move to a parallel position along the mid-piece, the latter consisting of a cytoplasmic medial projection. Ciliary rootlets (RT, Figs. 106, 108) are located near the centriole (CE); internally each possesses alternating light and dark crossbands. Axial filaments (AF, Figs. 106-108) arise from centrioles at right angles and extend outwardly from the spermatid body. The cytoplasm (CY, Fig. 108) is filled with ribosomes and mitochondria (M, Fig. 106). In subsequent development (Fig. 96), the nucleus (NU) migrates from the spermatid body into the mid-piece which extends to the (head) end of the future sperm. In a cross section through these projections of the spermatid at this stage (Fig. 95), the mid-piece (MP) and two adjacent axial filaments (AF) are clearly seen. Electron micrographs (Figs. 113, 115) illustrate the presence of large numbers of 9+1 axial filaments and dumbbell-shaped mid-pieces (MP). Several microtubules (MT, Figs. 113, 115) located in the bulbous ends of the mid-piece (MP) may provide support to this structure during migration of the nucleus through the center of

mid-piece. These microtubules correspond to the cytoplasmic microtubules previously described in mature sperm.

In the last stage of spermatid development (Fig. 97), the nucleus (NU) is shown within the mid-piece and the two axial filaments lie parallel to this projection. The nucleus now migrates to the distal end of the mid-piece (MP) and is followed by numerous mitochondria. Eventually the axial filaments fuse laterally with the mid-piece to form the mature sperm tail (Figs. 99, 100). This process of sperm tail formation is similar to that of Fasciola and Dicrocoelium reported by Hendelberg (1962). After sperm formation, the spermatid body containing mitochondria, ribosomes, and vesicles is retained within the testis as a residual cytoplasmic body.

Although further study of spermiogenesis must be undertaken, the developmental sequence (Figs. 93-97) proposed for Fibricola corresponds with the findings of Hendelberg (1962) and the preliminary ultrastructural study by Sato et al. (1967) on spermiogenesis of Paragonimus miyazakii. Additionally, it can be hypothesized that early workers in describing sperm as being uniflagellate, either were observing the mature sperm tail (containing two axial filaments) or the large mid-piece of an earlier developmental stage. Others (Dhingra,

1954a, b, 1955a, b; Nez and Short, 1957; Burton, 1960) who reported two flagella were probably seeing the two protruding axial filaments which arise before the formation of the mid-piece. Because nuclear migration and fusion of axial filaments into the sperm tail take place very rapidly (Hendelberg, 1962) and because many of these components are of small diameter, it is understandable that many stages of spermiogenesis were probably overlooked in previous light microscope studies. In any case, it can be stated that: 1) spermatozoa of Fibricola cratera are both nuclear and cytoplasmic in origin; 2) sperm nuclei migrate from the spermatid body to a distal position by means of a mid-piece, the latter derived from cytoplasm; and 3) single sperm tails of this species contain mitochondria, cytoplasmic microtubules and unique 9+1 axial filaments. Since platyhelminths also possess typical 9+2 cilia (as in flame cells, ciliated sensory receptors, sperm ducts, and vitelline ducts), the presence of the 9+1 axial filaments in their sperm has been considered by Hendelberg (1965) to be of phylogenetic significance. He hypothesized that the presence of these axial filaments is a secondarily derived characteristic of members of this phylum, thus suggesting that it is unlikely that "higher" metazoans evolved from turbellarians whose spermatozoa also have a flagellar

structure of this unusual 9+1 type. It is also interesting to note that these 9+1 axial filaments possess radial symmetry in contrast to the usual 9+2 bilateral ciliary pattern. It has been hypothesized that this radial arrangement could permit multidirectional movement, and Hendelberg (1965) indeed showed that free axial filaments of polyclad turbellarians were able to move in three planes, in contrast to the restricted "back and forth" movements of typical 9+2 cilia. Results of the present study of F. cratera confirm the unusual pattern of spermiogenesis common to certain trematodes and demonstrate the presence of distinctive 9+1 axial filaments in this biologically interesting group of flatworms.

Female Reproductive System (Vitelline Cells)

Trematode egg shell formation and the role of vitelline cells in this process has been the subject of much controversy. Early workers believed that the Mehlis' gland or "shell gland" secreted the shell or capsule of the egg, but more recently it has been confirmed that the vitelline cell globules form the bulk and possibly all of the shell (Stephenson, 1947b; review by Smyth and Clegg, 1959). Three precursors (proteins, phenols, and phenolase) have been localized histochemically in the vitelline globules. Recent ultrastructural and histochemical studies on the Mehlis' gland (Burton, 1967a; Threadgold and Irwin, 1970)

have shown that two types of secretory gland cells and their products occur. Although the fate of these secretions has not been determined conclusively, it has been hypothesized by these authors that one secretory product may serve a lubricatory function in the oötype and uterus, whereas the other may act on vitelline cells to cause release of vitelline globules which coalesce upon a basic shell membrane to form the main egg shell. Final oxidation and tanning of the shell occurs within the uterus where shells assume their characteristic yellow-brown color.

In this study, detailed investigations on the female reproductive system of Fibricola cratera were not conducted, but a careful examination of the vitelline follicles and vitelline ducts indicates that a regular developmental sequence of vitelline cells occurs, including the release of secretory products from such cells. Vitelline follicles of F. cratera are limited almost exclusively to the forebody, and extend from the intestinal bifurcation to the posterior margin of the forebody. Vitelline cells (VC, Fig. 129) are located throughout the parenchyma, and surround the intestinal crura (I), the holdfast organ (HF) and associated holdfast gland cells (GC). Vitelline cells display a developmental sequence as they mature. Young cells (Fig. 122) are small, possess few vitelline granules, a cytoplasm filled with innumerable ribosomes (R)

(170-200 A diam.), and strands of endoplasmic reticulum (ER). Nuclei (NU, Fig. 120) of such vitelline cells are typically elongate, and internally a granular nucleolus (NUC) is seen. As the vitelline cell matures, its cytoplasm becomes filled with vitelline granules of varying size (0.2-0.8 μ) which aggregate to form large clusters of vitelline granules within the surrounding secretory cytoplasm (Fig. 121). In this species, mature vitelline cells appear to break down structurally, thus releasing individual vitelline granules (VG, Figs. 119, 123, 124) from the cell proper prior to their movement into vitelline ducts. Cytoplasmic remnants of vitelline cells (CY, Fig. 123) persist after vitelline granules (VG) have been released and such remnants are also frequently seen along the wall of the vitelline ducts (Figs. 127, 128). The mechanism whereby vitelline materials pass through vitelline ducts is not known (Dawes, 1940), but in Fibricola numerous cilia (0.2 μ diam.) displaying the typical 9+2 microtubule pattern lie within the duct wall and may serve in movement of material through the duct. Cilia are either grouped (Fig. 125) or are arranged linearly (Fig. 126).

In addition to the prominent vitelline granules mentioned above, densely staining yolk droplets (Y, Figs. 119, 127) occur within vitelline cells and ducts of

F. cratera. These droplets, also known to occur in Fasciola hepatica and described in the latter species by Björkman and Thorsell (1963), are considered to serve a nutritive function in egg development (Smyth and Clegg, 1959).

After their release, vitelline materials pass through longitudinal and transverse vitelline ducts to the vitelline reservoir, located intertesticularly in the hindbody (VR, Figs. 89, 90). Peripherally within the vitelline reservoir (VR, Fig. 130) where temporary storage of vitelline products occurs, large clusters of vitelline granules (1.4-1.5 μ) and vitelline cell cytoplasm (CY), the latter filled with ribosomes and endoplasmic reticulum, may be observed.

The above findings indicating that individual vitelline cells undergo progressive granulation and vacuolation are in agreement with conclusions by Björkman and Thorsell (1963) who studied the vitelline maturation process in Fasciola hepatica and of Tulloch and Shapiro (1957) who dealt with Haematoloechus sp. Although conflicting views exist as to the mechanism and release site of vitelline granules in various species, it appears that in Fibricola some of the vitelline products are freed long before they reach the vitelline reservoir, as was first reported by Sommer (1880) in Distomum hepaticum and later by Tulloch

and Shapiro (1957) in Haematoloechus sp. The evidence of the presence of typical cilia within vitelline duct walls has been previously unreported and it appears that they may serve either a motile or a sensory role. This study of the vitelline cells illustrates that two types of secretory products (vitelline granules as well as yolk droplets) are involved. It also indicates that partial release of vitelline granules from vitelline cells occurs in the regions of the forebody prior to movement of the granules via vitelline ducts to the vitelline reservoir, Mehlis' gland, and associated reproductive organs located in the hindbody.

Excretory System

The excretory system of strigeoid trematodes is distinctive in possessing both a primary (protonephridial) system as well as a reserve excretory system. The former consists of flame cells, capillaries, collecting tubules, ducts and an excretory bladder. The reserve (secondary) excretory system lacks flame cells and consists of lacunar spaces (ducts) and numerous smaller tubular vessels, the latter terminating in short saccate branches. In metacercariae, these branches contain numerous calcareous corpuscles, but in adults, concretions are far less numerous. The entire reserve system forms an extensive network of vessels throughout the forebody

parenchyma of F. cratera. It is continuous with the primary system at specific points, and is considered to be a ramification of the excretory bladder, which in Fibricola opens posteriorly by a terminal excretory pore. Because of the large size and numerous small ramifications of the reserve system throughout the body, it has been implicated in circulatory, absorptive and hydrostatic roles.

Hughes (1927) described the extensive reserve excretory system of strigeoid trematodes in his study of Neascus ambloplitis; additional contributions by Van Haitsma (1931), LaRue (1932), Erasmus and Öhman (1963) and Öhman (1966a, b) have provided data on the morphology and histochemistry of this system in related species. Erasmus (1967a) reported on the ultrastructure of the reserve bladder system of Cyathocotyle bushiensis, noting the formation of lipid inclusions within ducts of this system.

In Fibricola, the reserve excretory system in the hindbody consists of a large expanded portion connected to many smaller reserve excretory ducts (lacunae) in the forebody. These spaces (RD, Fig. 21), especially prominent in the lateral forebody lobes, are also present throughout the forebody parenchyma, being well developed adjacent to the holdfast tegument (large arrow, Fig. 21; EL, Figs. 24, 29, 32). Although an extensive study of the excretory system of this species has not been undertaken, several

observations of both primary and reserve excretory systems seem of interest.

The ultrastructure of trematode flame cells was first reported by Kümmel (1958) in Fasciola hepatica miracidia. Kruidenier (1959), Lautenschlager and Cardell (1961), Senft et al. (1961), Pantelouris and Threadgold (1963), Gallagher and Threadgold (1967), Wilson (1969), and Ebrahimzadeh and Kraft (1971) have since described trematode flame cell and excretory duct ultrastructure. Additionally, the system has been studied in a variety of cestodes, turbellarians, and rotifers (see reviews by Howells (1969) and by Warner (1969)). Structurally, flame cells in Fibricola are comparable to those described by Howells (1969) in the cestode Monieza expansa. The "flame cell" seen at the light level actually is composed of two cells--a primary cell with cilia, and a funnel-shaped collar cell formed by the terminal portion of an excretory tubule. The two cells are connected by interlocking cytoplasmic rods (Howells, 1969). The primary cell (flame cell) in Fibricola possesses 68-75 typical cilia of the 9+2 pattern (C, Fig. 131) and a large oval-shaped nucleus (NU, Fig. 123). The funnel-shaped flame cell collar (FCC, Figs. 131, 132) is formed by cytoplasmic arms extending from the terminal portion of the capillary (terminal ductule); a desmosome (CJ, Fig. 131) marks the

junction of the arms at one side of the flame cell collar. Cilia of the flame cells possess basal bodies (BB, Figs. 133, 134) embedded within the cytoplasm (CY) of the flame cell, but no ciliary rootlets were observed. Basal bodies seen in Fig. 133 (sectioned at level of dotted line, Fig. 134) indicate that centrally located cilia are probably longer than more peripheral ones as reported by Gallagher and Threadgold (1967) in their study of flame cells in Fasciola hepatica. Cilia (C, Fig. 132) display a uniform orientation of centrally situated microtubules (plane of line, Fig. 132), thus indicating a unidirectional plane of movement. Cilia are densely packed in a homogeneous matrix in distinct diagonal rows.

The wall of a primary excretory tubule (ED, Figs. 131, 133, 135, 136) consists of a syncytium varying in thickness (0.2-1.0 μ) depending on the number and position of surface lamellae. Large nuclei located within the cytoplasm of the wall protrude into the lumen; additionally, the cytoplasm is filled with individual ribosomes and a few elongated mitochondria. The inner surface of the wall is covered with stacked lamellae (EL, Figs. 131, 135, 136) usually lying parallel with the surface but sometimes projecting into the lumen. Such excretory lamellae (200-240 A thick), bound by typical plasma membranes, often link adjacent cytoplasmic regions (e.g., EL, Figs. 135,

136). Lamellae may traverse the entire lumen, thus greatly increasing the surface area. Similar lamellae (microvilli, microrugae) have been reported from excretory ducts of both larval and adult trematodes (Stephenson, 1947c; Senft et al., 1961; Lautenschlager and Cardell, 1961; Kruidenier, 1959; Pantelouris and Threadgold, 1963; Gallagher and Threadgold, 1967; Erasmus, 1967a, 1969). Although the function of such lamellae remains unknown, Erasmus (1967a) reported alkaline phosphatase localization on them, thus suggesting their role in metabolic transport. Dense lipid droplets (L, Figs. 133, 135) were observed within the cytoplasm of cells of excretory tubules; such droplets frequently extend into the lumen and are covered with one or more excretory lamellae (Fig. 135). Since droplets of this type also appear within excretory ducts, it is hypothesized that lipid substances accumulate within the walls and later are released into the lumen. Lipid droplets within trematode excretory ducts were first reported by Sommer (1880) and later by numerous investigators (see review, Erasmus, 1967a), but their function remains unknown. It has been suggested that they may serve to remove excess sterols from the trematode parenchyma, that they provide a source of reserve energy storage, or that possibly they represent an excretory product of anaerobic glycolysis. Similar lipid droplets (L, Fig. 137) appear in lacunar

spaces of the reserve excretory system (RD, Figs. 137, 138) and below the surface lamellae (EL), the latter also characteristic of these duct walls. Additionally, numerous whorled membrane bodies (WM, Fig. 138) were seen within reserve excretory ducts. These bodies structurally resemble cestode calcareous corpuscles reported by von Brand et al. (1960). Erasmus (1967a) described similar bodies from the excretory system of Cyathocotyle bushiensis and reported their "nuclei" to consist of degraded membrane-bound organelles. A similar explanation for the formation of trematode excretory concretions was proposed by Martin and Bils (1964). Various developmental stages may account for the variety of loose and tightly coiled concretions observed within Fibricola excretory ducts. Frequently, large accumulations of glycogen (G, Figs. 137, 138), both alpha and beta forms, were observed near reserve excretory duct walls. Their proximity to the lamellate excretory wall suggests that this surface may be involved in the transport and/or absorption of this substance. Nieland and Weinbach (1968), studying excretory ducts within a larval cestode (cysticercus) bladder, noted similar adjacent areas of high glycogen concentrations. They suggested an absorptive and circulatory role for the excretory system in transport of glycogen to regions of high metabolism such as the

scolex, etc. The present study emphasizes that the excretory system of Fibricola is complex and that in addition to excretion and/or osmoregulation, various components may be involved in absorption and transport of nutrients.

HISTOCHEMISTRY

General histochemical tests on adult Fibricola cratera were conducted to determine concentrations of various chemical groupings within various body organs and structures. Histochemical techniques used were those described by Pearse (1968), Lillie (1965), Bancroft (1967), and Luna (1968). Because several comprehensive light level studies on the histochemistry of closely related strigeoid trematodes are already known, detailed histochemical determinations on F. cratera were not conducted. In a series of publications, Erasmus and Öhman (1963) and later Öhman (1965, 1966a, b) reported on the histochemistry of various strigeoids including Cyathocotyle bushiensis, Diplostomum spathaceum, Apatemon gracilis, and Holostephanus luhei. These studies centering on the structure and function of the adhesive (holdfast) organ also included observations on the tegument, parenchymal tissue, the alimentary tract (including caecal contents) and various glandular cells. Detailed investigations on carbohydrates, nucleic acids, lipids, and proteins (including a wide variety of enzymes-alkaline and acid phosphatases, leucine aminopeptidase, nonspecific esterases, and cholinesterases) were also included. Structurally, the strigeoid Diplostomum spathaceum studied by Öhman (1966a) closely resembles Fibricola cratera, both species having similarly shaped

fore- and hindbodies and the same type of acetabular holdfast. Lee (1962) also reported on the histochemistry of Diplostomum phoxini, specifically the localization of alkaline phosphatases and nonspecific esterases within the holdfast organ and pseudosuckers. The present study supplements the ultrastructural studies mentioned above. Four major chemical groupings (carbohydrates, proteins, nucleic acids, and lipids) were investigated. A summary of all histochemical tests is presented in Table 1.

Carbohydrates

Histochemically, carbohydrates are identified by the periodic acid-Schiff (P.A.S.) reaction which stains all groups of carbohydrates including: 1) simple polysaccharides (including glycogen), 2) mucopolysaccharides, 3) mucoproteins, 4) glycoproteins, and 5) glycolipids. Carbohydrates comprise one of the largest chemical groups present in helminths and are known to be an excellent source of anaerobic energy (von Brand, 1966). In F. cratera, carbohydrates demonstrated by the P.A.S. reaction occur throughout the body (Table 1), being especially concentrated within the tegument, alimentary tract (including caecal contents), vitelline cells, and the vitelline reservoir). P.A.S. control tests proved negative. Localization of glycogen (the principle stored simple polysaccharide found in helminths) was

Table 1. Histochemistry* of adult Fibricola cratera

	P.A.S.	P.A.S. control	P.A.S. amylase digestion	P.A.S. diastase digestion	Best's Carmine
Tegument	+	0	+	+	0
Subtegumental cells	+	0	+/-	0	0
Holdfast lobes	0	0	0	0	0
Holdfast gland cells	0	0	0	0	0
Holdfast tegument	+/-	0	0	0	0
Oral sucker	0	0	0	0	0
Acetabulum	0	0	0	0	0
Foregut epithelium	+	0	+	+	0
Hindgut epithelium	+	0	+	+	0
Caecal contents	+++	0	++	++	+
Vitellaria	++	0	0	0	+++
Vitelline ducts	+	0	0	0	++
Vitelline reservoir	+++	0	0	0	+++
Excretory ducts	0	0	0	0	0
Ovary	0	0	0	0	0
Oviduct	0	0	0	0	0
Testes	0	0	0	0	0
Vas deferens	0	0	0	0	0
Seminal Vesicle	0	0	0	0	0
Egg shell	0	0	0	0	0
Intrauterine egg (contents)	++	0	0	0	+++

* Symbols denote the following: +++ Strong reaction; ++ Moderate reaction; + Positive reaction; +/- Slight reaction; 0 No reaction

Alcian blue pH 6.5	Alcian blue pH 2.5	Alcian blue pH 1.0	HgBPBl	Napthol yellow Y	Feulgen reaction	Pyronin Y-M. green	Millon	Lipid
+	0	0	+	+	0	0	0	0
++	0	0	+	++	+	+	0	0
0	0	0	+	+	0	0	0	0
0	0	0	+++	+++	++	++	0	0
0	0	0	+	+	0	0	0	0
0	0	0	+	+	+	+	0	0
0	0	0	+	+	+	+	0	0
++	+	+	+	0	+	+	+/-	0
++	+	+	+	0	+	+	+/-	0
+++	++	++	+	0	0	0	0	0
0	0	0	+++	++	+	+	++	+
0	0	0	+	+	0	0	+	+
0	0	0	+	+	+/-	0	+	++
0	0	0	+/-	+	0	0	0	++
0	0	0	++	++	+	+	0	0
0	0	0	+	+	+/-	0	0	0
0	0	0	+++	+++	++	++	0	0
0	0	0	+	++	++	++	0	0
0	0	0	++	++	++	++	0	0
0	0	0	+	+	0	0	+++	0
+/-	0	0	+	+	+	+	+/-	0

determined in two ways. Best's carmine, a selective stain for glycogen, clearly demonstrated that high concentrations of this substance occur in vitelline cells, vitelline reservoir, and within egg capsules. A negative P.A.S. reaction following alpha-amylase and malt diastase digestion of glycogen showed glycogen to be lacking in these areas but still present in the tegument and alimentary tract, thus suggesting that another carbohydrate group still remains. Acid mucopolysaccharides can be localized with alcian blue stains at various pH levels. All acid mucopolysaccharides are stained at a pH of 6.5, whereas weakly acid sulfated mucosubstances are demonstrated at a pH of 2.5 and only sulfated mucosubstances are seen at a pH of 1.0 with this stain. In Fibricola, the tegument, subtegumental cells, gut epithelium, and caecal contents were positive for acid mucopolysaccharides (Table 1). At lower pH levels (2.5 and 1.0), staining was absent in the tegument and reduced in the gut epithelium. Öhman (1966a) reported similar concentrations of acid mucopolysaccharides in the gut epithelium, caecal contents and tegument of Diplostomum spathaceum.

Proteins

Proteins have been shown to make up a large percentage of body weight in parasites and are actively synthesized by them (see review, von Brand, 1966). Histochemical

determination of proteins is difficult for only infrequently do simple proteins (albumins, globulins, histones) occur within tissues without the presence of conjugated proteins (lipoproteins, mucoproteins, glycoproteins, and nucleoproteins). General protein stains including mercuric bromphenol blue (HgBPBl) and napthol Y were utilized in determination of protein concentrations within tissues. In Fibricola, general protein staining occurs throughout all regions of the body, and high protein concentrations are seen in the reproductive organs (testes, seminal vesicle, ovary, vitellaria), the tegument, and the holdfast organ. Each of these areas are sites of high protein synthesis. The holdfast organ of Fibricola stains intensely for protein, indicating its high synthetic capabilities, involving various enzymes. Lee (1962), Erasmus and Öhman (1963), Öhman (1965, 1966a, b) have all shown high levels of esterase activity in holdfast gland cells of all strigeoid species studied. Öhman (1965) additionally has shown that esterase substances released from holdfast tegumental surfaces are capable of degrading gelatin, thus suggesting a proteolytic activity. It is interesting to note that the holdfast (HF, Fig. 42) of F. cratera also stained intensely with an acetylcholinesterase staining technique, thus indicating high levels of nonspecific esterase within this

organ, again suggestive of a secretory proteolytic function.

The Millon reaction, a specific protein test for tyrosine, indicated this substance to be present within developing vitelline cells, vitelline ducts and the vitelline reservoir, as well as constituting a major component of the tanned egg shell present in this trematode.

Nucleic Acids

Concentrations of both DNA and RNA can be determined by a variety of histochemical and biochemical methods. Using the Feulgen reaction which is specific for DNA and the pyronin Y-methyl green staining technique for both DNA and RNA, high concentrations of these substances within F. cratera were localized. The reproductive organs (including testes, seminal vesicle, and ovary) as well as the tightly packed holdfast gland cells contain high nucleic acid levels. These structures have in common high nuclear concentrations and cell cytoplasm of high protein synthetic capabilities, thus indicating extensive nucleic acid transcriptive activity.

Lipids

Although lipids of F. cratera were only briefly examined by means of general broad spectrum lipid stains

(osmium tetroxide and Sudan IV), various neutral lipids and phospholipids were observed within excretory ducts and vitelline cells, respectively. As mentioned previously, the occurrence of lipid droplets within trematodes has been reported by many workers. It has been suggested by von Brand (1966) that lipids may 1) either serve as energy sources or storage reserves (e.g., vitelline material) or 2) may represent waste products of metabolism.

In general, the above histochemical findings compare favorably with similar studies on other strigeoid trematodes. With regard to the holdfast (tribocytic) organ, high esterase activity and acid phosphatase have been repeatedly demonstrated at the light microscope level in all species thus far studied. Additionally, Erasmus (1968, 1970) has shown ultrastructurally that acid phosphatase is localized on the holdfast tegument, in holdfast gland ducts, and within cisternae of endoplasmic reticulum of holdfast gland cells. Although its definite function remains unknown, structural and histochemical evidence point to a complex secretory and/or absorptive role for the strigeoid holdfast organ.

SUMMARY AND CONCLUSIONS

1. Ultrastructural and histochemical studies on adult Fibricola cratera (Trematoda: Diplostomatidae) were conducted. The tegument, holdfast (tribocytic) organ, nervous system (including sensory receptors), alimentary tract, male and female reproductive systems, and the excretory systems of this species were investigated.
2. The tegument of F. cratera, a syncytial layer characterized by mitochondria, vesicles, and spines, is connected by means of protoplasmic channels to underlying subtegumental cell bodies. Considerable variation in structure of the tegument as to its thickness, presence of spines, surface contour, is apparent in various body regions.
3. Tegumental spines possessing a lattice infrastructure are more numerous on the ventral surface of the forebody, especially near the holdfast organ. Spines appear either as blunt, blade-like structures (e.g., on the ventral forebody surface) or as pointed tegumental projections (e.g., on the holdfast cleft). The entire hindbody tegument is aspinose.
4. The ventrally situated acetabular holdfast of F. cratera is characterized by a highly folded tegumental surface, gland ducts, and numerous

peripherally arranged secretory gland cells. Membrane-bound "microvillar" processes project from holdfast tegumental folds and fill the central chamber of the holdfast. High mitochondrial concentrations and numerous lamellate ducts of the reserve excretory system near the holdfast tegument suggest a partial absorptive role for the holdfast and a circulatory role for the reserve excretory system. Holdfast gland cells possess an extensive endoplasmic reticulum characteristic of secretory cells. Similar densely staining vesicles were observed within gland cells, holdfast gland ducts and in tegumental folds of the holdfast surface.

5. The nervous system of F. cratera consists of a ladder-like network formed by major nerve cords and transverse nerve commissures. Two large "unipolar cells" observed near the cerebral ganglia are considered to be modified sensory receptors.
6. Ultrastructurally, cerebral ganglia and nerves and F. cratera possess synaptic vesicles, synaptic junctions, mitochondria, dense vesicles, and microtubules. Tegumental nerves lie between the fibrous layer of the tegument and the underlying circular muscle bands.
7. Sensory structures of F. cratera were studied by means

of transmission and scanning electron microscopy. Tegumental sensory receptors are of at least four distinct types. Ciliated and nonciliated sensory bulbs are more numerous around the oral sucker, acetabulum, and genital aperture but are also located over the entire forebody surface.

8. The oral sucker, esophagus, and pharynx of the alimentary tract are lined with a modified tegument. Intestinal crura are comprised of flattened gastrodermal cells characterized by numerous microvilli projecting into the gut lumen. Cytoplasm of such cells is filled with extensive endoplasmic reticulum, ribosomes, and dense vesicles, thus indicating both secretory and absorptive capabilities.
9. Ultrastructural studies on the male reproductive system of F. cratera were conducted with emphasis on spermiogenesis and mature sperm structure. F. cratera male germ cells undergo a developmental mitotic and meiotic sequence common to other trematodes.
10. Mature thread-like spermatozoa consist of a head with an elongated nucleus, and a tail portion internally composed of mitochondria, cytoplasmic microtubules and two unique 9+1 axial filaments. Such axial filaments possess nine peripheral microtubule doublets, radiating spokes, and a central column with

a superficial cortical sheath and a dense inner axial rod.

11. Spermiogenesis involves the migration of the elongated spermatid nucleus to the distal end of a tubular, cytoplasmically-derived mid-piece and subsequent lateral fusion of two axial filaments with this structure.

12. Ultrastructural studies of vitelline follicles indicate that vitelline cells undergo progressive granulation and become filled with vitelline globules of varying size. Partial release of vitelline materials from cells occurs prior to their movement into the hindbody. Typical 9+2 cilia were observed along vitelline duct walls.

13. Both primary (protonephridial) and secondary (reserve) excretory systems of this species were examined. Flame cells possess numerous 9+2 cilia which internally possess microtubules arranged in one plane, thus providing evidence for the "back and forth" beating of flame cells. Both primary excretory capillaries and ducts as well as reserve excretory ducts are lined with membrane-bound lamellae projecting into the lumen. Various lipid droplets and whorled-membrane concretions were observed within excretory ducts.

14. Histochemical tests on F. cratera adults included those used for the following chemical groups: carbohydrates, proteins, nucleic acids, and lipids. Carbohydrates are distributed throughout the body, being concentrated in the tegument, alimentary tract, vitelline follicles and the vitelline reservoir. Glycogen is highly concentrated within vitelline materials, but also occurs throughout the parenchyma, muscle cells and spermatozoan tails. Acid mucopolysaccharides were principally localized in gastrodermal cells and caecal contents. Proteins and nucleic acids occur in all body tissues, but are highly concentrated in the holdfast organ and reproductive organs (testes, seminal vesicle, ovary). High nonspecific esterase levels within the holdfast organ were noted. Tyrosine was detected within vitelline cells, the vitelline reservoir, and intrauterine egg shells. Neutral lipid and phospholipids were localized within excretory ducts and vitelline follicles, respectively.

LITERATURE CITED

Afzelius, B. 1959. Electron microscopy of the sperm tail. Results obtained with a new fixative. J. Biophys. Biochem. Cytol. 5: 269-278.

Anderson, W. A., and R. A. Ellis. 1965. Ultrastructure of Trypanosoma lewisi: flagellum, microtubules and the kinetoplast. J. Protozool. 12: 483-499.

Babero, B. B., and J. R. Shepperson. 1958. Some helminths of raccoons in Georgia. J. Parasitol. 44: 519.

Baer, J. G. 1951. Ecology of animal parasites. University of Illinois Press, Urbana, Ill. 224 p.

Bancroft, J. D. 1967. An introduction to histochemical technique. Butterworth and Co., Ltd., London. 268 p.

Barker, F. D. 1915. Parasites of the American muskrat (Fiber zibethicus). J. Parasitol. 1: 184-197.

Bettendorf, H. 1897. Ueber Musculatur und Sinneszellen der Trematoden. Zool. Jahrb. Abt. Anat. 10: 307-358.

Bils, R. F., and W. E. Martin. 1966. Fine structure and development of the trematode tegument. Trans. Amer. Micro. Soc. 85: 78-88.

Björkman, N., and W. Thorsell. 1963. On the fine morphology of the formation of egg-shell globules in the vitelline glands of the liver fluke (Fasciola hepatica L.). Exp. Cell Res. 32: 153-156.

Björkman, N., and W. Thorsell. 1964. On the fine structure and resorptive function of the cuticle of the liver fluke Fasciola hepatica. Exp. Cell Res. 33: 312-329.

Bogitsh, B. J. 1968. Cytochemical and ultrastructural observations on the tegument of the trematode Megalodiscus temperatus. Trans. Amer. Micr. Soc. 87: 477-486.

Bogitsh, B. J. 1970. Observations on the cytochemistry of the Mehlis gland cells of Haematoloechus medioplexus. J. Parasitol. 56: 1084-1094.

Bogitsh, B. J., and F. P. Aldridge. 1967. Histochemical observations on Posthodiplostomum minimum. IV. Electron microscopy of tegument and associated structures. Exp. Parasitol. 21: 1-8.

Bogitsh, B. J., D. A. Davis, and D. A. Nunnally. 1968. Cytochemical and biochemical observations on the digestive tracts of digenetic trematodes. II. Ultrastructural localization of acid phosphatase in Haematoloechus medioplexus. Exp. Parasitol. 23: 303-308.

Bogitsh, B. J., and W. A. Shannon. 1971. Cytochemical and biochemical observations on the digestive tracts of digenetic trematodes. VIII. Acid phosphatase activity in Schistosoma mansoni and Schistosomatium douthitti. Exp. Parasitol. 29: 337-347.

Bueding, E. 1952. Acetylcholinesterase activity of Schistosoma mansoni. Brit. J. Pharmacol. 7: 563-566.

Bueding, E., E. L. Schiller, and J. G. Bourgeois. 1967. Some physiological biochemical and morphologic effects of Tris (p-aminophenyl) carbonium salts (TAC) on Schistosoma mansoni. Amer. J. Trop. Med. Hyg. 16: 500-515.

Bullock, T. H., and G. A. Horridge. 1965. Structure and function in the nervous systems of invertebrates. Vol. 1. W. H. Freeman and Co., San Francisco. 798 p.

Burton, P. R. 1960. Gametogenesis and fertilization in the frog lung fluke, Haematoloechus medioplexus Stafford (Trematoda: Plagiorchiidae). J. Morph. 107: 93-122.

Burton, P. R. 1964. The ultrastructure of the integument of the frog lung-fluke, Haematoloechus medioplexus (Trematoda: Plagiorchiidae). J. Morph. 115: 305-317.

Burton, P. R. 1966. The ultrastructure of the integument of the frog bladder fluke, Gorgoderina sp. J. Parasitol. 52: 926-934.

Burton, P. R. 1967a. Fine structure of the reproductive system of a frog lung fluke. I. Mehlis gland and associated ducts. J. Parasitol. 53: 540-555.

Burton, P. R. 1967b. Fine structure of the unique central region of the axial unit of lung-fluke spermatozoa. J. Ultr. Res. 19: 166-172.

Byrd, E. E., J. Reiber, and M. V. Parker. 1942. Mammalian trematodes. I. Trematodes from the opossum, Didelphis virginiana Kerr. J. Tenn. Acad. Sci. 17: 130-142.

Chance, M. R. A., and T. E. Mansour. 1953. A contribution to the pharmacology of movement in the liver fluke. Brit. J. Pharmacol. 8: 134-138.

Chandler, A. C. 1942. The morphology and life cycle of a new strigeid, Fibricola texensis, parasitic in raccoons. Trans. Amer. Micr. Soc. 61: 156-167.

Chandler, A. C., and R. Rausch. 1946. A study of strigeids from Michigan mammals with comments on the classification of mammalian strigeids. Trans. Amer. Micr. Soc. 65: 328-337.

Chandler, A. S., and C. P. Read. 1965. Introduction to parasitology with special reference to the parasites of man. 10th ed. John Wiley and Sons, Inc., New York. 822 p.

Chapman, H. D., and R. A. Wilson. 1970. The distribution and fine structure of the integumentary papillae of the cercaria of Himasthla secunda (Nicoll). Parasitology 61: 219-227.

Cuckler, A. C. 1940. The life cycle of Fibricola cratera (Barker and Noll, 1915) Dubois, 1932 (Trematoda: Strigeata). J. Parasitol. 26: 32-33 (Suppl.).

Cuckler, A. C. 1949. Morphological and biological studies on certain strigeid trematodes of mammals. Summaries Ph.D. Theses, Univ. Minnesota 4: 45-47.

Davis, D. A., B. J. Bogitsh, and D. A. Nunnally. 1968. Cytochemical and biochemical observations of the digestive tracts of digenetic trematodes. I. Ultrastructure of Haematoloechus medioplexus. Exp. Parasitol. 22: 96-106.

Davis, D. A., B. J. Bogitsh, and D. A. Nunnally. 1969. Cytochemical and biochemical observations on the digestive tracts of digenetic trematodes. III.

Non-specific esterase in Haematoloechus medioplexus. Exp. Parasitol. 24: 121-129.

Davis, D. A., and B. J. Bogitsh. 1971a. Arylsulfatase activity in Gorgoderina attenuata and Haematoloechus medioplexus: Cytochemical and biochemical observations on the digestive tracts of digenetic trematodes. Exp. Parasitol. 29: 302-308.

Davis, D. A., and B. J. Bogitsh. 1971b. Gorgoderina attenuata: Cytochemical and biochemical observations on the digestive tracts of digenetic trematodes. Exp. Parasitol. 29: 320-329.

Dawes, B. 1940. Notes on the formation of the egg capsules in the monogenetic trematode Hexacotyle extensicauda Dawes, 1940. Parasitology 32: 287-295.

Dawes, B. 1962. A histological study of the caecal epithelium of Fasciola hepatica L. Parasitology 52: 483-493.

DeGiusti, D. L. 1957. Parasites of rats collected in the city of Detroit. Amer. J. Trop. Med. Hyg. 6: 375.

Dhingra, O. P. 1954a. Gametogenesis and fertilization in Isoparorchis eurytremum. Res. Bull. Panjab Univ. 44: 21-47.

Dhingra, O. P. 1954b. Spermatogenesis of a digenetic trematode, Cyclocoelum bivesiculatum. Res. Bull. Panjab Univ. 61: 159-168.

Dhingra, O. P. 1955a. Spermatogenesis of a digenetic trematode, Cotylophoron elongatum. Res. Bull. Panjab Univ. 64: 1-10.

Dhingra, O. P. 1955b. Spermatogenesis of a digenetic trematode Gastrothylax crumenifer. Res. Bull. Panjab Univ. 65: 11-17.

Dike, S. C. 1967. Ultrastructure of the ceca of the digenetic trematodes Gorgoderina amplicava and Haematoloechus medioplexus. J. Parasitol. 53: 1173-1185.

Dike, S. C. 1969. Acid phosphatase activity and ferritin incorporation in the ceca of digenetic trematodes. J. Parasitol. 55: 111-123.

Dike, S. C. 1971. Ultrastructure of the esophageal region in Schistosoma mansoni. Amer. J. Trop. Med. Hyg. 20: 552-568.

Dixon, K. E., and E. H. Mercer. 1965. The fine structure of the nervous system of the cercaria of the liver fluke, Fasciola hepatica L. J. Parasitol. 51: 967-976.

Dogiel, V. A. 1964. General parasitology. Academic Press, New York. 516 p.

Dönges, J. 1964. Der Lebenszyklus von Posthodiplostomum cuticola (v. Nordmann 1832) Dubois 1936 (Trematoda: Diplostomatidae). Z. Parasitenk. 24: 169-248.

Dubois, G. 1932. Révision des 'Hemistomes' et étude de formes nouvelles. Bull. Soc. Neuchât. Sci. Nat. 56: 375-412.

Dubois, G. 1953. Systématique des Strigeida. Complément de la Monographie. Mém. Soc. Neuchâtel Sci. Nat. 8: 1-141.

Dubois, G. 1963. Statut des Alariinae Hall et Wigdor 1918 (Trematoda: Diplostomatidae) et revision de quelques alariens. Bull. Soc. Neuchâtel Sci. Nat. 86: 107-142.

Ebrahimzadeh, H., and M. Kraft. 1971. Ultrastruckturelle Untersuchungen zur Anatomie der Cercarien von Schistosoma mansoni II. Das Exkretionsystem. Z. Parasitenk. 36: 265-290.

Erasmus, D. A. 1967a. Ultrastructural observations on the reserve bladder system of Cyathocotyle bushiensis Khan, 1962 (Trematoda: Strigeoidea) with special reference to lipid excretion. J. Parasitol. 53: 525-536.

Erasmus, D. A. 1967b. The host-parasite interface of Cyathocotyle bushiensis Khan, 1962 (Trematoda: Strigeoidea). II. Electron microscope studies of the tegument. J. Parasitol. 53: 703-714.

Erasmus, D. A. 1968. The host-parasite interface of Cyathocotyle bushiensis Khan, 1962 (Trematoda: Strigeoidea). III. Electron microscope observations on nonspecific phosphatase activity. Parasitology 58: 371-375.

Erasmus, D. A. 1969. Studies on the host-parasite interface of strigeoid trematodes. V. Regional differentiation of the adhesive organ of Apatemon gracilis minor Yamaguti, 1933. Parasitology 59: 245-256.

Erasmus, D. A. 1970. The host-parasite interface of strigeoid trematodes. VII. Ultrastructural observations on the adhesive organ of Diplostomum phoxini Faust, 1918. Z. Parasitenk. 33: 211-224.

Erasmus, D. A., and C. Öhman. 1963. The structure and function of the adhesive organ in strigeid trematodes. Ann. N.Y. Acad. Sci. 113: 7-35.

Erasmus, D. A., and C. Öhman. 1965. Electron microscope studies of the gland cells and host-parasite interface of the adhesive organ of Cyathocotyle bushiensis Khan, 1962. J. Parasitol. 51: 761-769.

Ercoli, N., A. E. Sorell, A. Omedas, and V. de Gimenez. 1963. Ultrastructure of Schistosoma mansoni. Trans. Roy. Soc. Trop. Med. Hyg. 57: 239.

Faust, E. C. 1918. Eye-spots in digenea. Biol. Bull. 35: 117-127.

Gallagher, S. S. E., and L. T. Threadgold. 1967. Electron-microscope studies of Fasciola hepatica. II. The interrelationship of the parenchyma with other organ systems. Parasitology 57: 627-632.

Gomori, G. 1952. Microscopic histochemistry, principles and practice. University of Chicago Press, Chicago. 273 p.

Gorirossi, F., and D. L. DeGiusti. 1950. A modified gold chloride impregnation method for trematode nerve tissue. Trans. Amer. Micr. Soc. 69: 183-185.

Gresson, R. A. R. 1965. Spermatogenesis in the hermaphroditic Digenea (Trematoda). Parasitology 55: 117-125.

Gresson, R. A. R., and M. M. Perry. 1961. Electron microscope studies of spermateleosis in Fasciola hepatica. Exp. Cell Res. 22: 1-8.

Gresson, R. A. R., and L. T. Threadgold. 1959. A light and electron microscope study of the epithelial cells of the gut of Fasciola hepatica L. J. Biophys. Biochem. Cytol. 6: 157-162.

Guilford, J. H. 1954. A survey of muskrat helminths in Illinois. J. Parasitol. 40: 702-703.

Guilford, A. G. 1961. Gametogenesis, egg-capsule formation, and early miracidial development in the digenetic trematode, Halipegus eccentricus. J. Parasitol. 47: 757-764.

Halton, D. W. 1966. Occurrence of microvilli-like structures in the gut of digenetic trematodes. Experientia 22: 828-829.

Halton, D. W. 1967. Studies on phophatase activity in trematoda. J. Parasitol. 53: 46-54.

Halton, D. W., and G. P. Morris. 1969. Occurrence of cholinesterase and ciliated sensory structures in a fish gill-fluke, Diclidophora merlangi (Trematoda: Monogenea). Z. Parasitenk. 33: 21-30.

Hendelberg, J. 1962. Paired flagella and nucleus migration in the spermiogenesis of Dicrocoelium and Fasciola (Digenea, Trematoda). Zool. Bidr. Uppsala 35: 569-587.

Hendelberg, J. 1965. On different types of spermatozoa in Polycladida, Turbellaria. Ark. Zool. Uppsala 18: 267-304.

Hoffman, G. L. 1955. Notes on the life cycle of Fibricola cratera (Trematoda: Strigeida). J. Parasitol. 41: 327.

Howells, R. E. 1969. Observations on the nephridial system of the cestode Moniezia expansa. Parasitology 59: 449-459.

Hughes, R. C. 1927. Studies on the trematode family Strigeidae (Holostomatidae). No. VI. A new metacercaria, Neascus ambloplitis sp. nov., representing a new larval group. Trans. Amer. Micr. Soc. 47: 248-267.

Huxley, H. E. 1965. The mechanism of muscle contraction. Sci. Amer. 206: 18-27.

Hyman, L. H. 1951. The invertebrates. Vol. II. Platyhelminths and Rhynchocoela. McGraw-Hill Book Co., New York. 550 p.

Inatomi, S., Y. Tongu, D. Sakumoto, K. Itano, and S. Suguri. 1968. The ultrastructure of helminths. I. The body wall of Clonorchis sinensis (Cobbold, 1875) Loos, 1907. Jap. J. Parasitol. 17: 395-401.

Isseroff, H. 1964. Fine structure of the eyespots in the miracidum of Philophthalmus megalurus (Cort, 1914). J. Parasitol. 50: 549-554.

Jennings, J. B. 1968. Digestion in flatworms, p. 303-326. In M. Florkin and B. Scheer, (Ed.) Chemical zoology. Vol 2. Academic Press, Inc., New York.

Koelle, G. B., and J. S. Friedenwald. 1949. A histochemical method for localizing cholinesterase activity. Proc. Soc. Exp. Biol. Med. 70: 617-622.

Kruidenier, F. J. 1959. Ultrastructure of the excretory system of cercariae. J. Parasitol. 45: 59. (Abstr.)

Kümmel, V. G. 1958. Das Terminalorgan der Protonephridien, Feinstruktur und Deutung der Funktion. Z. Naturforsch. 13b: 677-679.

Kümmel, V. G. 1960. Die Feinstruktur des Pigmentbecherocells bei Miracidien von Fasciola hepatica L. Zool. Beitr. 5: 345-354.

LaRue, G. R. 1932. Morphology of Cotylurus communis Hughes (Trematoda: Strigeidae). Trans. Amer. Micr. Soc. 51: 28-47.

Lautenschlager, E. W., and R. R. Cardell. 1961. Ultrastructure of the cuticular region and flame-cell system of the metacercaria, Diplostomulum trituri. J. Parasitol. 47: 46. (Abstr.)

Law, R. G., and A. H. Kennedy. 1932. Parasites of fur-bearing animals. Bull. Dept. Game and Fisheries Ont. 4: 1-30.

Lee, D. L. 1962. Studies on the function of the pseudosuckers and holdfast organ of Diplostomum phoxini Faust (Strigeida, Trematoda). Parasitology 52: 103-112.

Lee, D. L. 1966. The structure and composition of helminth cuticle. p. 187-254. In B. Dawes (ed.) Advances in parasitology. Vol IV. Academic Press, Inc., New York.

Leigh, W. H. 1954. Notes on the life history of Fibricola texensis Chandler, 1942, in Florida. J. Parasitol. 40: 45. (Abstr.)

Lillie, R. D. 1965. Histopathologic technic and practical histochemistry. 3rd ed. McGraw-Hill Book Co., New York. 715 p.

Lumsden, R. D. 1961. The white ibis, Eudocimus albus (Linn.) host for the diplostomatid trematode Fibricola cratera (Barker and Noll, 1915) Dubois, 1932, in Louisiana. J. Parasitol. 47: 897.

Lumsden, R. D. 1965. Macromolecular structure of glycogen in some cyclophyllidean and trypanorhynch cestodes. J. Parasitol. 51: 501-515.

Lumsden, R. D. 1970. Preparatory technique for electron microscopy, p. 215-228. In MacInnis, A. J. and M. Voge (eds.) Experiments and techniques in parasitology. W. H. Freeman and Co., San Francisco.

Lumsden, R. D., and J. A. Zischke. 1961. Seven trematodes from small mammals in Louisiana. Tulane Studies Zool. 9: 87-98.

Luna, L. G. 1968. Manual of histologic staining methods of the Armed Forces Institute of Pathology. 3rd ed. McGraw-Hill Book Co., New York. 258 p.

Lyons, K. M. 1969a. Sense organs of monogenean skin parasites ending in a typical cilium. Parasitology 59: 611-623.

Lyons, K. M. 1969b. Compound sensilla in monogenean skin parasites. Parasitology 59: 625-636.

Martin, W. E., and R. F. Bils. 1964. Trematode excretory concretions: formation and fine structure. J. Parasitol. 50: 337-344.

Marszalek, D. S., and E. B. Small. 1969. Preparation of soft biological materials for scanning electron microscopy. Proc. Ann. Scan. Electron Microscop. Symp. 2: 231-239.

Miller, M. J. 1940. A new trematode, Fibricola laruei, from the raccoon in Canada. Can. J. Res. 18: 135-140.

Millonig, G. 1961. Advantages of a phosphate buffer for osmium tetroxide solutions in fixations. J. Appl. Phys. 32: 1627.

Mollenhauer, H. H. 1964. Plastic embedding mixtures for use in electron microscopy. Stain Tech. 39: 111-114.

Morgan, B. B., and E. F. Waller. 1940. Severe parasitism in a raccoon (Procyon lotor lotor Linnaeus) Trans. Amer. Micr. Soc. 59: 523-527.

Morris, G. P. 1968. Fine structure of the gut epithelium of Schistosoma mansoni. Experientia 24: 480-482.

Morris, G. P. 1971. The fine structure of the tegument and associated structures of the cercaria of Schistosoma mansoni. Z. Parasitenk. 36: 15-31.

Morris, G. P., and L. T. Threadgold. 1967. A presumed sensory structure associated with the tegument of Schistosoma mansoni. J. Parasitol. 53: 537-539.

Morris, G. P., and L. T. Threadgold. 1968. Ultrastructure of the tegument of the adult Schistosoma mansoni. J. Parasitol. 54: 15-27.

Morseth, D. J. 1967. Observations on the fine structure of the nervous system of Echinococcus granulosus. J. Parasitol. 53: 492-500.

Muller, W. 1923. Die Nahrung von Fasciola hepatica und ihre Verdauung. Zool. Anz. 57: 273-281.

Nieland, M. L., and E. C. Weinbach. 1968. The bladder of Cysticercus fasciolaris: electron microscopy and carbohydrate content. Parasitology 58: 489-496.

Nez, M. M., and R. B. Short. 1957. Gametogenesis in Schistosomatium douthitti (Cort) (Schistosomatidae: Trematoda). J. Parasitol. 43: 167-177.

Odlaug, T. O. 1948. The finer structure of the body wall and parenchyma of three species of digenetic trematodes. Trans. Amer. Micr. Soc. 67: 236-253.

Öhman, C. 1965. The structure and function of the adhesive organ in strigeid trematodes. II. Diplostomum spathaceum Braun, 1893. Parasitology 55: 481-502.

Öhman, C. 1966a. The structure and function of the adhesive organ in strigeid trematodes. Part III. Apatemon gracilis minor Yamaguti, 1933. Parasitology 56: 209-226.

Öhman, C. 1966b. The structure and function of the adhesive organ in strigeid trematodes. IV. Holostephanus lühei Szidat, 1936. Parasitology 56: 481-491.

Osborn, H. L. 1903. On the habits and structure of Cotylaspis insignis Leidy. Zool. Jahrb. Abt. Anat. 21: 201-242.

Pantelouris, E. M., and L. T. Threadgold. 1963. The excretory system of the adult Fasciola hepatica L. Cellule 64: 63-67.

Parducz, B. 1967. Ciliary movement and coordination in ciliates. Int. Rev. Cytol. 21: 91-127.

Pearse, A. G. E. 1968. Histochemistry theoretical and applied. 3rd ed. Vol I. Little Brown and Co., Boston. 759 p.

Pearson, J. C. 1959. Neodiplostomum intermedium n. sp. from the allied rat, Rattus assimilis, with remarks on the genera Neodiplostomum and Fibricola (Trematoda: Diplostomatidae). Parasitology 49: 111-120.

Pearson, J. C. 1961. Observations on the morphology and life cycle of Neodiplostomum intermedium (Trematoda: Diplostomatidae). Parasitology 51: 133-172.

Pond, G. G., and R. M. Cable. 1966. Fine structure of photoreceptors in three types of ocellate cercariae. J. Parasitol. 52: 483-493.

Rausch, R., and J. Tiner. 1948. Studies on the parasitic helminths of the North Central States. I. Helminths of Sciuridae. Amer. Midl. Natur. 39: 728-747.

Read, C. P. 1948. Strigeids from Texas mink with notes on the genus Fibricola Dubois. Trans. Amer. Micr. Soc. 67: 165-168.

Read, C. P. 1966. Nutrition of intestinal helminths, p. 101-126. In E. Soulsby (Ed.) Biology of parasites. Academic Press, Inc., New York

Rees, G. 1968. Macrolecithus papilliger sp. nov. (Digenea: Allocreadiidae, Stossich, 1904) from Phoxinus phoxinus L. Morphology, histochemistry and egg capsule formation. Parasitology 58: 855-878.

Reissig, M. 1970. Characterization of cell types in the parenchyma of Schistosoma mansoni. Parasitology 60: 273-279.

Reynolds, E. S. 1963. The use of lead citrate at high pH as an electron opaque stain in electron microscopy. J. Cell Biol. 17: 208-212.

Reznik, G. K. 1966. New interpretation of the structure of the integument in the trematode Dicrocoelium lanceatum. Akad. Nauk S.S.S.R. Dokl. 171: 839-840.

Robson, R. T., and D. A. Erasmus. 1970. The ultrastructure, based on stereoscan observations, of the oral sucker of the cercaria of Schistosoma mansoni with special reference to penetration. Z. Parasitenk. 35: 76-86.

Rogers, W. P. 1962. The nature of parasitism. Academic Press, Inc., New York. 287 p.

Rohde, K. 1968. Lichtmikroskopische Untersuchungen an den Sinnesrezeptoren der Trematoden. Z. Parasitenk. 30: 252-277.

Rosario, B. 1964. An electron microscope study of spermatogenesis in cestodes. J. Ultr. Res. 11: 412-427.

Sato, M., M. Oh, and K. Sakoda. 1967. Electron microscopic study of spermatogenesis in the lung fluke (Paragonimus miyazakii). Z. Zellforsch. 77: 232-243.

Sawyer, T. K. 1958. Metagonimoides oregonensis Price, 1931 from a Georgia raccoon with a note on Sellacotyle mustelae Wallace, 1935. J. Parasitol. 44: 63.

Schiller, E. L., and B. B. Morgan. 1949. The incidence of parasites of Rattus norvegicus in Wisconsin. J. Parasitol. 35: 40 (Suppl.).

Senft, A. W., D. E. Philpott, and A. H. Pelofsky. 1961. Electron microscope observations of the integument, flame cells and gut of Schistosoma mansoni. J. Parasitol. 47: 217-229.

Shannon, W. A., Jr., and B. J. Bogitsh. 1969. Cytochemical and biochemical observations on the digestive tracts of digenetic trematodes. V. Ultrastructure of Schistosomatium douthitti gut. Exp. Parasitol. 26: 344-353.

Shapiro, J. E., B. R. Hershenov, and G. S. Tulloch. 1961. The fine structure of Haematoloechus spermatozoan tail. J. Biophys. Biochem. Cytol. 9: 211-217.

Silk, M. H., I. M. Spence, and J. H. S. Gear. 1969. Ultrastructural studies of the blood fluke-Schistosoma mansoni. I. The integument. S. Afr. J. Med. Sci. 34: 1-10.

Silveira, M. 1969. Ultrastructural studies on a "nine-plus-one" flagellum. J. Ultr. Res. 26: 274-288.

Smith, J. H., E. S. Reynolds, and F. von Lichtenburg. 1969. The integument of Schistosoma mansoni. Amer. J. Trop. Med. Hyg. 18: 28-49.

Smyth, J. D. 1962. Introduction to animal parasitology. C. C. Thomas Co., Springfield, Illinois. 470 p.

Smyth, J. D., and J. A. Clegg. 1959. Egg-shell formation in trematodes and cestodes. Exp. Parasitol. 8: 286-323.

Sommer, F. 1880. Zur Anatomie des Leberegels Distomum hepaticum L. Z. wiss. Zool. 34: 539-640.

Stempak, J. G., and R. T. Ward. 1964. An improved staining method for electron microscopy. J. Cell Biol. 22: 697-701.

Stephenson, W. 1947a. Physiological and histochemical observations on the adult liver fluke. Fasciola hepatica. II. Feeding. Parasitology 38: 123-127.

Stephenson, W. 1947b. Physiological and histochemical observations on the adult liver fluke, Fasciola hepatica L. III. Egg-shell formation. Parasitology 38: 128-139.

Stephenson, W. 1947c. Physiological and histochemical observations on the adult liver fluke. Fasciola hepatica. L. IV. The excretory system. Parasitology 38: 140-144.

Stunkard, H. W. 1967. Platyhelminth parasites of invertebrates. J. Parasitol. 53: 673-682.

Thorsell, W., and N. Björkman. 1965. Morphological and biochemical studies on absorption and secretion in the alimentary tract of Fasciola hepatica. J. Parasitol. 51: 217-223.

Threadgold, L. T. 1963a. The ultrastructure of the 'cuticle' of Fasciola hepatica. Exp. Cell Res. 30: 238-242.

Threadgold, L. T. 1963b. The integument and associated structures of Fasciola hepatica. Quart. J. Micr. Sci. 104: 505-512.

Threadgold, L. T. 1967. Electron microscope studies of Fasciola hepatica. III. Further observations on the tegument and associated structures. Parasitology 57: 633-637.

Threadgold, L. T. 1968a. The tegument and associated structures of Haplometra cylindracea. Parasitology 58: 1-7.

Threadgold, L. T. 1968b. Electron microscope studies of Fasciola hepatica. VI. The ultrastructural localization of phosphatases. Exp. Parasitol. 23: 264-276.

Threadgold, L. T., and S. W. B. Irwin. 1970. Electron microscope studies of Fasciola hepatica. IX. The fine structure of Mehlis gland. Z. Parasitenk. 35: 16-30.

Tulloch, G. S., and J. Shapiro. 1957. The ultrastructure of the vitelline cells of Haematoloechus. J. Parasitol. 43: 628-632.

Turner, H. F. 1957. Preliminary notes on the life cycle of Fibricola cratera (Barker and Noll, 1915) Dubois, 1932 (Trematoda: Diplostomatidae). J. Ala. Acad. Sci. 29: 43-44.

Turner, H. F. 1958. The life history of Fibricola cratera (Barker and Noll, 1915) Dubois, 1932 (Trematoda: Diplostomatidae) Diss. Abst. 19: 609.

Ulmer, M. J. 1954. Experimental definitive hosts for Fibricola cratera (Barker and Noll, 1915) Dubois,

1932 (Trematoda: Diplostomatidae). J. Parasitol. 40: 33. (Abstr.)

Ulmer, M. J. 1955. Notes on the morphology and host-parasite specificity of Fibricola cratera (Barker and Noll, 1915) Dubois, 1932 (Trematoda: Diplostomatidae). J. Parasitol. 41: 460-466.

Ulmer, M. J. 1971. Site-finding behaviour in helminths in intermediate and definitive hosts, p. 123-160. In A. M. Fallis (ed.) Ecology and physiology of parasites: A symposium. University of Toronto Press, Toronto, Canada.

Van Haitsma, J. P. 1931. Studies on the trematode family Strigeidae (Holostomidae) No. XXII: Cotylurus flabelliformis (Faust) and its life history. Pap. Mich. Acad. Sci. 13: 447-480.

von Bonsdorff, C-H. and A. Telkka. 1965. The spermatozoon flagella in Diphyllobothrium latum (fish tapeworm). Z. Zellforsch. 66: 643-648.

von Brand, T. 1966. Biochemistry of parasites. Academic Press, Inc., New York. 429 p.

von Brand, T., T. I. Mercado, M. U. Nylen, and D. B. Scott. 1960. Function, composition, and structure of cestode calcareous corpuscles. Exp. Parasitol. 9: 205-214.

Warner, F. D. 1969. The fine structure of the protonephridia in the rotifer Asplanchna. J. Ultr. Res. 29: 499-524.

Wilson, R. A. 1969. The fine structure of the protonephridial system in the miracidium of Fasciola hepatica. Parasitology 59: 461-467.

Wilson, R. A. 1970. Fine structure of the nervous system and specialized nerve endings in the miracidium of Fasciola hepatica. Parasitology 60: 399-410.

Wotton, R. M., and F. Sogandares-Bernal. 1963. A report on the occurrence of microvillus-like structures in the caeca of certain trematodes (Paramphistomatidae). Parasitology 53: 157-161.

Yosufzai, H. K. 1952. Cytological studies on the spermatogenesis of Fasciola hepatica L. Cellule 55: 7-19.

Zailer, O. 1914. Zur Kenntnis der Anatomie der Muskulatur und des Nervensystems der Trematoden. Zool. Anz. 44: 358-396.

ACKNOWLEDGMENTS

The author wishes to express sincere appreciation to Dr. Martin J. Ulmer for his unselfish help, counseling, and generous contributions of time and patience throughout this investigation. His leadership, inspiration for excellence and concern for others as well as his personal friendship will never be forgotten.

Thanks are also due to Messrs. Eain M. Cornford, David W. Fredericksen, Richard O. McCracken, and Dr. Harvey D. Blankespoor in providing assistance and encouragement during this study. Appreciation is also expressed to Dr. Harry T. Horner for his excellent instruction in electron microscopy and histochemical techniques. A special note of thanks is due Dr. Stanley Boertje who first stimulated my career through his excellent teaching efforts.

This study was supported in part by National Science Foundation Grant No. GB-5465X1 under the direction of Dr. Martin J. Ulmer, in part by the Iowa State University College of Science and Humanities Research Institute, and by a gift from Houston Endowment Co., Inc., Houston, Texas. Appreciation is expressed for Thomas H. MacBride Scholarships for study at the Iowa Lakeside Laboratory during the summers of 1967 and 1968.

PLATES

Abbreviations

A - Acetabulum

AF - Axial filament

AR - Axial rod

AT - Anterior testis

BB - Basal body

BL - Basal lamina

BM - Basal membrane

C - Cilium

CC - Cerebral commissure

CCH - Central chamber of holdfast

CE - Centriole

CG - Cerebral ganglion

CH - Chromosome

CJ - Cell junction

CM - Circular muscle

CR - Mitochondrial crista

CS - Cortical sheath

CY - Cytoplasm

DB - Doublet microtubules

DV - Dense vesicle

ED - Excretory duct

EL - Excretory lamella

ER - Endoplasmic reticulum

FB - Forebody

FC - Flame cell

FCC - Flame cell collar

FL - Fibrous layer

G - Glycogen

GA - Genital aperture

GC - Gland cell(s) of holdfast

GD - Gland duct

GDC - Gastrodermal cell

GP - Genital pore

HB - Hindbody

HC - Holdfast cleft

HG - Holdfast gland tissue

HO - Holdfast opening

HR - Horizontal rods

I - Intestine

IC - Intestinal crus

IM - Ingested material

L - Lipid

LM - Longitudinal muscle

LN - Lateral nerve

LU - Lumen

M - Mitochondrion or mitochondria

MO - Mouth

MP - Mid-piece

MT - Microtubule

MU - Muscle

MV - Microvillus

N - Nerve

NC - Nerve commissure

NP - Nuclear pore

NU - Nucleus

NUC - Nucleolus

OM - Oblique muscle

OS - Oral sucker

OV - Ovary

P - Pharynx

PB - Protein body

PC - Protoplasmic channel

PM - Plasma membrane

PT - Posterior testis

R - Ribosome

RD - Reserve excretory duct

RT - Rootlet

S - Spoke

SB - Sensory bulb

SD - Septate desmosome

SJ - Synaptic junction

SMV - Seminal vesicle

SP - Spine

SPE - Spermatozoon (sperm)

ST - Sperm tail

STB - Subtegumental cell body

SV - Synaptic vesicle

T - Tegument

TF - Tegumental fold

TJ - Tight junction

TW - Testis wall

UC - Unipolar cell

UT - Uterus

V - Vesicle

VC - Vitelline cell

VD - Vitelline duct

VG - Vitelline granule

VN - Ventral nerve

VR - Vitelline reservoir

WM - Whorled membrane body

Y - Yolk droplet

Plate I

Fig. 1. Dorsal tegument of F. cratera. Note infoldings of basal membrane (BM) into surface syncytium and several junctions (TJ) of underlying tegumental cell body with surrounding parenchyma. (X 27,750)


1

Plate II

Fig. 2. Dorsal tegument. Note especially the two types of muscle fibers seen in cross sections of longitudinal muscle bands (LM). Tegumental spines (SP) rest basally on the fibrous layer and do not project from the surface. (X 27,750)

Fig. 3. Dorsal tegument. Note the two types of tegumental vesicles (V), mitochondria (M) and spines (SP) within the tegument (T). Externally the tegument is bounded by a trilaminate plasma membrane (PM). (X 46,600)

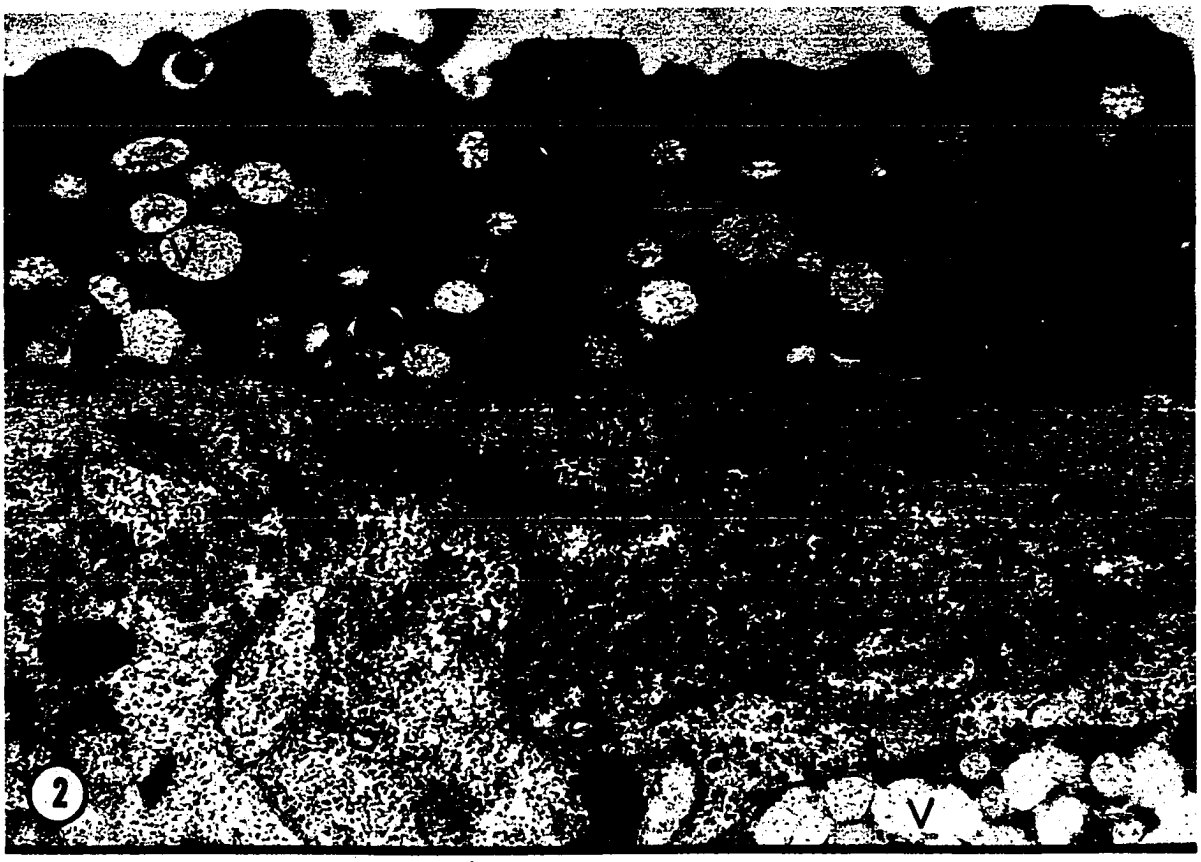
2
V

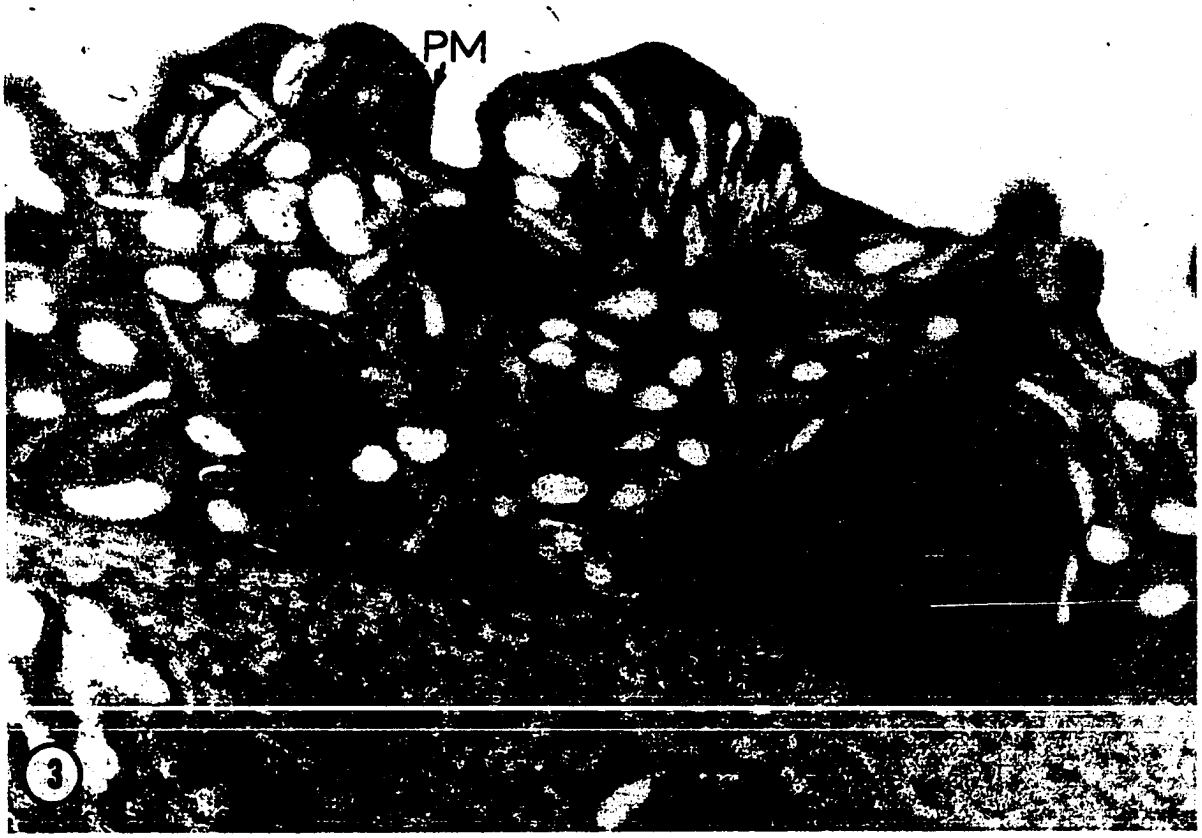
PM
3

Plate III

Fig. 4. High magnification micrograph of dorsal tegument. Note elongate vesicles near the surface plasma membrane (PM) and larger vesicles filled with particulate matter. A spine (SP) appears in oblique section. (X 85,500)

Fig. 5. Hindbody tegument. The roughened aspinose tegument contains mitochondria (M) and few small vesicles. Invaginations of the basal membrane (BM) into the surface layer are shown. Note underlying fibrous layer (FL) and subtegumental nerve (N). (X 22,250)


PM
4
5

Plate IV

Figs. 6-9. Scanning electron micrographs of tegument of *Fibricola cratera*

Fig. 6. Dorsal tegument. Note foliate tegumental folds and absence of protruding spines. Two sensory bulbs (type II) are seen in the lower part of the micrograph. (X 9,600)

Fig. 7. Ventral tegument near edge of forebody. Broad blunt tegumental spines projecting from the surfaces are oriented at right angles to the longitudinal axis of the body. (X 7,200)

Fig. 8. Ventral tegument. Numerous terminally-branched blade-like spines project from the surface. (X 3,200)

Fig. 9. Hindbody tegument. Aspinose tegument of this region is characterized by irregular surface folds. (X 2,600)

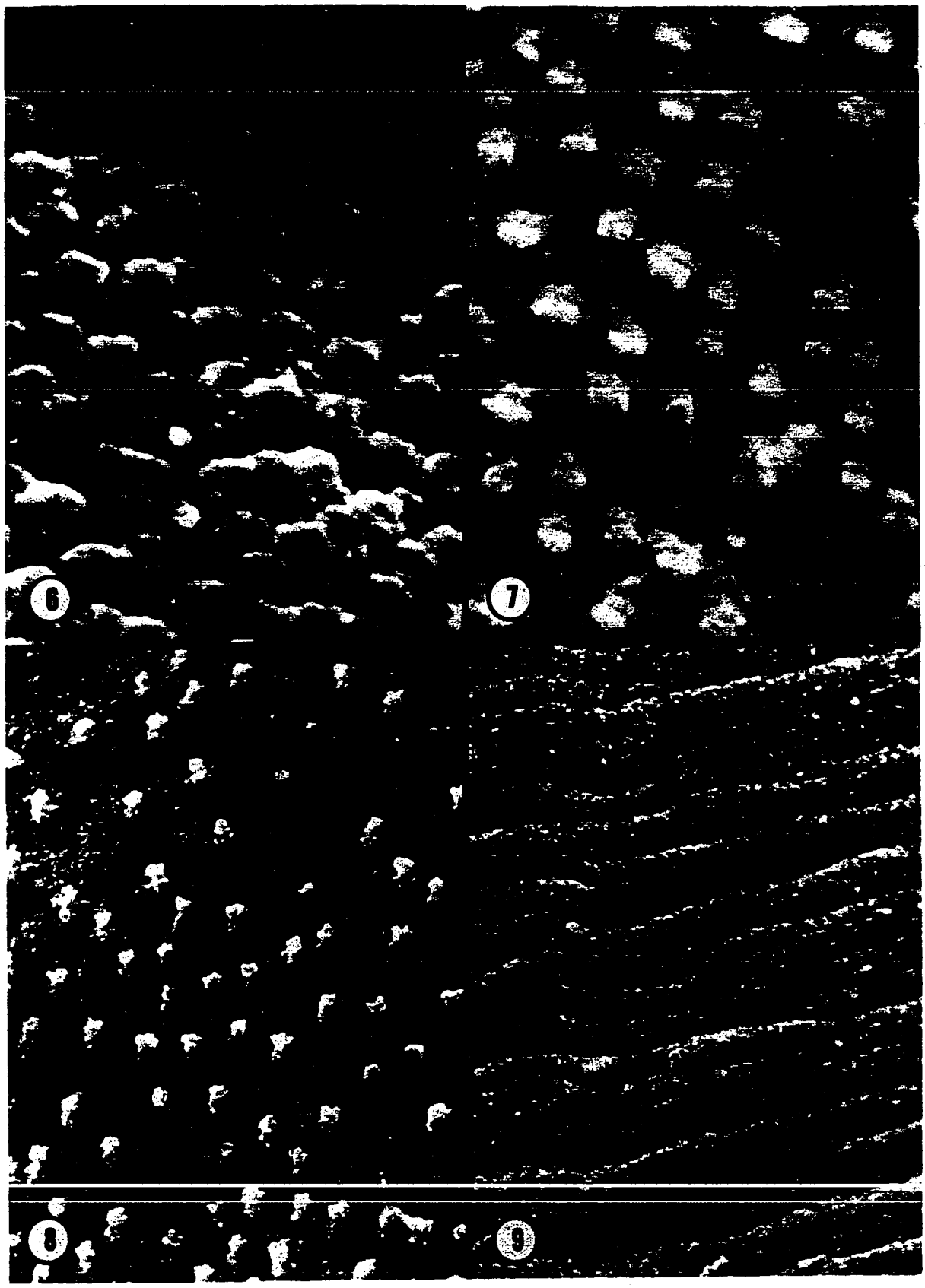
6
7
0
9

Plate V

Fig. 10. Ventral tegument. Note tegumental spines (SP) projecting from roughened tegument (T) and the underlying fibrous layer (FL). (X 38,900)

Fig. 11. Tegument of holdfast cleft. Large numbers of elongate pointed spines (SP) and numerous vesicles characterize this surface. Note protoplasmic channel (PC) connecting surface syncytium with underlying subtegumental cell body. (X 14,300)

Fig. 12. Tegument of edge of forebody lobe. Pointed spines protrude from tegument near junction of dorsal and ventral forebody surfaces. Note the two types of vesicles within tegument. (X 29,000)


V
10


11


12

Plate VI

Fig. 13. Ventral tegument of anterior forebody. Note close proximity and shape of adjacent spines. (X 27,400)

Fig. 14. Ventral tegument of anterior forebody. Note size relationship between tegumental vesicles and those of the underlying parenchyma. (X 14,300)

Fig. 15. Pointed tegumental spine from holdfast cleft. Note basal membrane (BM) and outer plasma membrane (PM). (X 48,500)

Fig. 16. Tegumental spine, ventral surface of forebody. (X 36,800)

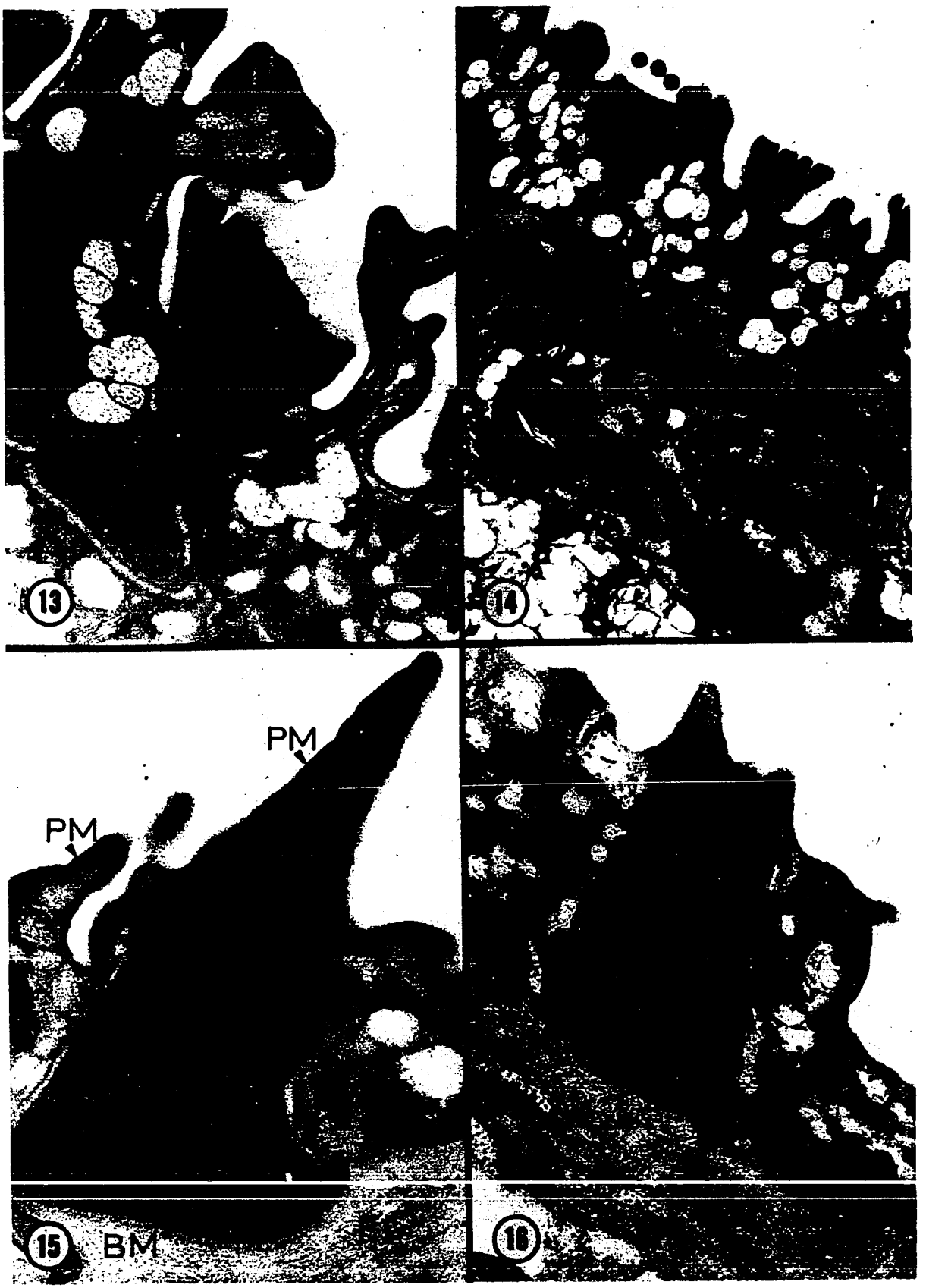
13
14
PM
PM
15
BM
16

Plate VII

Fig. 17. High magnification micrograph of tegumental spine of F. cratera. Note internal lattice network formed by horizontal rods (HR) and more numerous vertical bars between them. The basal membrane (BM) and the surface plasma membrane (PM) are also clearly seen. (X 104,000)


PM
T
BM
17

Plate VIII

Fig. 18. Scanning electron micrograph of holdfast (tribocytic) organ (HF) of F. cratera, ventral view. Note transition of external tegument to an irregular chambered surface typical of the holdfast cleft (HC) and dorsal holdfast chamber. (X 1,900)


18

Plate IX

Fig. 19. Diagram of adult F. cratera, ventral view. Note position of holdfast (HF)

Fig. 20. Cross section of adult F. cratera at level of holdfast (dotted line, Fig. 19). Note gland cells (GC) forming the bulk of the holdfast and holdfast cleft (HC) leading to dorsal holdfast chamber

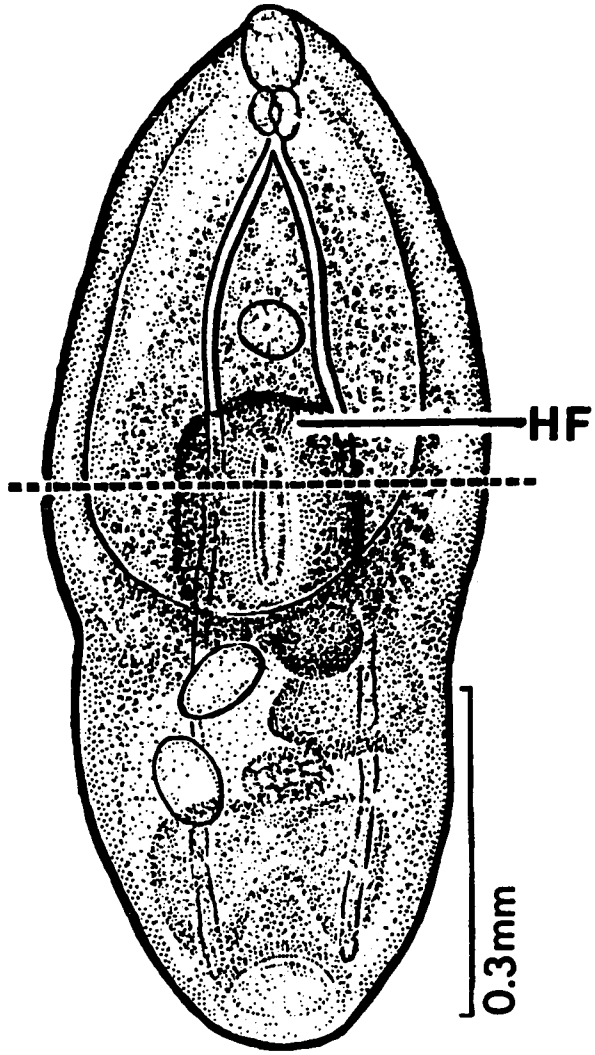

19

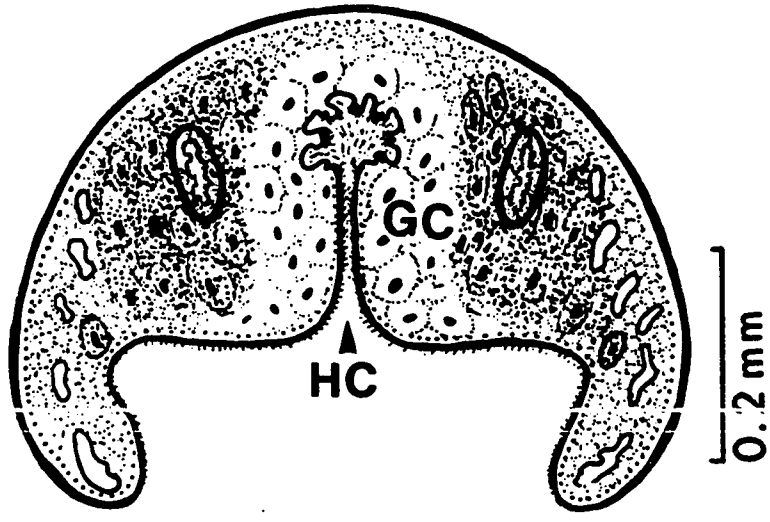

20

Plate X

Fig. 21. Cross section of F. cratera depicting the holdfast central chamber (CCH) and associated gland cells (GC). Reserve excretory ducts (RD) appear within the lateral forebody lobes and near the holdfast (large arrow). (X 565)

Fig. 22. High magnification of the holdfast cleft (HC) and dorsal holdfast chamber. Note tegumental folds (TF) characteristic of the chamber and numerous spines within holdfast cleft tegument. (X 1,250)

Fig. 23. Holdfast gland cells (GC). Note large dense nuclei of these tightly packed cells, resulting in dense nuclear staining of this region at the light level. (X 1,330)

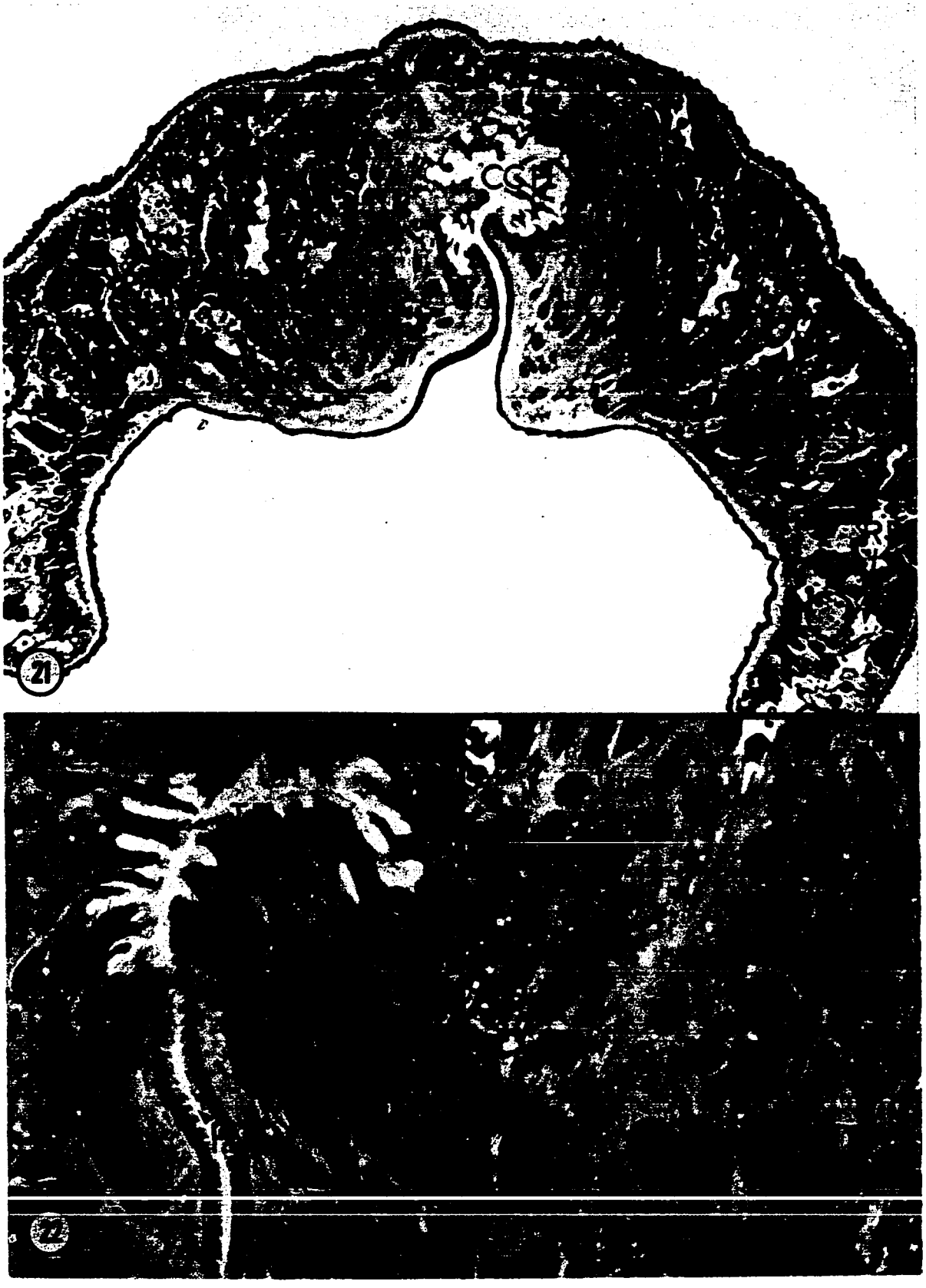
CS
21
22

Plate XI

Fig. 24. Survey electron micrograph of junction of holdfast cleft (HC) with central holdfast chamber. Note numerous spines (SP) within holdfast cleft tegument (T) and transition to the folded surface. Large numbers of mitochondria (M) surround the holdfast chamber, which is filled with microvillous processes (MV). (X 11,000)


MV
HC
HC
24

Plate XII

Fig. 25. High magnification of holdfast junctional zone. Numerous tegumental folds (TF) form extensive surface amplifications in the holdfast chamber, whereas the tegument (T) of the holdfast cleft resembles that of the external tegument. (X 25,500)

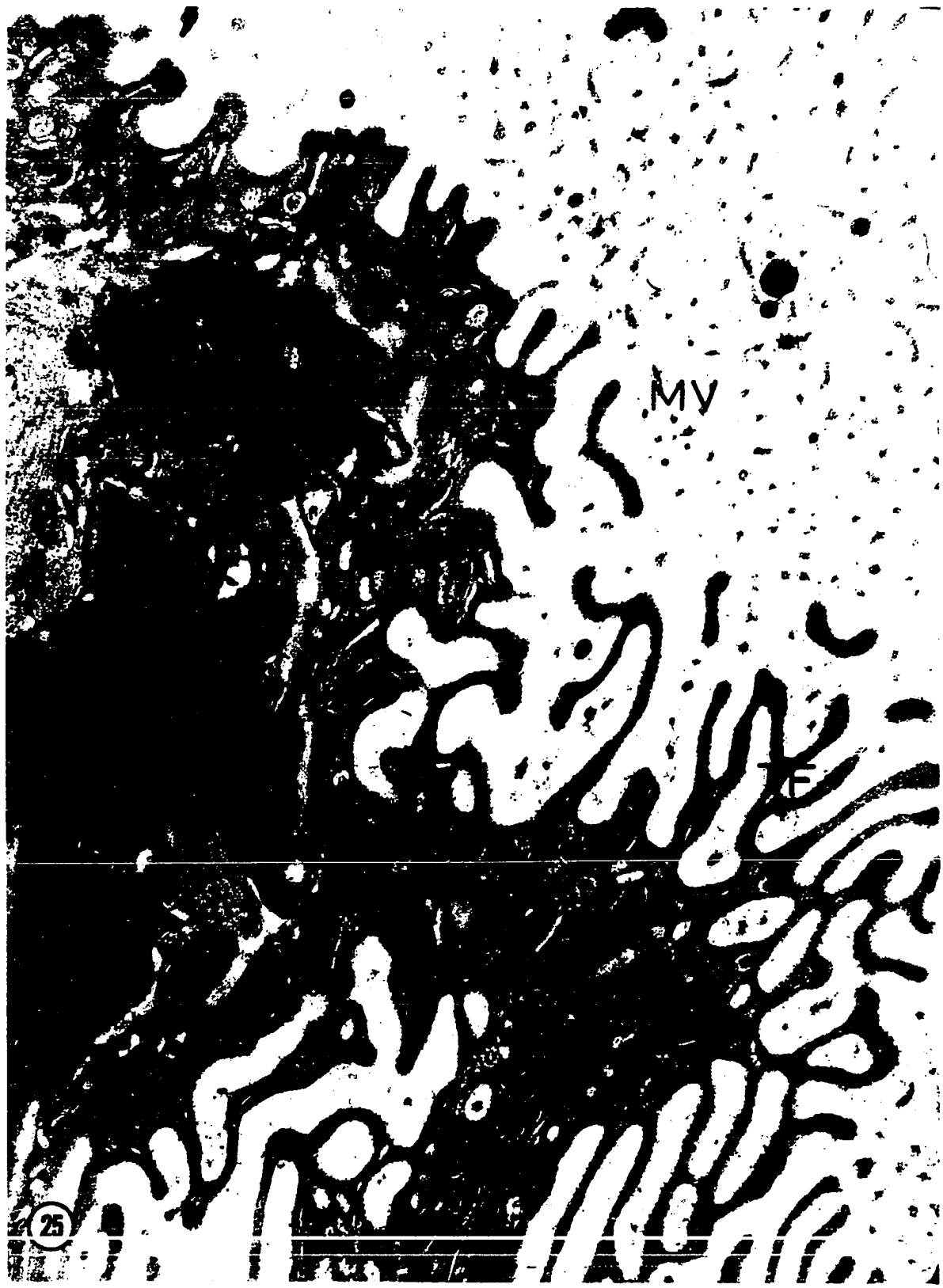
MY
25

Plate XIII

Fig. 26. High magnification electron micrograph of holdfast tegumental folds (TF). Trilaminate plasma membranes (PM) bound both the tegumental folds and digitiform microvilli (MV) arising from such folds. (X 76,700)

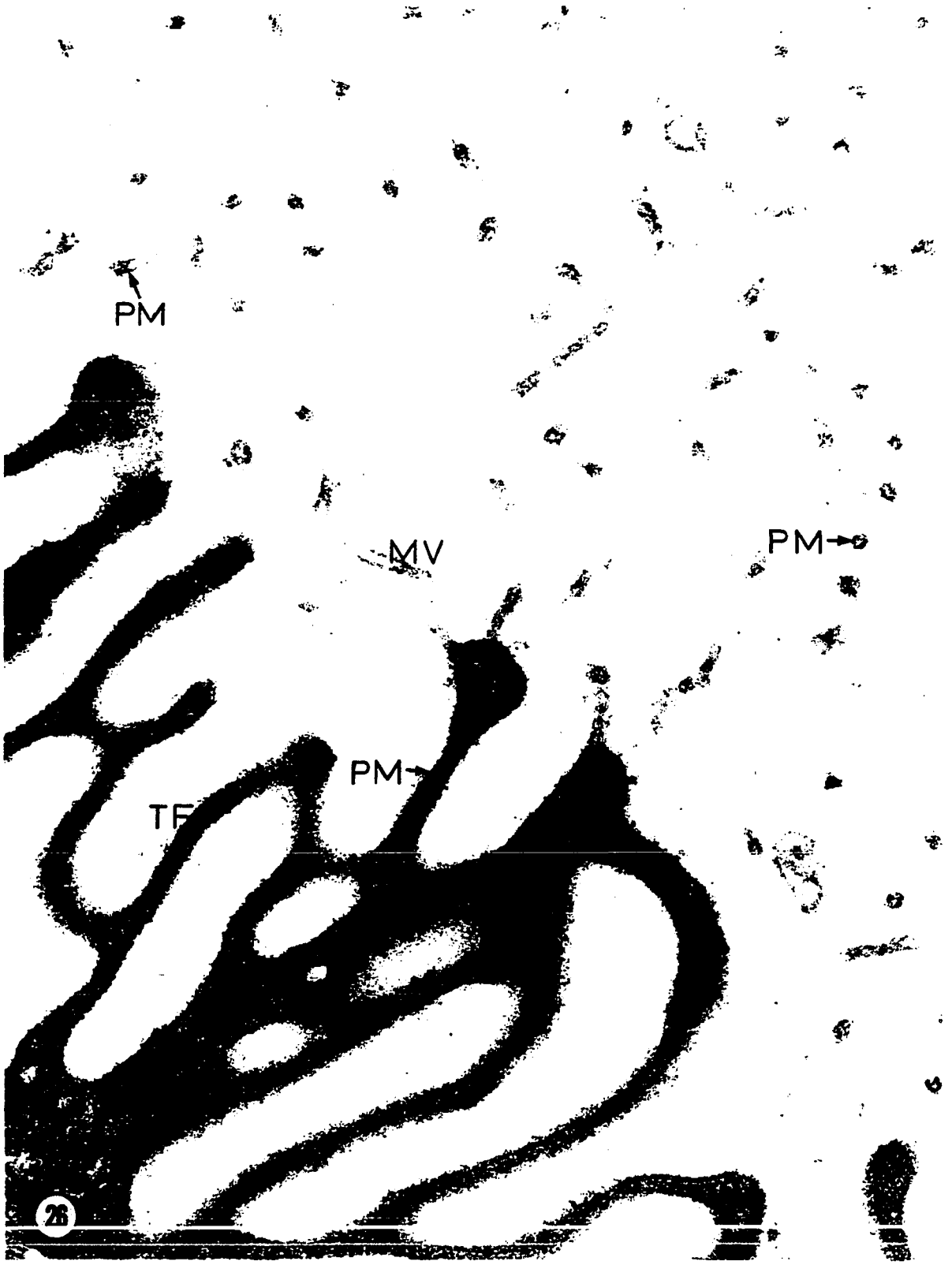
PM
MV
PM
PM
TF
26

Plate XIV

Figs. 27-30. Holdfast tegumental surfaces

Fig. 27. Note numerous dense vesicles (DV) within the tegumental syncytium and the greatly folded basal membrane (BM) underlying it. (X 23,350)

Fig. 28. Note large numbers of mitochondria (M) adjacent to the tegumental folds (TF), thus suggesting a highly metabolic region. Dense vesicles are seen within the tegument and in gland ducts (GD), the latter arising from holdfast gland cells. (X 20,250)

Fig. 29. Note extensive surface amplification provided by tegumental folds (TF). An excretory duct with numerous stacked lamellae (EL) lies close to this surface. (X 20,900)

Fig. 30. Note presence of dense vesicles (DV) within tegumental folds. Microvilli (MV) fill the holdfast central chamber. (X 14,250)

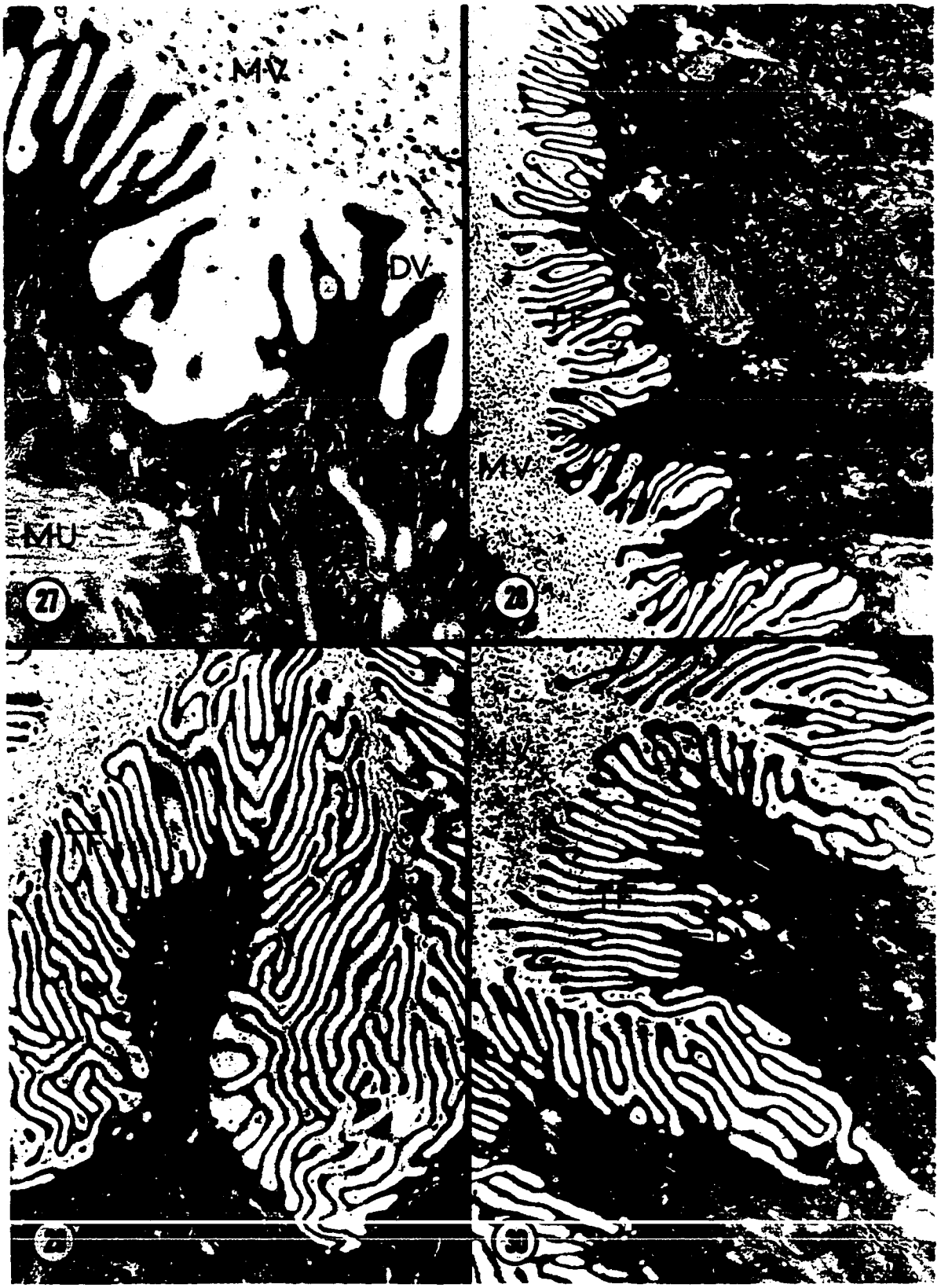
MV
DV
MU
27
28
29
30

Plate XV

Fig. 31. Electron micrograph demonstrating basal membrane (BM) of the holdfast tegument. (X 50,100)

Fig. 32. An excretory duct near holdfast tegument. Note numerous membrane-bound lamellae (EL). (X 25,500)

Fig. 33. Dense protein body (PB) within excretory duct walls. Note small subunits comprising this body. (X 48,200)

Fig. 34. High magnification of cristate mictochondria found adjacent to holdfast tegument. (X 63,800)

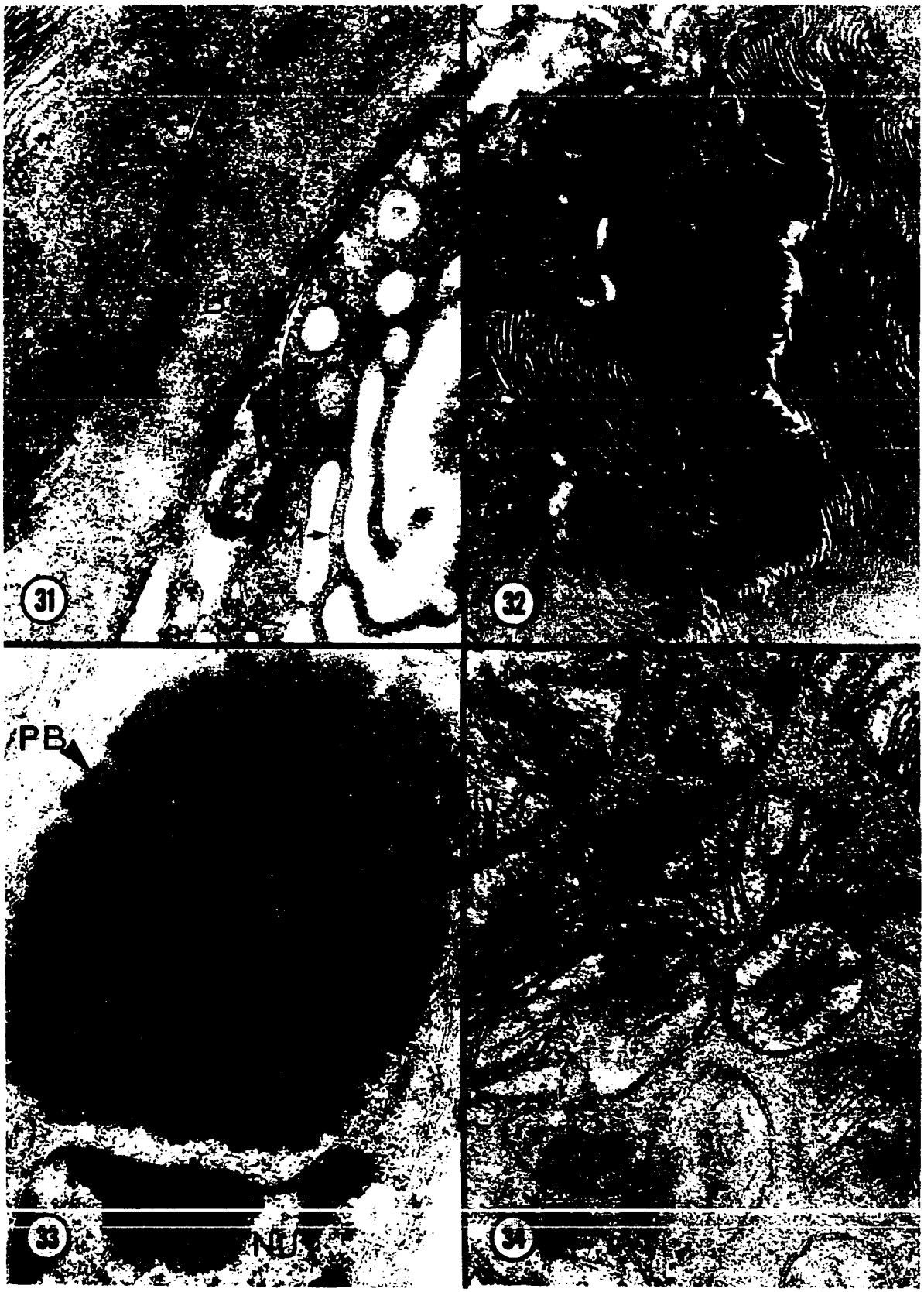
31
32
PB
33
NU
34

Plate XVI

Fig. 35. Survey micrograph of holdfast gland cells (GC). Note large nucleus (NU) and indistinct cell boundaries. In the lower part of the micrograph a subtegumental cell body (STB) as well as its cytoplasmic connection to the ventral tegument (T) can be seen. (X 8,900)


35

Plate XVII

Fig. 36. High magnification electron micrograph of a holdfast gland cell. Several nuclear pores (NP) connect the nucleoplasm with the surrounding cytoplasm (CY). The latter is filled with endoplasmic reticulum cisternae (ER) and ribosomes (R). (X 48,700)

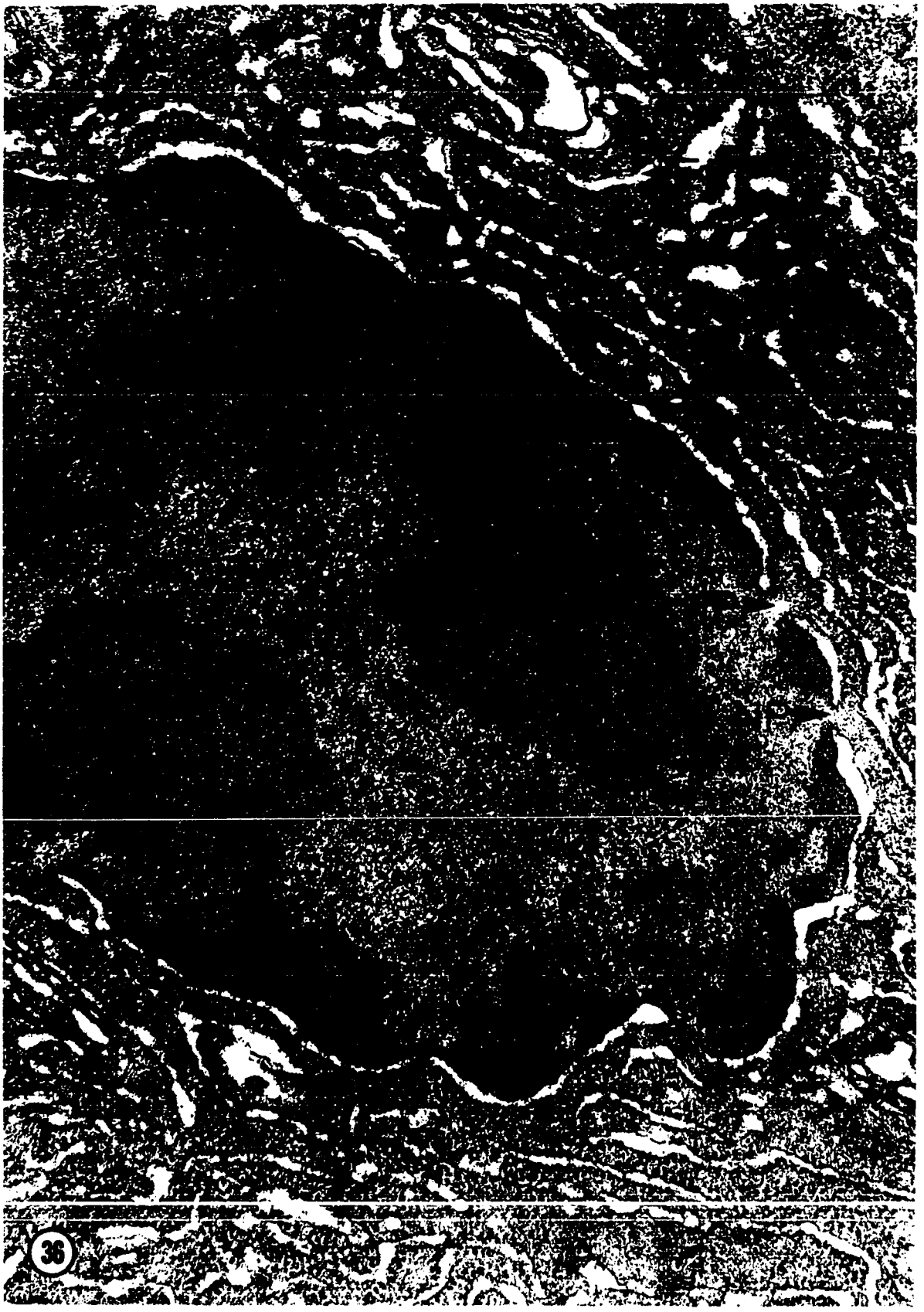
36

Plate XVIII

Figs. 37-40. Holdfast gland cells

Fig. 37. Survey micrograph of holdfast gland cells (GC) showing proximity of their nuclei (NU). (X 15,400)

Fig. 38. Note plasma membranes (PM) between individual cells, as well as cristate mitochondria and extensive endoplasmic reticulum within these cells. (X 22,750)

Fig. 39. Gland cell cytoplasm. Note dense vesicles (DV) similar to those observed near the holdfast tegument. (X 11,900)

Fig. 40. Nucleus of gland cell. Note dense heterochromatin and lighter euchromatin within nucleus (NU). Dense vesicles (DV), ribosomes (R) and endoplasmic reticulum cisternae (ER)are seen within the cytoplasm. (X 22,600)

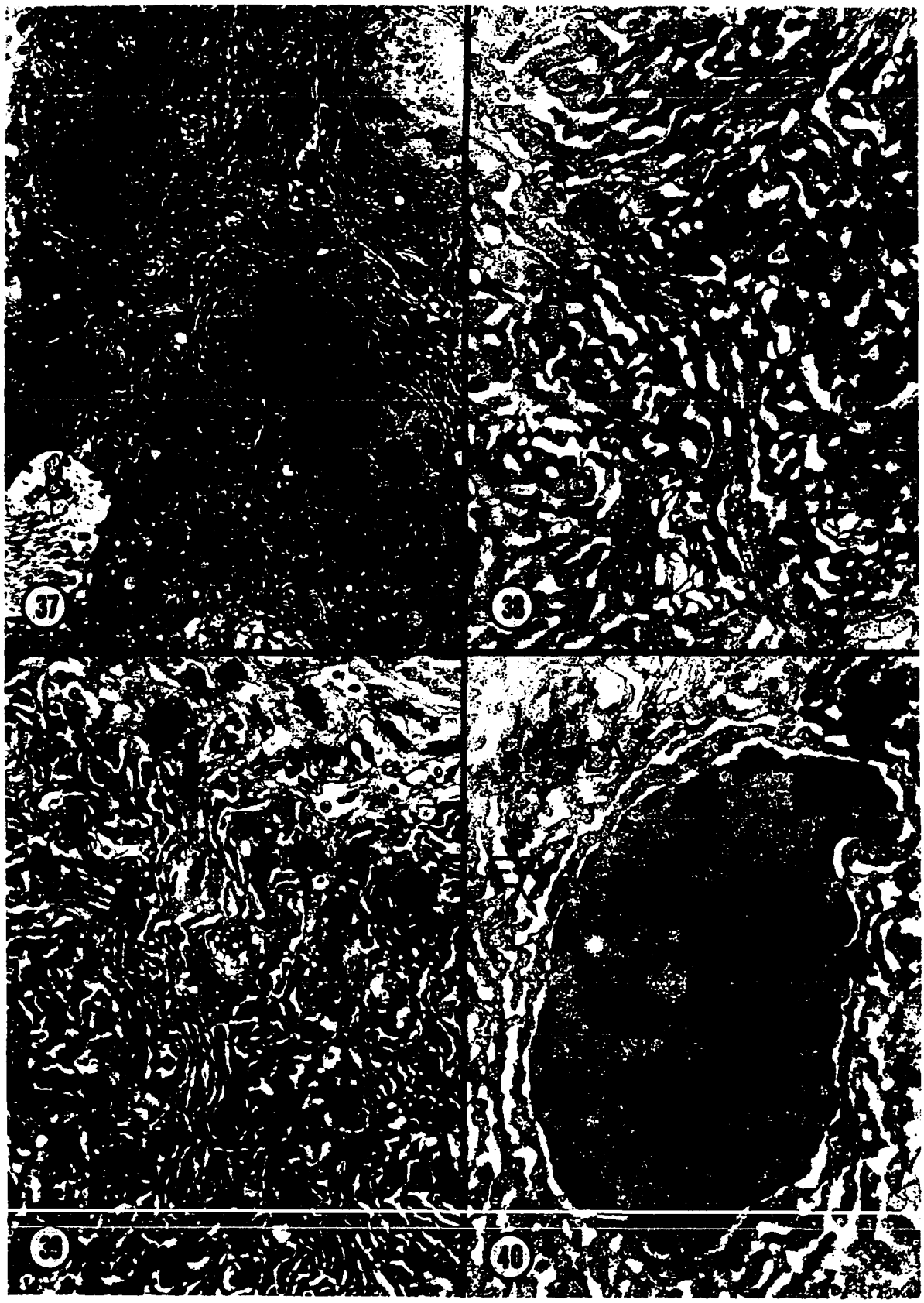
37
38
39
40

Plate XIX

Fig. 41. Diagram of adult Fibricola cratera depicting major components of the nervous system

Legend:
A - Acetabulum
AT - Anterior testis
CG - Cerebral ganglion
GP - Genital pore
HF - Holdfast organ
IC - Intestinal crus
LN - Lateral nerve
OS - Oral sucker
OV - Ovary
P - Pharynx
PT - Posterior testis
VN - Ventral nerve
VR - Vitelline reservoir

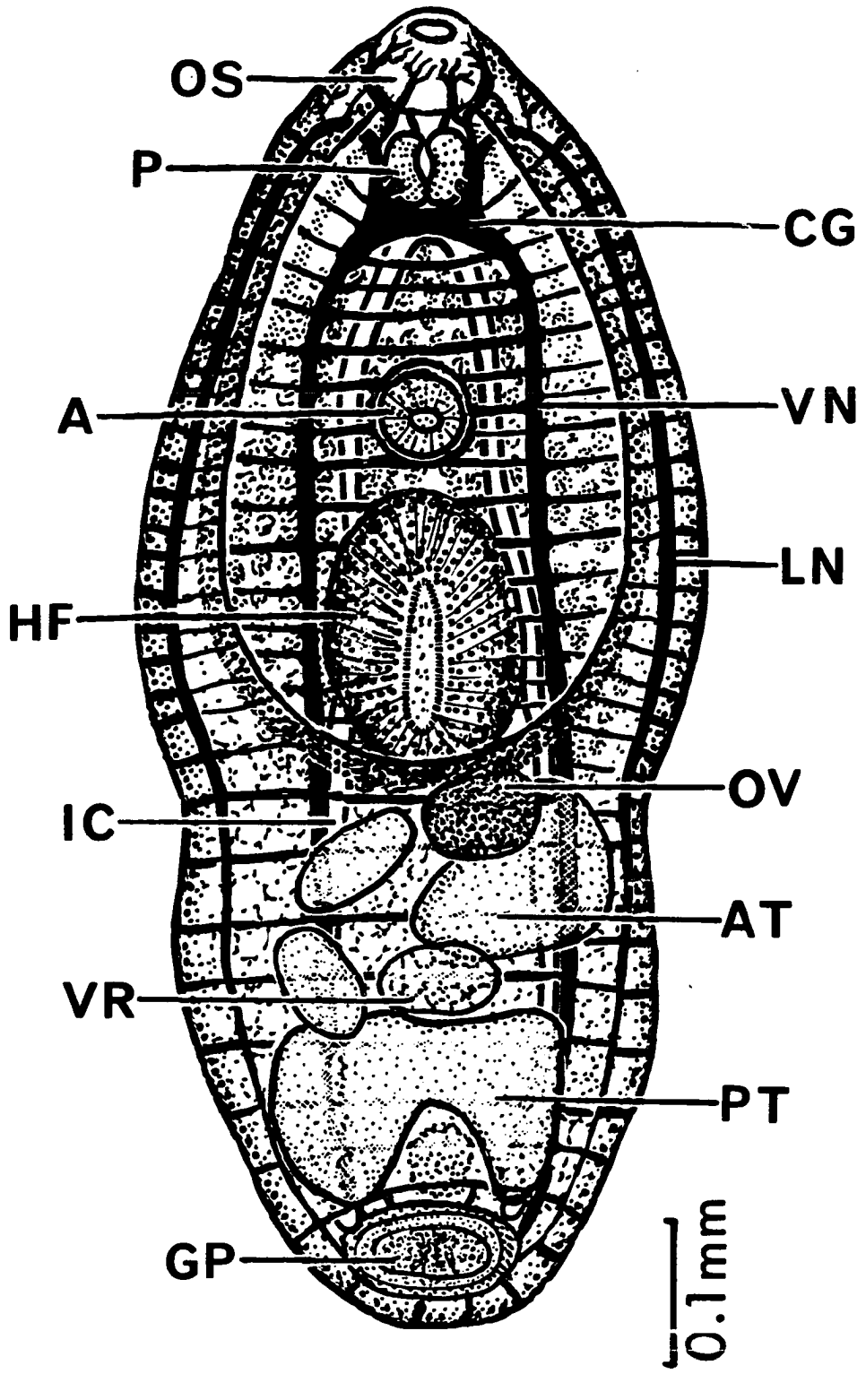

41

Plate XX

Fig. 42. Forebody of adult F. cratera showing cerebral ganglia (CG), ventral nerve cords (VN), nerve commissures (NC) and lateral nerve cords (LN). Note the dense staining of the oral sucker (OS) and acetabulum (A), indicating presence of large numbers of nerve fibers. Note also the staining of nonspecific esterases within the holdfast (HF). Acetylthiocholinesterase staining technique. (X 320)


OS
LN
VN
NC
A
42

Plate XXI

Figs. 43-46. Light micrographs of nervous system of *F. cratera*

Fig. 43. Unipolar cells (UC) located anteromedial to the cerebral ganglia (CG). (X 790)

Fig. 44. Survey micrograph of major nerve trunks within forebody. Note dorsal cerebral commissure (CC) located at the posterior edge of pharynx. (X 160)

Fig. 45. High magnification of cerebral ganglion (CG), cerebral commissure (CC) and unipolar cells (UP). (X 755)

Fig. 46. Micrograph depicting the large ventral nerve cord (VN) and smaller nerve commissures (NC) connecting with it at right angles. (X 750)

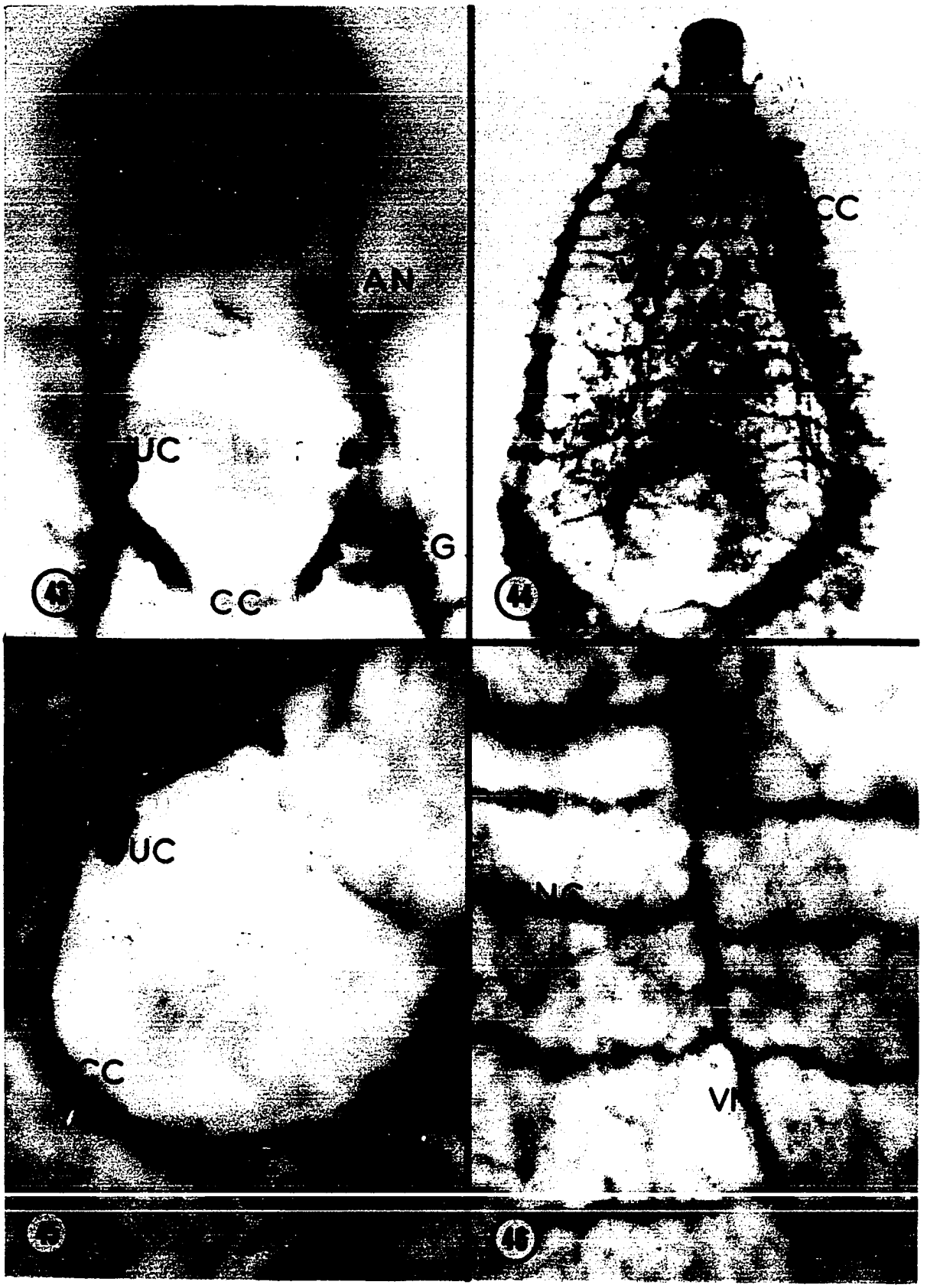
AN
UC
G
CC
4
CC
4
UC
CC
VI
4B

Plate XXII

Fig. 47. Electron micrograph of cerebral ganglion. Note numerous synaptic vesicles (SV) and larger dense rounded vesicles. Arrow indicates probable synaptic junction. (X 71,000)

Figs. 48-49. Sections of major nerve cords. Note large numbers of synaptic vesicles (SV) and dense bodies within these nerves. (Fig. 48, X 43,000; Fig. 49, X 62,100)

Fig. 50. Section of nerve with a gastrodermal cell. Note synaptic vesicles (SV) and proximity of nerve to gut lumen (LU). (X 59,000)


LU
49
50

Plate XXIII

Fig. 51. Subtegumental nerve (N) below fibrous layer (FL) of tegument. Note vertical striations within tegumental spine (SP). (X 41,500)

Fig. 52. Small nerve fiber with synaptic vesicles within cytoplasm of a holdfast gland cell. (X 41,000)

Fig. 53. Subtegumental nerve (N). Note its position between fibrous layer (FL) and underlying circular muscle (MU). Synaptic vesicles (SV), and large dense vesicles are seen within nerves. (X 71,000)

Fig. 54. Subtegumental nerve (N) within the hindbody. Note synaptic vesicles (SV) and fibrous elements of the tegumental fibrous layer (FL). (X 74,500)

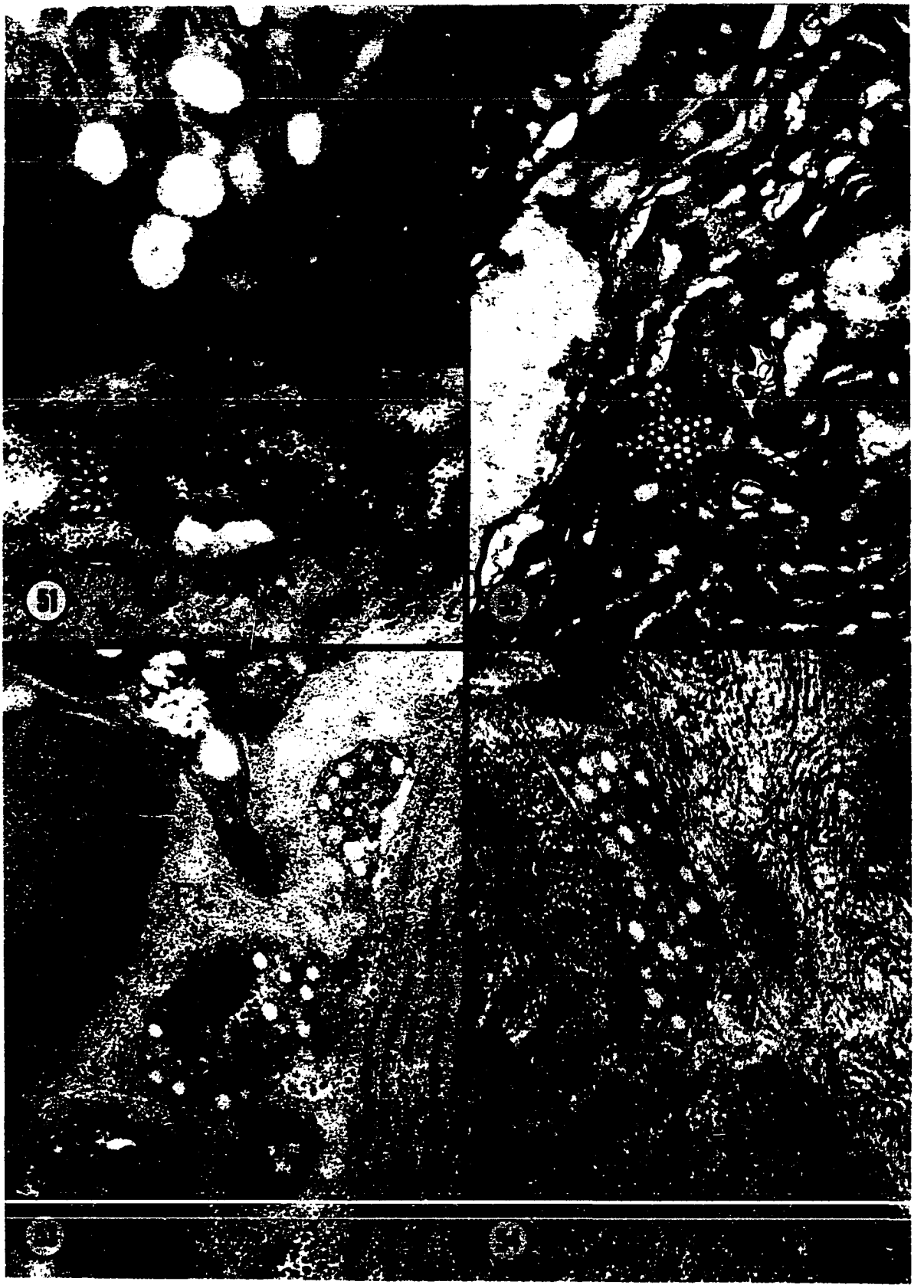
51

Plate XXIV

Fig. 55. Ciliated sensory bulb, type I. Note terminal projecting cilium, ciliary basal body (BB), mitochondria (M) and synaptic vesicles (SV). Bulbs of this type are located on ventral and lateral surfaces of forebody. (X 65,500)


V
SD
B
SV
55

Plate XXV

Fig. 56. Type I ciliated sensory bulb. Note central microtubules within terminal cilium. Septate desmosomes (SD) appear between sensory bulb and surrounding tegument. Synaptic vesicles (SV) and mitochondria fill the dense matrix of the bulb. (X 83,500)


C
PM
V
56

Plate XXVI

Fig. 57. Diagram of type I ciliated sensory bulb. Note its position relative to tegument (T), basal lamina (BL) (fibrous layer), and circular (CM) and longitudinal muscle (LM) bands. Numerous microtubules (MT) occur within the bulb and its connecting nerve (N) which joins larger nerves by means of a synaptic junction (SJ)

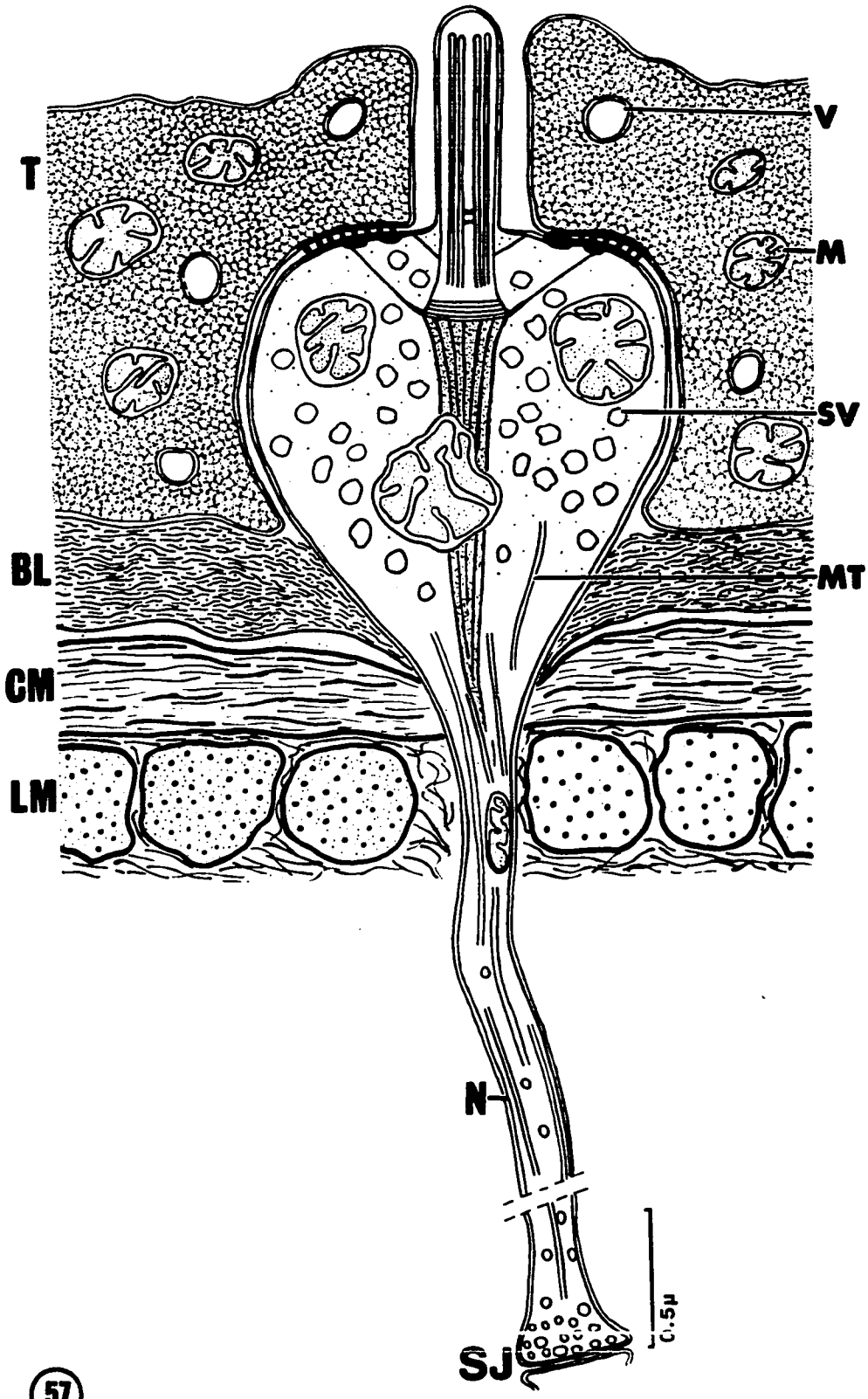

57

Plate XXVII

Figs. 58-61. Tegumental sensory bulbs of *F. cratera*

Fig. 58. Ciliated sensory bulb of type I. Note microtubules (MT) within nerve process (N) extending to the underlying parenchymal tissue. (X 22,000)

Fig. 59. Bulbous nonciliated type III sensory bulb. Note synaptic vesicles (SV) within sensory bulb projecting from surface but covered with the tegumental layer (T). (X 27,200)

Fig. 60. Ciliated type I sensory receptor. Note structure of terminal cilium (C) and numerous mitochondria (M) within sensory bulb. A small tegumental nerve (N) is also shown. (X 23,000)

Fig. 61. Type I ciliated sensory bulb. Note microtubules within cilium (C) and dense bodies adjacent to septate desmosomes (SD). (X 67,000)


C
SV
MT
M.U
58
59
C
60
61

Plate XXVIII

Fig. 62. Transmission electron micrograph of domed type III sensory bulb. Internally, mitochondria (M), synaptic vesicles (SV) and ribosomes are seen within the dense matrix. Sensory bulbs of this type are covered with a tegumental layer (T). Note external plasma membrane (PM). (X 82,500)


PM
S
82

Plate XXIX

Figs. 63-66. Scanning electron micrographs of four types of sensory receptors of Fibricola cratera

Fig. 63. Ciliated type IV sensory bulb. Note that the bulbous portion (SB) is elevated above the surrounding tegument. Bulbs of this type are located around the acetabulum and genital atrium. (X 40,000)

Fig. 64. Domed nonciliated type III sensory bulb (SB). Large numbers of type III receptors are located near the genital aperture (see Figs. 68 and 69). (X 24,000)

Fig. 65. Ciliated type I sensory bulb. Note depressed circular pit around centrally projecting cilium (C). The bulb proper is embedded in the tegument as seen in transmission electron micrographs (Figs. 55-58, 60, 61). (X 30,500)

Fig. 66. Ciliated type II sensory receptor. Sensory bulbs of this type closely resemble type I receptors but lack a circular depression around the cilium. Cilia (C) project between adjacent tegumental folds (TF). Sensory bulbs of this type are the most numerous and are located over dorsal and ventral forebody surfaces. (X 26,400)

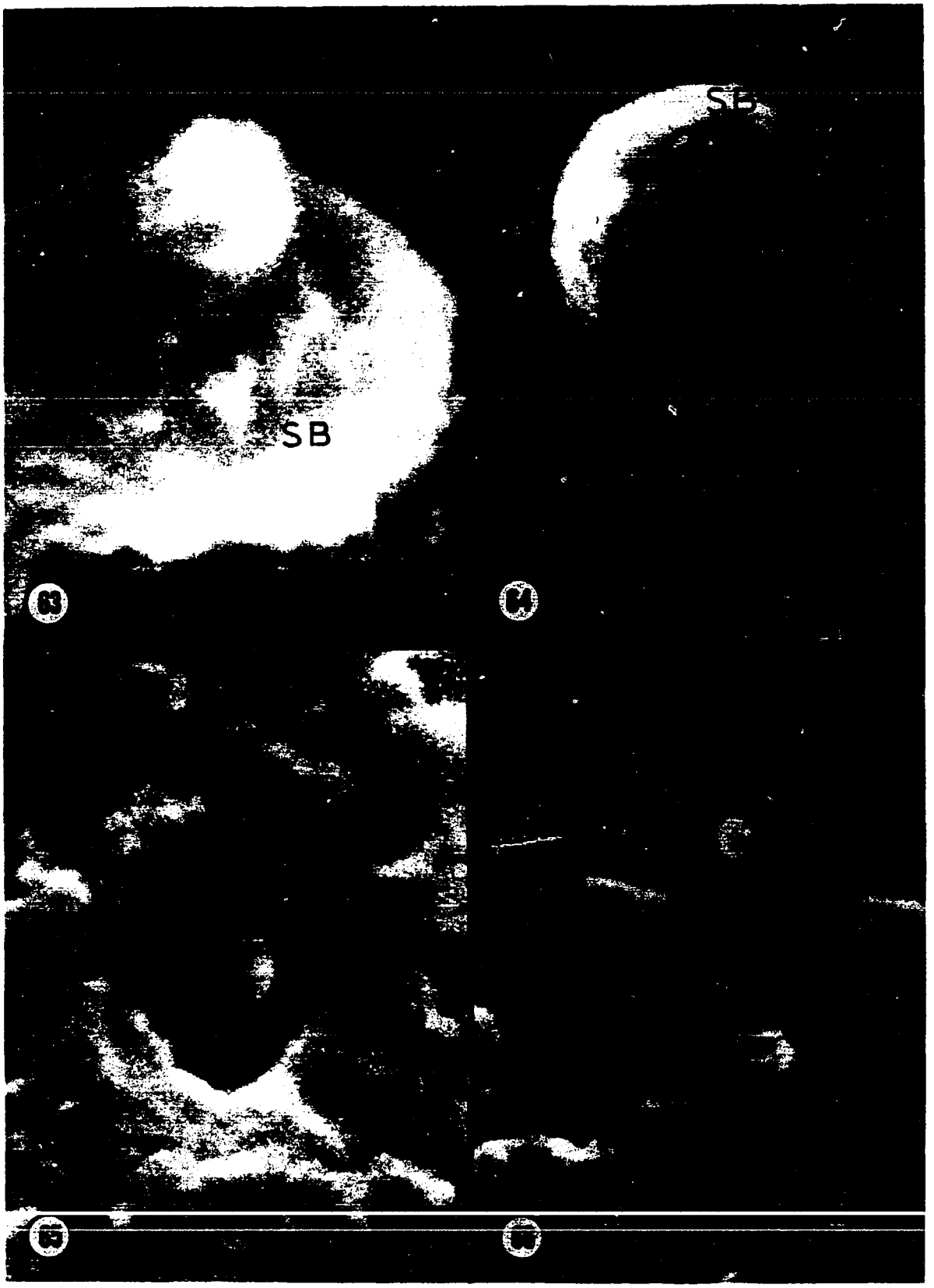
SB
SB
B
C
D
E

Plate XXX

Fig. 67. Survey scanning electron micrograph of the acetabulum (A) of F. cratera, lateral aspect. Note cilia (C) projecting from type IV sensory bulbs (SB) which lie at the periphery of the acetabulum. (X 7,500)

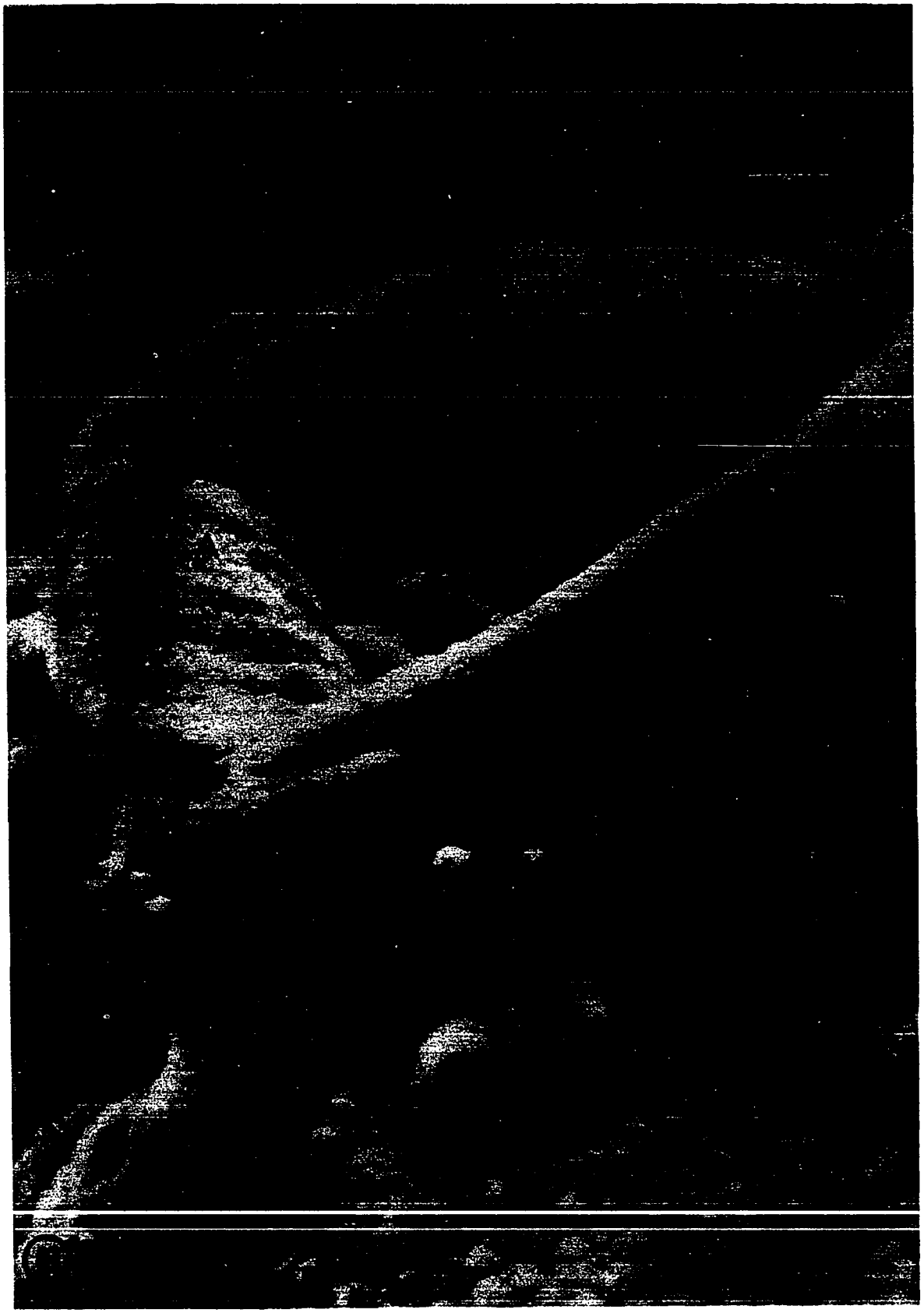

Plate XXXI

Fig. 68. Scanning electron micrograph of genital region of F. cratera. Note numerous sensory bulbs (SB) (types III and IV) surrounding the inverted genital cone and genital aperture (GA). (X 3,400)

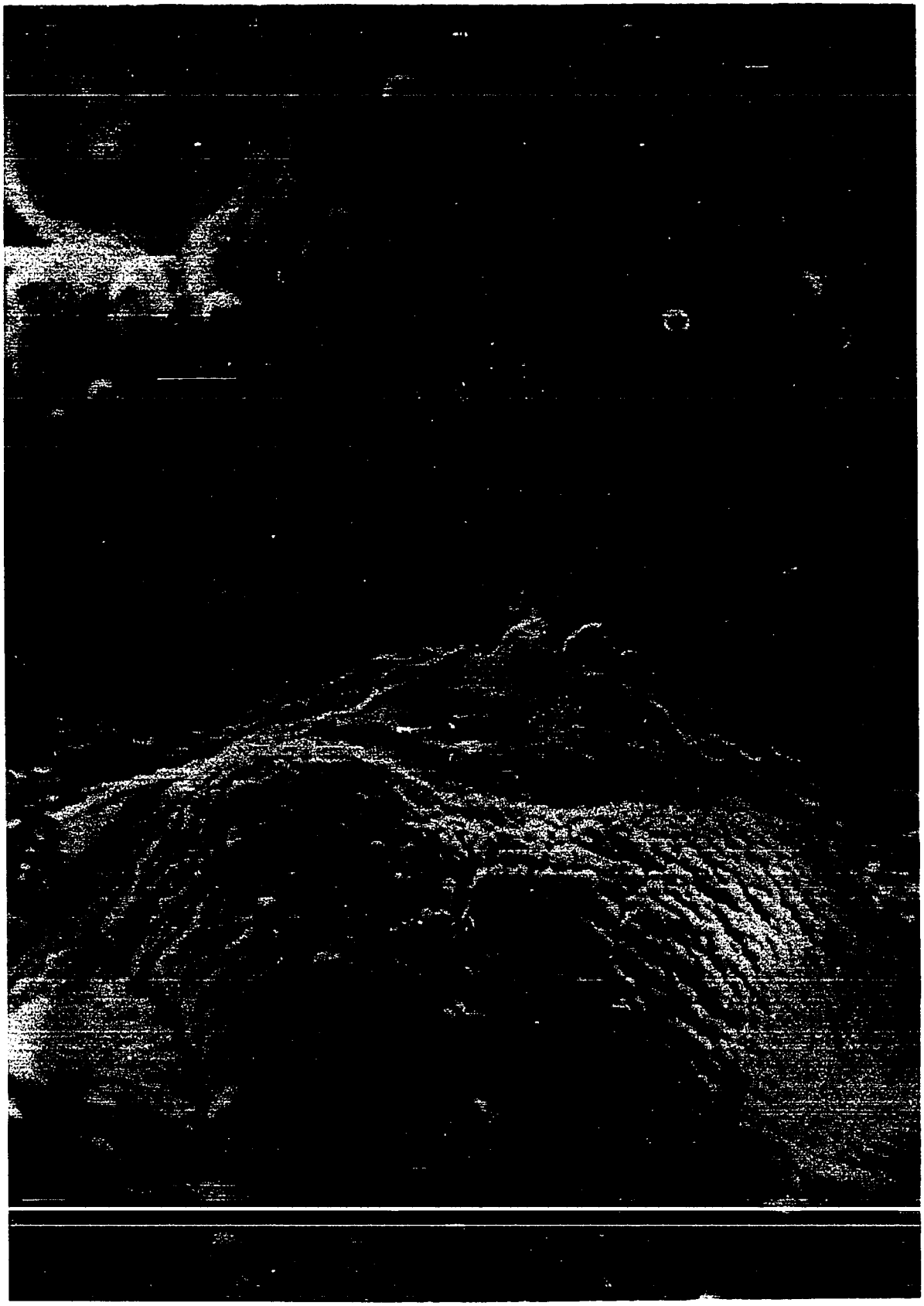

Plate XXXII

Fig. 69. Survey scanning electron micrograph of the genital region of F. cratera. Note everted genital cone and genital aperture. Numerous types III and IV sensory receptors (SB) characterize the genital region and surrounding tegument. (X 1,350)


B

Plate XXXIII

Fig. 70. Scanning electron micrograph of mouth and oral sucker of Fibricola cratera. Note continuation of the external tegument with the lining of the oral sucker and numerous sensory bulbs (SB) of types III and II surrounding the oral sucker rim. (X 6,350)

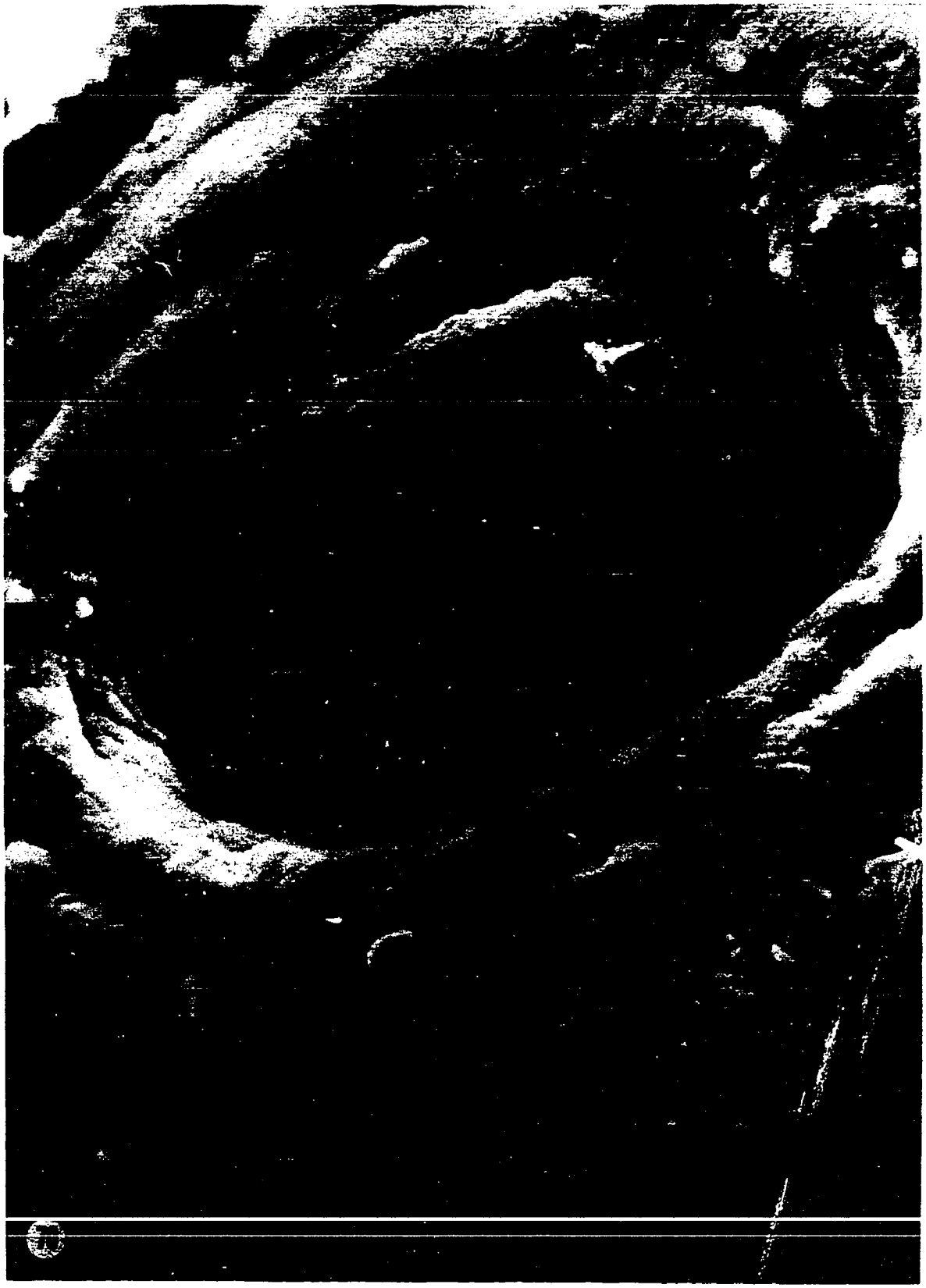

Plate XXXIV

Fig. 71. Light micrograph of anterior end of adult F. cratera. Note mouth (MO), muscular oral sucker (OS) and pharynx (P), and branched intestinal crura. (X 415)

Fig. 72. Electron micrograph of lining of the oral sucker (OS). Note roughened tegument (T), underlying fibrous layer (FL), and large muscle bands (MU) surrounding the central oral cavity. (X 8,000)

Fig. 73. Section through pharynx of F. cratera. Note mitochondria (M) and vesicles within tegumental lining (T). Large muscle bands (MU) lie peripheral to the translucent fibrous layer (FL). Ingested food material (IM) fills the lumen of the pharynx. (X 29,600)

Fig. 74. High magnification of oral sucker tegumental (T) lining. Note trilaminate surface plasma membranes (PM), tegumental vesicles (V) and basal membrane (BM) separating the tegument from the underlying fibrous layer (FL). (X 73,500)

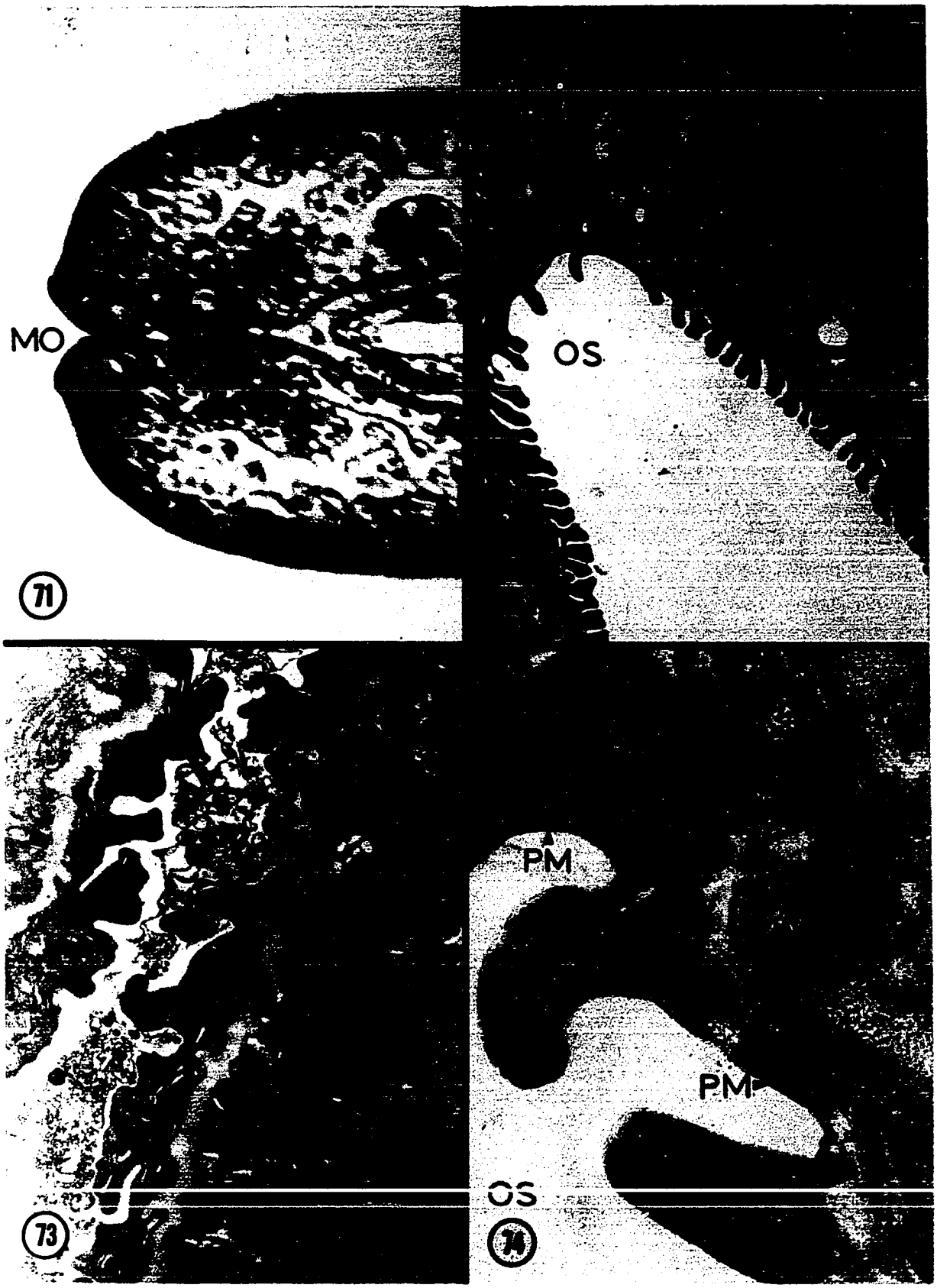
MO
OS
71
PM
PM
OS
73
74

Plate XXXV

Fig. 75. Survey transmission electron micrograph of cross section of an intestinal crus of F. cratera. Prominent large nuclei (NU) and numerous microvilli (MV) characterize these gastrodermal cells. Dense septate desmosomes (SD) are contiguous with adjacent cells near the lumenal surface. Muscle bands (MU) surround the crus; a flame cell (FC) in cross section is seen in the lower left of the micrograph. (X 10,750)


75

Plate XXXVI

Fig. 76. Cross section of an intestinal crus. Note large numbers of microvilli (MV) within lumen (LU) and septate desmosomes (SD) between gastrodermal cells. (X 11,900)

Fig. 77. Electron micrograph of gastrodermal cell. Note dense material between microvilli (MV) in the lumen. The cytoplasm (CY) is filled with numerous ribosomes (R). (X 43,700)

Fig. 78. High magnification of gastrodermal microvilli (MV). Note plasma membranes (PM) bounding the microvilli. (X 137,000)

Fig. 79. Edge of gastrodermal cell. Note septate desmosome (SD) near gut lumen (LU). (X 28,500)

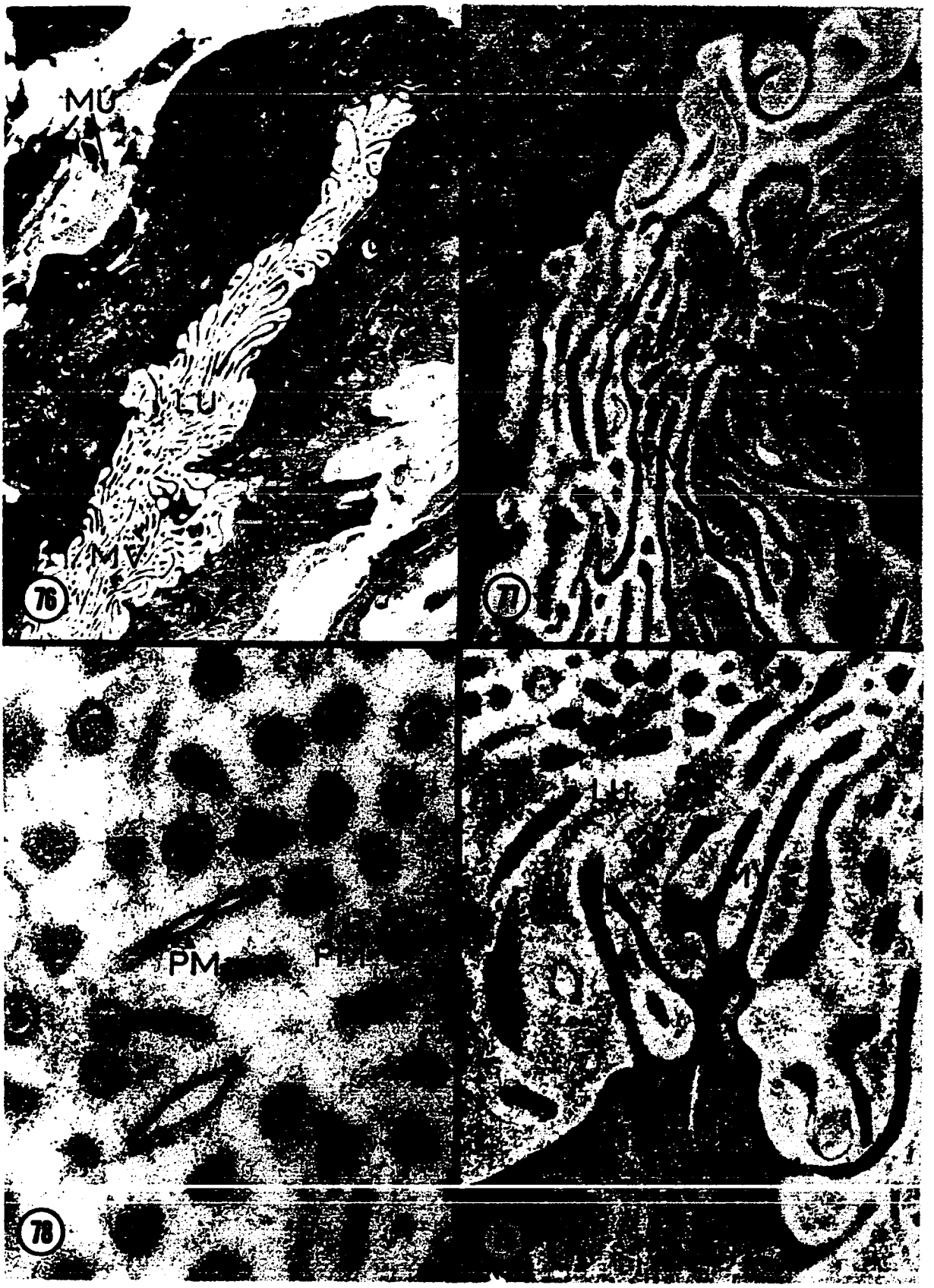
MU
LU
MV
76
77
PM
78

Plate XXXVII

Fig. 80. Cytoplasmic projection of a gastrodermal cell. Note the dense protein body (PB) and extensive granular endoplasmic reticulum (ER) within the cytoplasm. A whorled membrane body (WM) appears in the gut lumen (LU). (X 20,600)

Fig. 81. High magnification of protein body (PB) within gastrodermal cytoplasm (CY). Note small rounded subunits within the protein body. (X 46,750)

Fig. 82. Whorled membrane body (WM) within the gut lumen. (X 21,200)

Fig. 83. Section of gastrodermal cell. Note whorled membrane body (WM) and septate desmosomes (SD) at the edge of the lumen. (X 43,700)

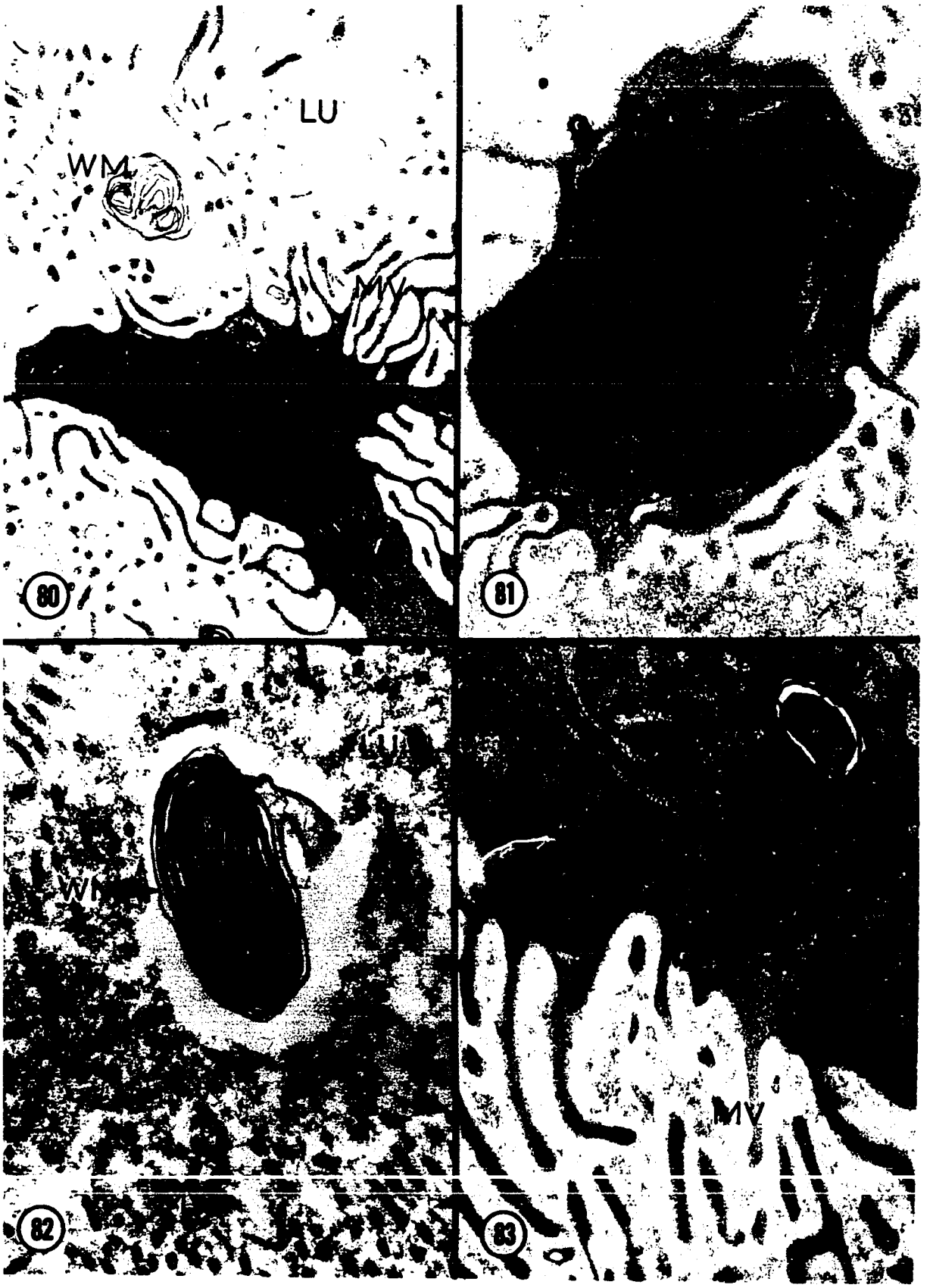
LU
WM
MV
80
81
WM
MV
82
83

Plate XXXVIII

Fig. 84. High magnification of gut cell cytoplasm. Note mitochondria (M), ribosomes (R) and plasma membranes (PM) between cells. (X 56,000)

Fig. 85. Edge of gastrodermal cell with lumen filled with ingested material (IM). Note vesicles (V) at cell border. (X 15,500)

Fig. 86. Hindbody gut epithelium. Note the few shortened microvilli (MV) projecting into the lumen and vesicles (V) near the cell border. (X 35,250)

Fig. 87. Low magnification micrograph of hindbody gastrodermis. Note the particulate droplets and particles within the lumen (LU). (X 12,900)

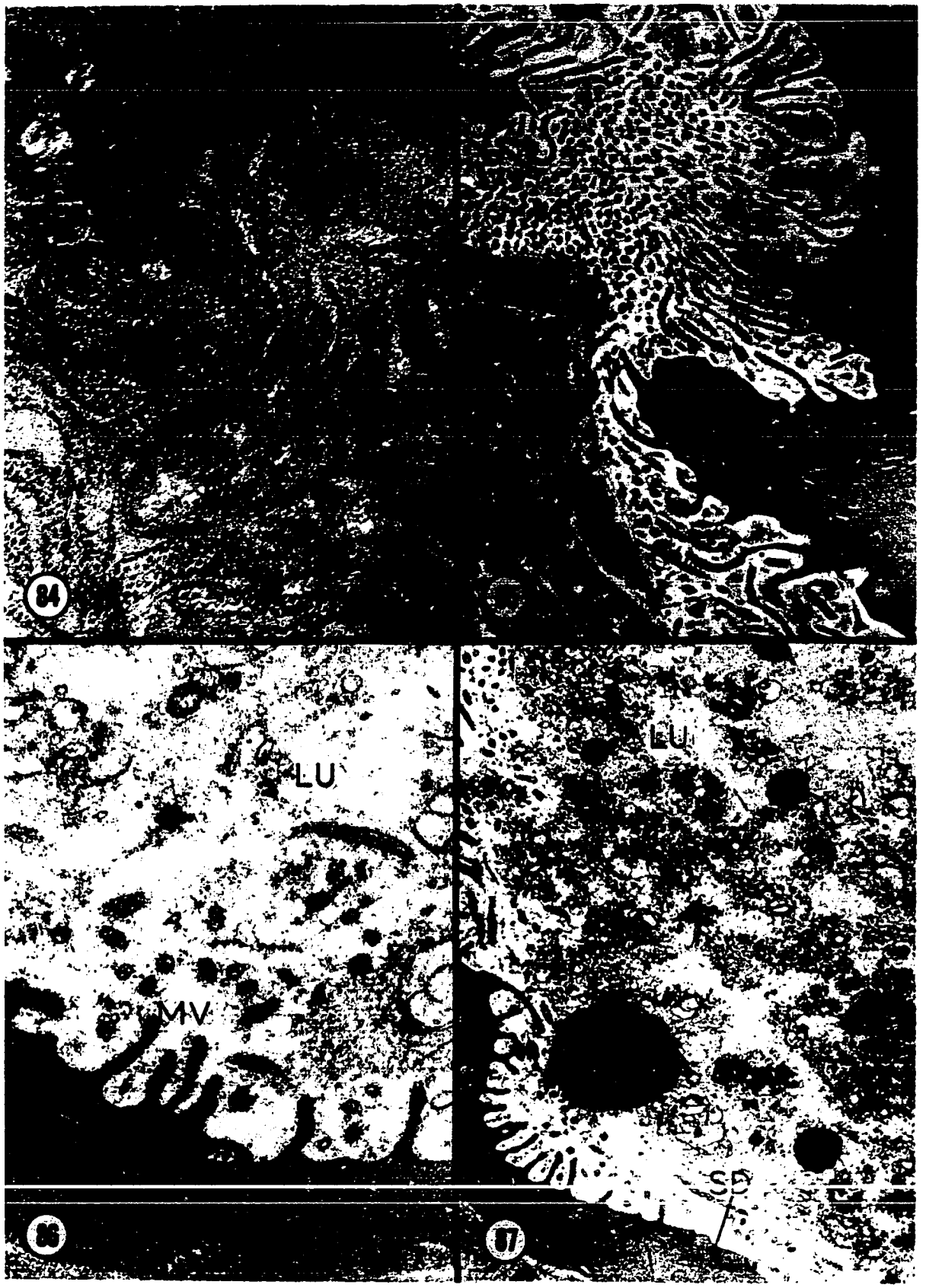
84
LU
MV
86
LU
CB
87

Plate XXXIX

Figs. 88-91. Light micrographs of the male reproductive system of *F. cratera*

Fig. 88. Whole mount. Note shape and position of anterior (AT) and posterior (PT) testes within hindbody (HB). (X 117)

Fig. 89. Frontal section of hindbody. Note individual oocytes within ovary (OV) and position of seminal vesicle (SMV) and genital aperture (GA). (X 180)

Fig. 90. Oblique section of hindbody demonstrating the intertesticular position of vitelline reservoir (VR). (X 490)

Fig. 91. Phase contrast micrograph of seminal vesicle (SMV) and genital aperture (GA). (X 635)

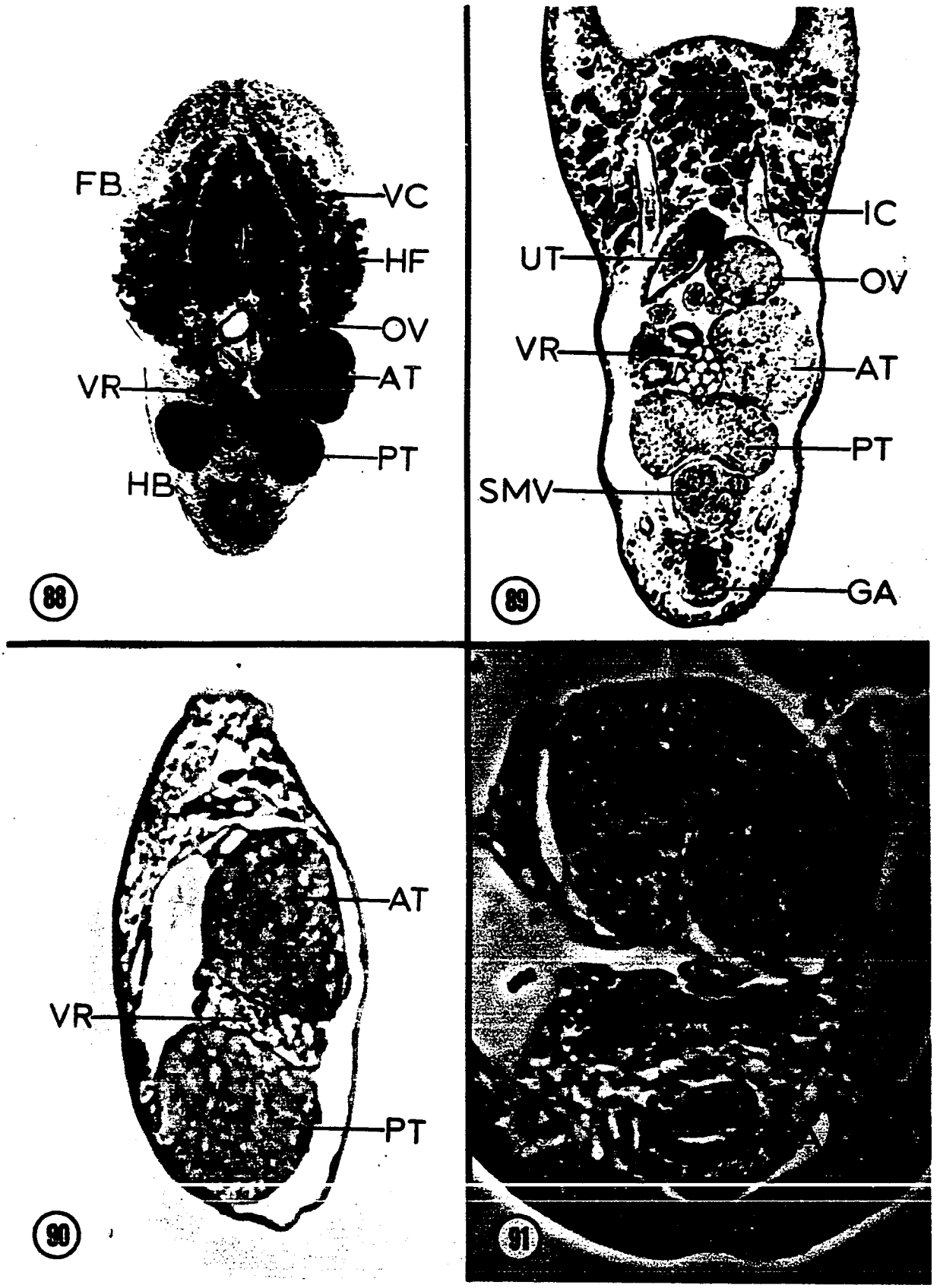
FB
VC
HF
OV
VR
AT
PT
HB
88
UT
IC
OV
VR
AT
PT
SMV
GA
89
AT
VR
PT
90
91

Plate XL

Fig. 92. Schematic diagram of trematode spermatogenesis. Note that both mitotic and meiotic divisions are involved. Numbers in parentheses denote numbers of germ cells at each stage of development. N and 2N denote haploid and diploid numbers of chromosomes, respectively

SPERMATOGENESIS

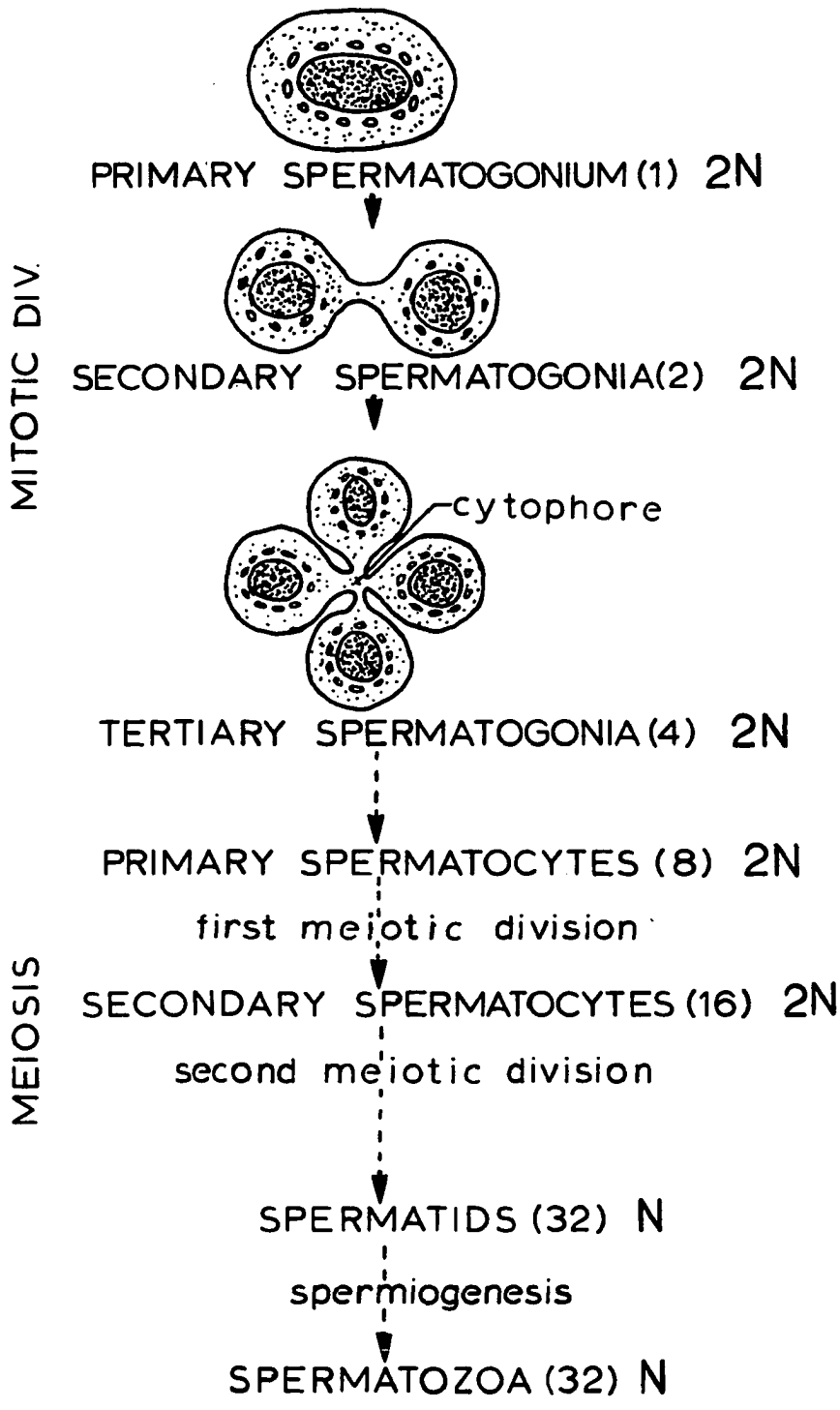

Plate XLI

Figs. 93-97. Schematic diagram of developmental stages of spermiogenesis

Fig. 93. Young undifferentiated spermatid. Note presence of a centriole (CE)

Fig. 94. Second stage of spermatid development. Note elongate nucleus (NU) and axial filaments (AF) arising from apical centriole (CE). Arrows depict direction of movement of axial filaments to a vertical position, characteristic of later stages

Fig. 95. Diagram of three components (two axial filaments (AF) plus single mid-piece (MP)) forming the spermatozoon tail

Fig. 96. Third spermatid developmental stage. Note movement of nucleus (NU) distally

Fig. 97. Last spermatid stage depicting elongate nucleus within mid-piece. Note also the rootlet fibers (RT) attached to axial filaments (AF)

Figs. 98-102. Diagrams of mature spermatozoon

Fig. 98. Section of sperm nucleus corresponding to plane A, Fig. 102. Note nucleus (NU), single axial filament, mitochondrion (M) and cytoplasmic microtubules within sperm head

Fig. 99. Section through neck region of sperm tail. (B, Fig. 102)

Fig. 100. Section through middle portion of sperm tail. Note the two axial filaments and cytoplasmic microtubules (MT). (C, Fig. 102)

Fig. 101. Section of terminal portion of sperm tail. (D, Fig. 102)

Fig. 102. Diagram of entire sperm. Note elongated nucleus (NU) and thread-like appearance of sperm

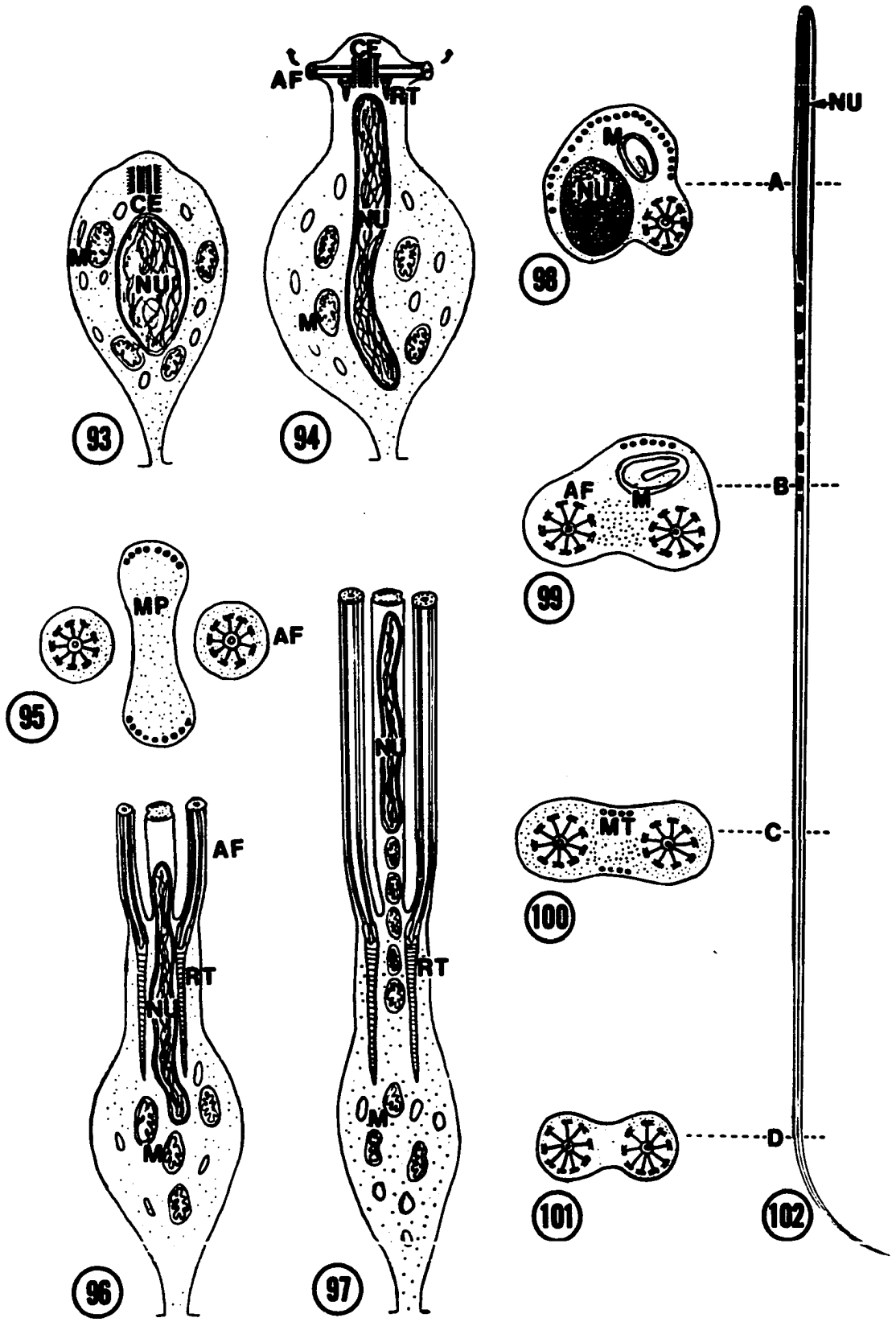
CE
NU
M
93
AF
CE
RT
NU
M
94
NU
M
98
A
NU
AF
M
99
B
MP
AF
95
MT
100
C
AF
RT
NU
M
96
RT
M
97
D
101
102

Plate XLII

Fig. 103. Electron micrograph of spermatogonium within testis of F. cratera. The large nucleus (NU) is surrounded by mitochondria (M). A centriole (CE) with attendant rootlet fibers is seen within the cytoplasm. (X 18,500)

Fig. 104. Spermatogonial cell. Note the nuclear/ cytoplasmic volume ratio and large numbers of mitochondria (M) within cytoplasm (CY). (X 15,850)

Fig. 105. Spermatocyte chromosomes (CH). Internal fibrous elements give a "scroll-like" appearance to chromosomes. The cytoplasm (CY) is filled with individual ribosomes. (X 19,900)

Fig. 106. Longitudinal section of spermatid with rootlet fibers (RT), centriole (CE), and a protruding axial filament (AF). (X 33,350)


103
104
105
106

Plate XLIII

Fig. 107. Spermatid of F. cratera showing an axial filament (AF) arising from a centriole (CE) and projecting from the cell body. (X 36,400)

Fig. 108. Section of spermatid depicting the nucleus (NU), and rootlet fibers (RT) within the ribosome-filled cytoplasm (CY). Note internal structure of centriole (CE) and protruding axial filament (AF). (X 36,400)

Fig. 109. Tangential section of spermatozoa (SPE) within testis. Note axial filaments (AF) and mitochondria (M) within sperm tails. (X 15,400)

Fig. 110. Longitudinal section of an axial filament (AF). Note peripheral microtubules (MT), connecting spokes (S) and helical pattern of the cortical sheath (CS) around the central axial rod. (X 56,800)

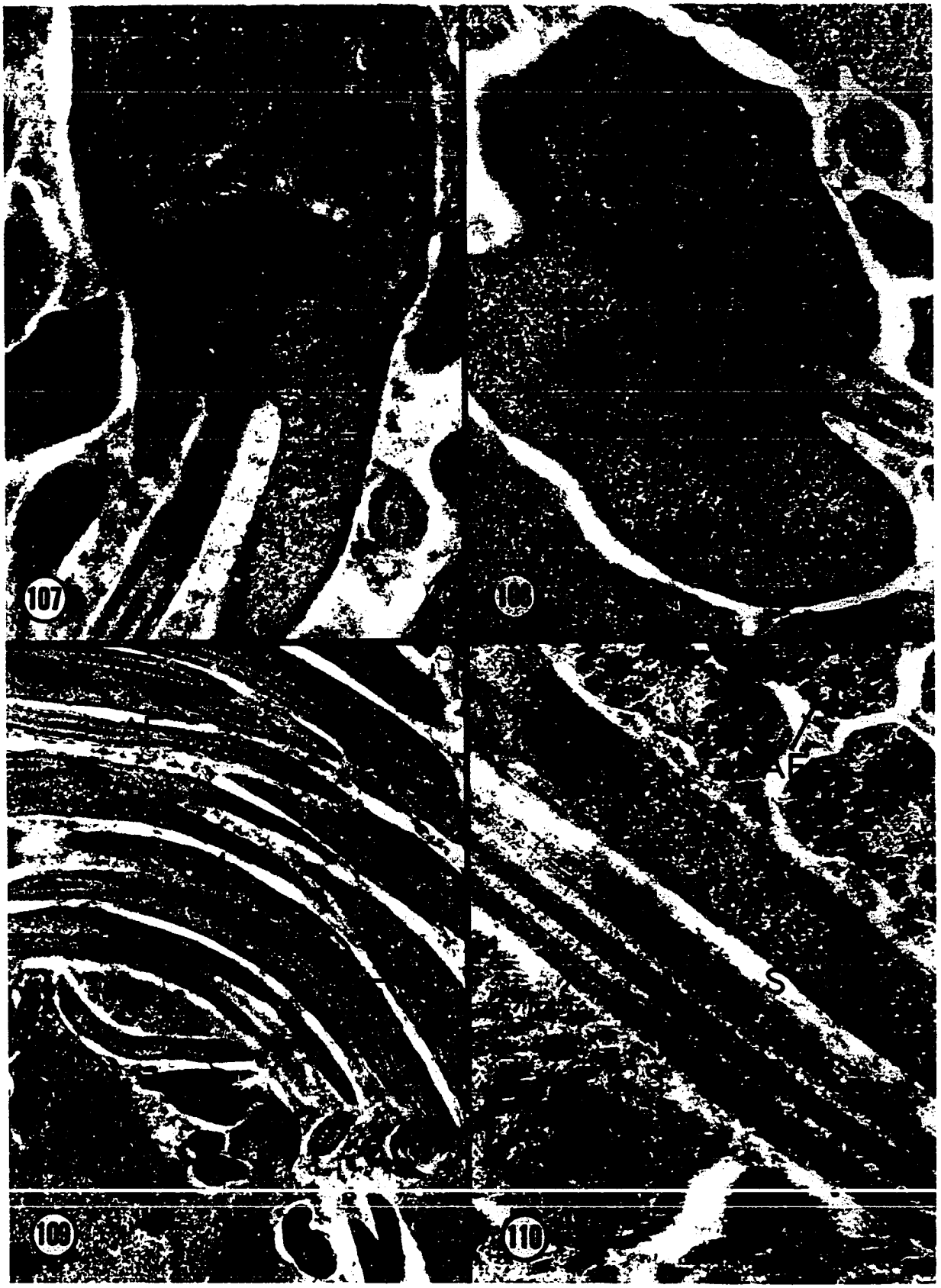
107
108
109
110

Plate XLIV

Figs. 111-114. Sections of mature spermatozoa and sperm tail components

Fig. 111. Sections of sperm heads displaying nucleus (NU), single axial filament (AF) and microtubules. (X 34,300)

Fig. 112. Sections through neck region of spermatozoa of F. cratera. Note cytoplasmic microtubules (MT) and two axial filaments. (X 60,600)

Fig. 113. Section of sperm tail components of developing spermatids. Numerous single axial filaments (AF) lie among larger, elongate mid-pieces (MP). (X 42,850)

Fig. 114. High magnification of sperm tail displaying internal structure of axial filaments. Dense internal axial rods (AR), the cortical sheath (CS), as well as connecting spokes (S) and peripheral doublet microtubules (DB) are seen. (X 106,300)

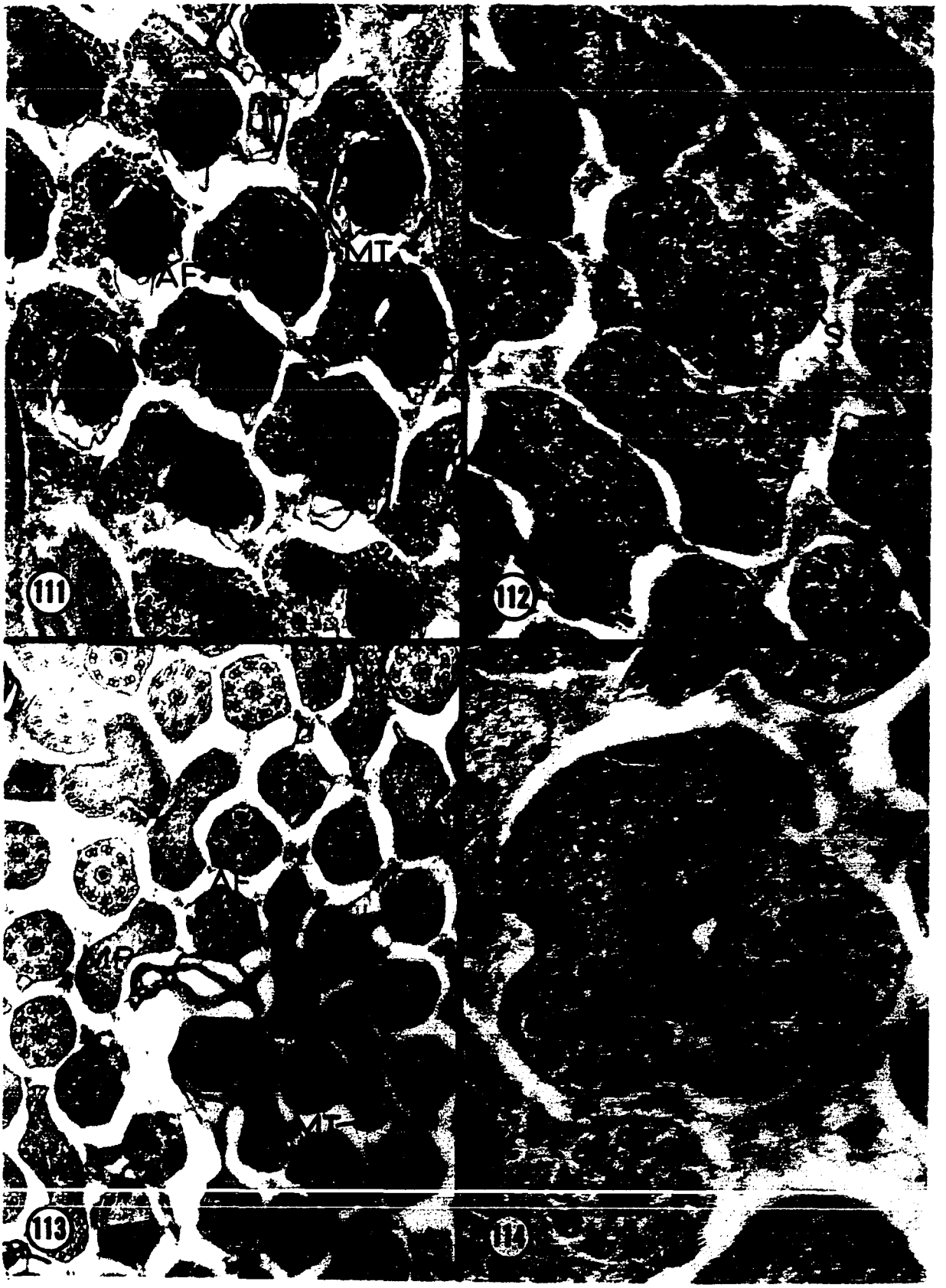
MT
AF
111
112
AF
AF
MT
113
114

Plate XLV

Fig. 115. High magnification of axial filaments (AF) and mid-pieces of developing spermatids. Note the cytoplasmic microtubules (MT) at the bulbous ends of mid-pieces (MP). (X 88,200)

Fig. 116. High magnification electron micrograph of 9+1 axial filaments (AF) within sperm tails. Note internal structure of the central axial column, radiating spokes (S), and doublet microtubules. (X 119,300)

Fig. 117. Section showing juncture of testis wall (TW) and seminal vesicle (SMV). Note spermatozoa (SPE) within testis and seminal vesicle as well as spermatogonia along the testis wall. (X 6,670)

Fig. 118. Micrograph of mature spermatozoa within the seminal vesicle. Light areas within sperm tails represent glycogen (G) concentrations. The terminal portion of a sperm tail (ST) is also shown. (X 6,750)

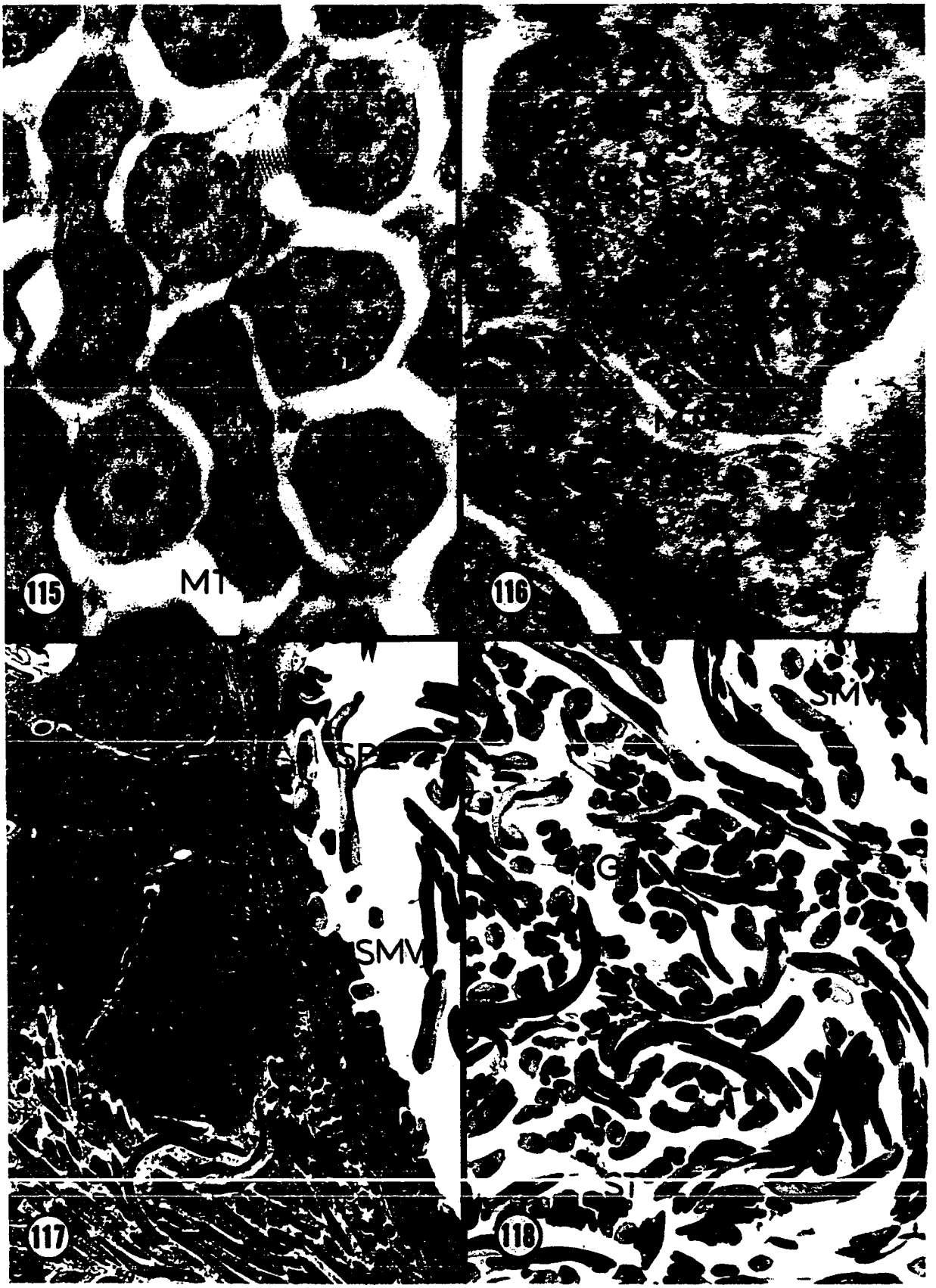
115
MT
116
117
SMV
118
SMV

Plate XLVI

Fig. 119. Survey micrograph of vitelline cells (VC) within forebody near the intestine (I). Note dense vitelline granules (VG) and yolk droplets (Y). (X 3,000)

Fig. 120. Nucleus of a vitelline cell illustrating nucleolus (NUC) and less dense surrounding euchromatin. Numerous ribosomes are seen in the cytoplasm. (X 25,000)

Fig. 121. Cytoplasm of mature vitelline cell containing large numbers of vitelline granules (VG) and endoplasmic reticulum (ER). (X 9,480)

Fig. 122. Cytoplasm of immature vitelline cell. Note large numbers of free ribosomes (R), strands of endoplasmic reticulum (ER) and dense vitelline granules. (X 29, 400)

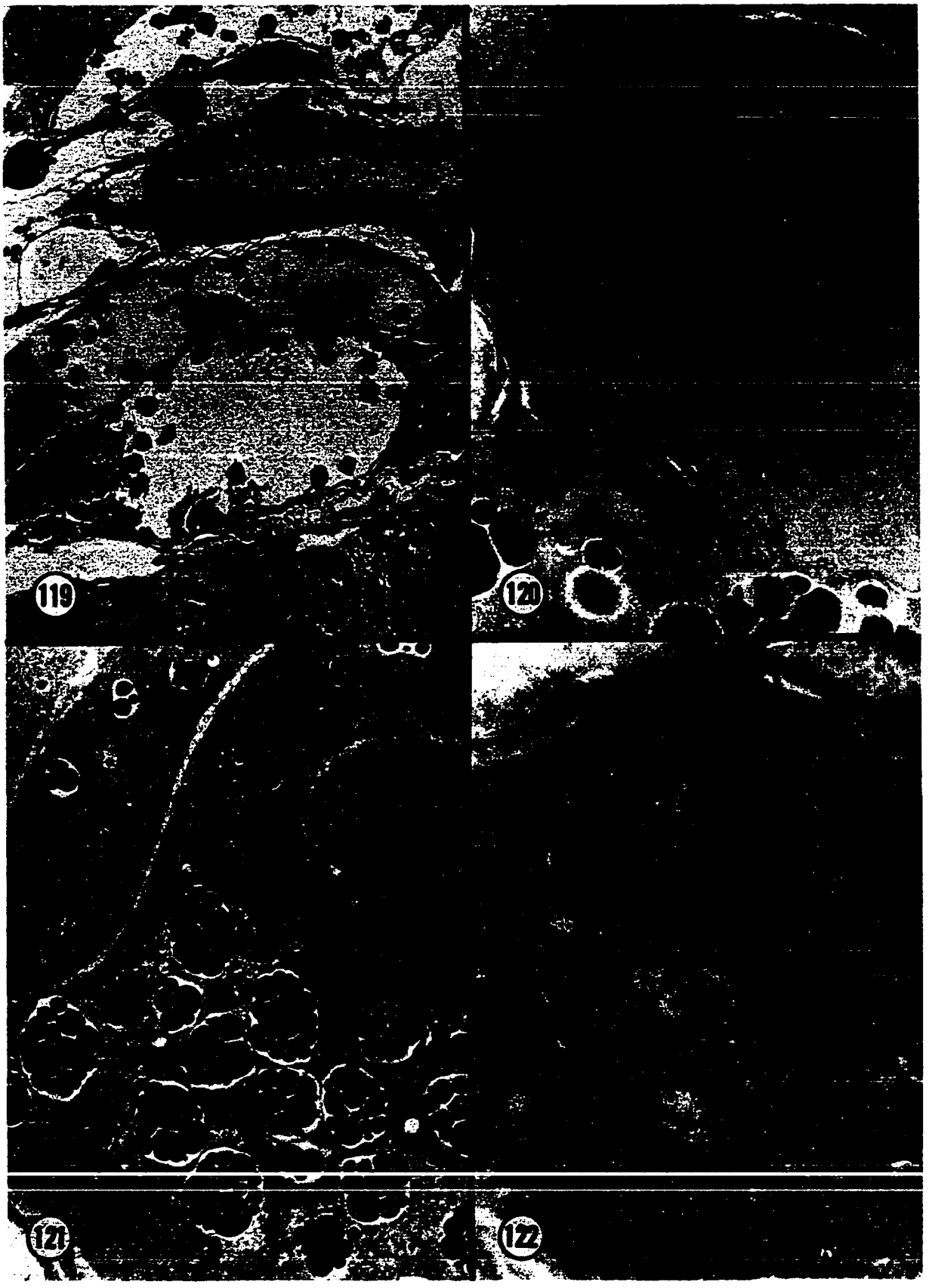
119
120
121
122

Plate XLVII

Fig. 123. Micrograph depicting accumulation of vitelline granules (VG) within vitelline cells. Note cytoplasmic (CY) remnants of vitelline cells. (X 28,800)

Fig. 124. Large vitelline granules formed by aggregation of smaller units. (X 14,150)

Fig. 125. Section of vitelline duct (VD) walls depicting 9+2 cilia (C), seen both in cross and longitudinal planes. (X 65,700)

Fig. 126. Micrograph of vitelline duct wall showing alignment of several 9+2 cilia (C). Certain cilia possess single peripheral microtubules indicating that sections are near the terminus of these cilia. (X 51,000)


VD

Plate XLVIII

Fig. 127. Section of vitelline duct depicting the two types of vitelline products: vitelline granules (VG) and dense yolk droplets (Y). (X 18,250)

Fig. 128. Large clusters of vitelline granules (VG) within vitelline duct (VD). (X 27,000)

Fig. 129. Light micrograph of section through forebody depicting arrangement of vitelline cells (VC) around the holdfast organ (HF), its gland cells (GC) and the intestine (I). (X 620)

Fig. 130. Vitelline granules (VG) within vitelline reservoir. (X 29,800)

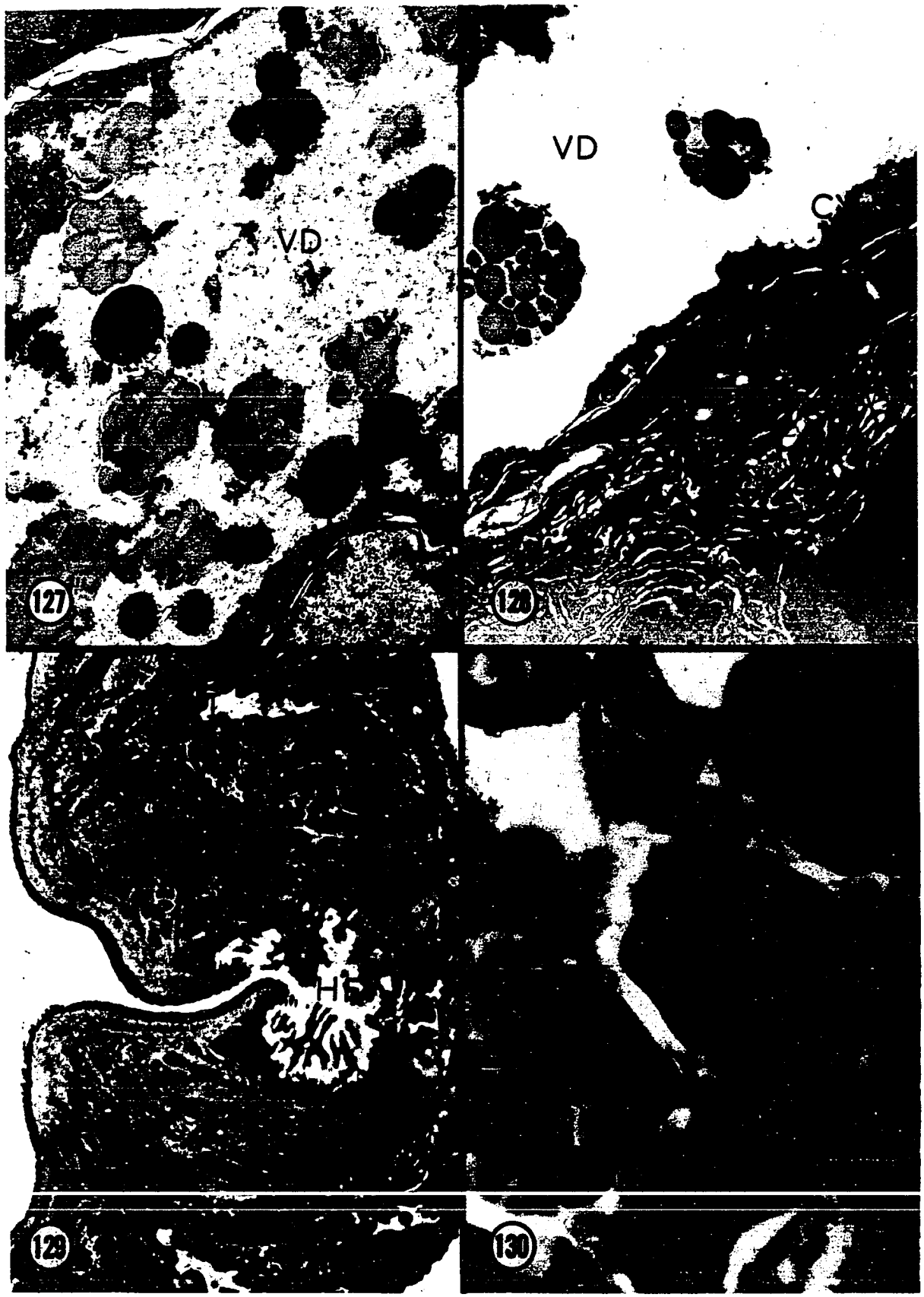
VD
127
VD
128
129
130

Plate XLIX

Fig. 131. Electron micrograph through flame cell and primary excretory duct (ED) of F. cratera. Note large number of internal cilia within the dense flame cell collar (FCC). (X 21,400)

Fig. 132. High magnification of 9+2 flame cell cilia depicting uniform orientation of central microtubules (indicated by plane of line). (X 65,000)

Fig. 133. Low magnification micrograph of section through basal bodies of flame cell cilia, and lamellate excretory duct. Section through basal bodies (BB) is at level of dotted line, Fig. 134. (X 18,600)

Fig. 134. Longitudinal section of primary flame cell, at junction of flame cell cilia (C) with their basal bodies (BB). (X 49,000)


ED
131
ED

Plate L

Fig. 135. Lamellate primary excretory duct with numerous lipid (L) inclusions. Note that several excretory lamellae (EL) usually surround the lipid droplets. (X 9,800)

Fig. 136. High magnification electron micrograph of a small excretory duct (ED) displaying membrane-bound excretory lamellae characteristic of its inner surface. (X 71,300)

Fig. 137. Reserve excretory duct (RD) depicting its lamellate walls (EL). Note that lipid droplets (L) occur in reserve excretory duct walls and also lie free within the duct lumen. Note also the high glycogen (G) concentrations adjacent to the duct wall. (X 31,400)

Fig. 138. Electron micrograph of a whorled membrane body (WM) within a reserve excretory duct (RD). Note presence of glycogen (G) near the excretory lamellae of duct walls. (X 37,000)

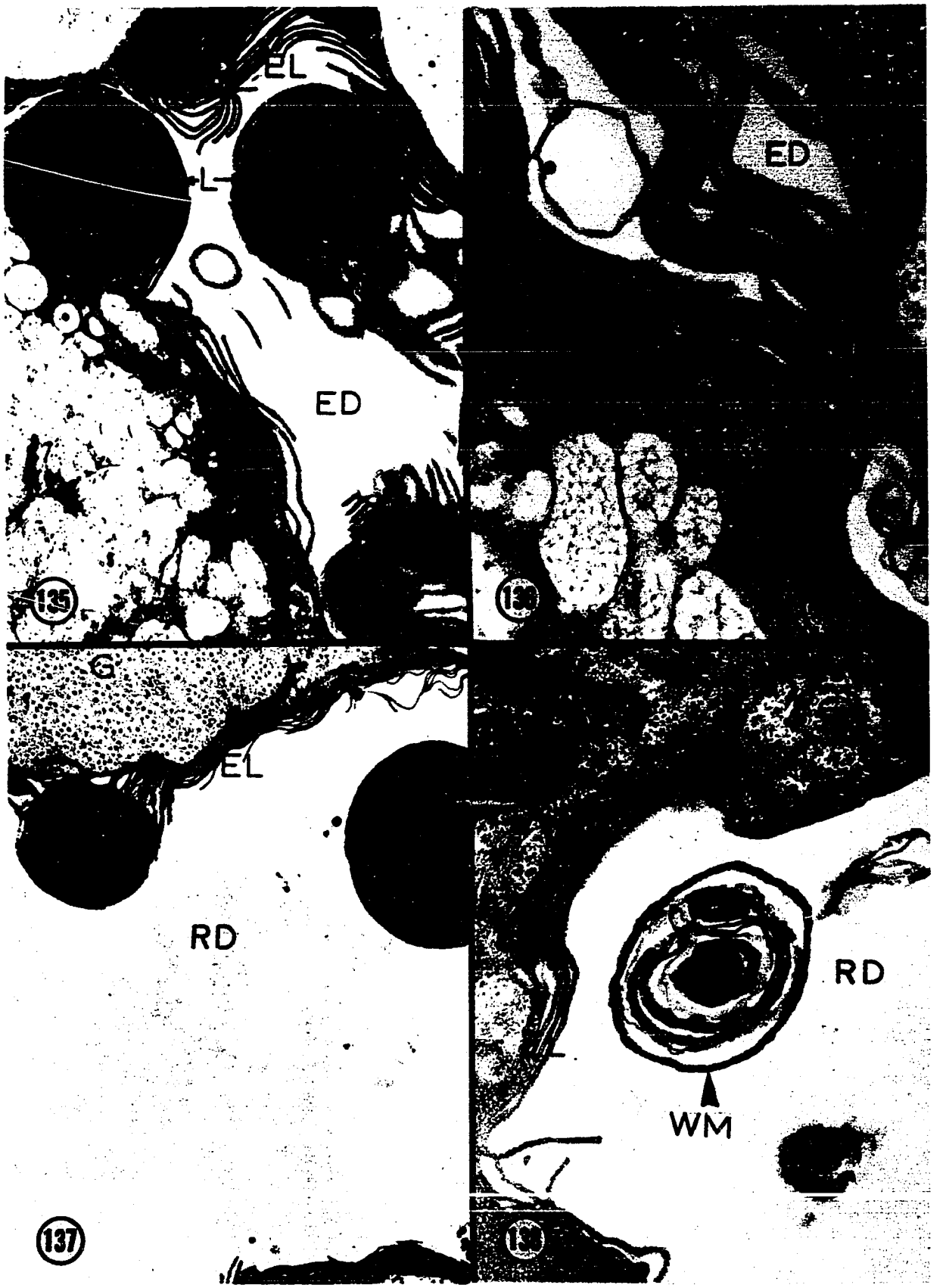
EL
L
O
ED
135
ED
136
G
EL
RD
137
RD
WM
138